

International Journal of Modern Physics A  
 © World Scientific Publishing Company

## FLAVOR MIXINGS AND TEXTURES OF THE FERMION MASS MATRICES

MANMOHAN GUPTA

*Department of Physics, Centre of Advanced Study, P.U., Chandigarh, India.  
 mmgupta@pu.ac.in*

GULSHEEN AHUJA

*Department of Physics, Centre of Advanced Study, P.U., Chandigarh, India.*

Received Day Month Year

Revised Day Month Year

A comprehensive review of several aspects of fermion mixing phenomenon and texture specific mass matrices have been presented. Regarding fermion mixings, implications of unitarity and certain new developments for the CKM paradigm have been discussed. In the leptonic sector, the question of possibility of CP violation has been discussed in detail from the unitarity triangle perspective. In the case of texture specific mass matrices, the issues of viability of Fritzsch-like as well as non Fritzsch-like mass matrices have been detailed for both the quark and leptonic sectors. The relationship of textures, naturalness and weak basis rotations has also been looked into. The issue of the compatibility of texture specific mass matrices with the SO(10) based GUT mass matrices has also been discussed.

*Keywords:* Fermion mixings, unitarity and CP violation, fermion mass matrices, SO(10) based mass matrices

PACS numbers: 12.15.Hh, 12.15.Ff, 12.10.-g, 14.60.Pq

### 1. Introduction

Understanding fermion masses and mixings, an important aspect of flavor physics, is one of the outstanding problems of present day High Energy Physics. Fermion mixing phenomena in the context of quarks was initiated by Cabibbo in 1963<sup>1</sup>, subsequently generalized to two generations by Glashow, Illiopoulos, Maiani<sup>2</sup> and finally to three generations by Kobayashi and Maskawa<sup>3</sup>. This is very well incorporated in the Standard Model (SM)<sup>4–8</sup> and has been tested to a great accuracy. Recently, flavor mixing has also been observed in the case of neutrinos implying the existence of non zero and non degenerate neutrino masses.

The complexity of the problem can be understood by considering the fermion masses which span over many orders of magnitudes. For example, considering the smallest neutrino mass to be of the order of a fraction of an eV and the top quark mass being of the order of  $10^{11}$  eV, the range of fermion masses looks to span over

13 orders of magnitudes. Similarly, fermion mixing angles again span several orders of magnitudes, these being quite small in the quark sector whereas in the leptonic sector these are somewhat ‘large’. The recent T2K<sup>9</sup>, MINOS<sup>10</sup>, DAYA BAY<sup>11</sup> and RENO<sup>12</sup> measurements regarding the mixing angle  $s_{13}$  also suggest a not so ‘small’ value. In fact, understanding the different patterns of mixing angles in the quark and lepton sector is a problem in itself. One may also mention that the non zero value of angle  $s_{13}$  has given a big impetus to the sharpening of the implications of the neutrino oscillations and has added another dimension to neutrino physics by implying the possibility of existence of CP violation in the leptonic sector.

At present, it seems that fermion masses and mixings provide a fertile ground to hunt for physics beyond the SM as well as pose a big challenge to understand these from more fundamental considerations. It may be noted that mixing angles and CP violating phases are very much related to the corresponding mass matrices, therefore in view of this relationship one has to essentially formulate the fermion mass matrices to unravel some of the deeper aspects of flavor physics. This becomes more challenging and interesting in case one attempts to understand the fermion masses and mixings in a unified framework. To this end, several ideas regarding the possible connections between quarks and leptons<sup>13</sup> are under investigation. One of the most seriously pursued idea is the quark-lepton symmetry wherein quarks and leptons may be two different manifestations of the same form of matter. This principle is enshrined in the Grand Unified Theories (GUTs) wherein both quarks and leptons form multiplets of the extended group. The most appealing such a group is SO(10) where all known components of quarks and leptons, including the right handed neutrinos, fit into the unique 16-plet spinor multiplet.

It may be noted that while on the one hand, GUTs have provided vital clues for understanding the relationship of fermion mass matrices between quarks and leptons, on the other hand, horizontal symmetries<sup>14–18</sup> have given clues for the relationship between different generation of fermions. Ideas such as extra dimensions<sup>19,20</sup> have also been invoked to understand fermion masses and mixings. Unfortunately, at present it seems that we do not have any theoretical framework which provides a viable and satisfactory description of flavor physics. The lack of a convincing fermion flavor theory from the ‘top down’ perspective necessitates a re-look at the issue from a ‘bottom up’ approach. The essential idea behind this complimentary approach is that one tries to find the phenomenological fermion mass matrices which are in tune with the low energy data and can serve as guiding stone for developing more ambitious theories. One may note that at present a ‘bottom up’ approach perhaps may be more useful, wherein apart from understanding the subtleties of mixing matrices of quarks and leptons, one has to also understand the texture structure, hierarchy of elements, phase structure, etc. of the corresponding mass matrices<sup>21,22</sup>. In particular, a viable strategy would be to examine general features of texture specific mass matrices of quarks and leptons which are in tune with the mixing parameters as well as are in accordance with the GUTs.

One may note that vital constraints on mass matrices can be obtained through

continuous refinements of the mixing parameters. In particular, in the last few years, the recent success of B factories<sup>23,24</sup>, analyzing over  $10^9$  decays of B-hadrons, has provided a wealth of data leading to a good deal of progress in our understanding of flavor physics. Precise measurements of CP asymmetry parameter  $\sin 2\beta$ , characterizing CP asymmetry  $a_{\psi K_s}$  in the  $B_d^0 \rightarrow \psi K_s$  decay, also referred to as the Golden Mode, the Cabibbo-Kobayashi-Maskawa (CKM)<sup>1,3</sup> matrix elements  $V_{us}, V_{cb}, V_{ud}$  as well as of several other parameters have been carried out. Based on these, several phenomenological analyses<sup>25–28</sup> have allowed us to conclude that the single CP violating phase, encoded in the CKM matrix, appears to be the dominant source of CP violation in the meson decays, at least to the leading order. Further, these refinements have also brought up several issues having potentiality of New Physics (NP). Therefore, one may conclude that continuous refinements of the mixing parameters, coupled with certain theoretical improvements in the lattice QCD calculations, not only sharpen the constraints on the mass matrices but also provide clues for finding NP.

The detailed plan of the article is as follows. Essentials regarding quark mixing phenomenology, unitarity and CP violation in the quark sector have been presented in Section (2). Section (3) presents the implications of unitarity, precision measurements and certain new developments for the CKM paradigm. Similarly, in Section (4) unitarity and CP violation in the leptonic sector have been discussed. Further, details pertaining to texture 6, 5, 4 zero quark and lepton mass matrices have been presented in Section (5). The concepts of natural mass matrices and weak basis (WB) transformations have been discussed in Section (6). Section (7) discusses the issue of compatibility of texture specific mass matrices with SO(10) inspired matrices. Finally, in Section (8) we summarize and conclude.

## 2. Essentials of quark mixing phenomenology

The idea of quark mixing was introduced by Cabibbo<sup>1</sup> in 1963 in order to explain the suppression of the strangeness-changing ( $\Delta S = 1$ ) weak interactions in comparison to the strangeness-conserving ( $\Delta S = 0$ ) weak interactions involving hadrons. To explain this anomalous behaviour, Cabibbo suggested that the electroweak eigenstates are a mixture of the flavor eigenstates ( $u, d, s$ ), e.g.,

$$\begin{pmatrix} u \\ d \end{pmatrix} \longrightarrow \begin{pmatrix} u \\ d' \end{pmatrix} \longrightarrow \begin{pmatrix} u \\ d \cos \theta_c + s \sin \theta_c \end{pmatrix}, \quad (1)$$

where  $\theta_c$  is the Cabibbo angle. The Cabibbo hypothesis was generalized by Glashow, Iliopoulos and Maiani (GIM)<sup>2</sup> to explain the absence of the flavor changing neutral currents by introducing a new quark, later on called the charm quark. In accordance with the GIM mechanism, the doublet consisting of c and s quarks takes the form

$$\begin{pmatrix} c \\ s' \end{pmatrix} \longrightarrow \begin{pmatrix} c \\ s \cos \theta_c - d \sin \theta_c \end{pmatrix}, \quad (2)$$

4 *Manmohan Gupta, Gulsheen Ahuja*

leading to

$$\begin{pmatrix} d' \\ s' \end{pmatrix} = V \begin{pmatrix} d \\ s \end{pmatrix} = \begin{pmatrix} \cos\theta_c & \sin\theta_c \\ -\sin\theta_c & \cos\theta_c \end{pmatrix} \begin{pmatrix} d \\ s \end{pmatrix}, \quad (3)$$

where  $V$  is the  $2 \times 2$  quark mixing matrix.

In 1974, Kobayashi and Maskawa<sup>3</sup> generalized the above mixing matrix to the case of three generations by defining the weak interaction eigenstates  $(d', s', b')$  in terms of the flavor eigenstates  $(d, s, b)$ , e.g.,

$$\begin{pmatrix} d' \\ s' \\ b' \end{pmatrix} = V \begin{pmatrix} d \\ s \\ b \end{pmatrix} = \begin{pmatrix} V_{ud} & V_{us} & V_{ub} \\ V_{cd} & V_{cs} & V_{cb} \\ V_{td} & V_{ts} & V_{tb} \end{pmatrix} \begin{pmatrix} d \\ s \\ b \end{pmatrix}. \quad (4)$$

This quark mixing matrix is a unitary matrix which describes the transition from one quark to another quark, mediated by the charged weak gauge currents. It may be added that a general  $n \times n$  unitary matrix has  $n^2$  parameters,  $n(n-1)/2$  of these are the Eulers angles and the remaining parameters are the phases. However, in the present case, some of the phases can be rotated away, leaving only  $(n-1)(n-2)/2$  measurable physical phases. Thus, for the case of two generations, it may be noted that one is left with no CP violation as the phase gets rotated away. However, for the case of three families, the mixing matrix is expressed in terms of three mixing angles and one phase, the latter being responsible for CP violation.

Originally, Kobayashi and Maskawa considered the following parameterization<sup>3</sup>, obtained by taking the product of three rotations, namely

$$\begin{aligned} V_{\text{KM}} &= R_{23}(\theta_3, \phi) R_{12}(\theta_1, 0) R_{23}(\theta_2, 0) \\ &= \begin{pmatrix} c_1 & -s_1 c_3 & -s_1 s_3 \\ s_1 c_2 & c_1 c_2 c_3 - s_2 s_3 e^{i\phi} & c_1 c_2 s_3 + s_2 c_3 e^{i\phi} \\ s_1 s_2 & c_1 s_2 c_3 + c_2 s_3 e^{i\phi} & c_1 s_2 s_3 - c_2 c_3 e^{i\phi} \end{pmatrix}, \end{aligned} \quad (5)$$

where  $s_i = \sin\theta_i$  and  $c_i = \cos\theta_i$  for  $i=1,2,3$ . It may be noted that apart from the above mentioned form, several other parameterizations of the quark mixing matrix have been proposed in the literature. In particular, altogether there are 36 different possible parameterizations which are all equivalent. These parameterizations can be arrived at easily if one notes that rotations in different planes do not commute, therefore for a given central rotation there are four possibilities related to left and right rotations. One may also mention that there are three possibilities for the central rotation, leading to 12 possible rotations. Further, corresponding to each of these there are three ways in which the phase can be introduced leading to 36 parameterizations in all. For details, the readers are referred to Ref. 29. In the following, we discuss some of the commonly used parameterizations of the quark mixing matrix.

One of the popular parameterization based on hierarchical expansion was proposed by Wolfenstein<sup>30</sup>. In this representation, each element is expanded as a power

series in the small parameter  $\lambda$ , leading to the quark mixing matrix  $V_{\text{CKM}}$  being

$$V_{\text{CKM}} = \begin{pmatrix} 1 - \frac{1}{2}\lambda^2 & \lambda & A\lambda^3(\rho - i\eta) \\ -\lambda & 1 - \frac{1}{2}\lambda^2 & A\lambda^2 \\ A\lambda^3(1 - \rho - i\eta) & -A\lambda^2 & 1 \end{pmatrix}, \quad (6)$$

where  $\lambda \sim 0.22$ ,  $A \sim 0.83$  and the magnitudes of  $\rho$  and  $\eta$  are smaller than one. It may be added that in the context of flavor physics, this parameterization has been extensively used, however, one may note that in this case the constraints of unitarity have to be satisfied order by order.

It needs to be mentioned that because of the smallness of  $\lambda$  and the fact that for each element the expansion parameter is actually  $\lambda^2$ , the Wolfenstein parameterization is a rapidly converging expansion. In case one requires sufficient level of accuracy, the terms of  $\mathcal{O}(\lambda^4)$  and  $\mathcal{O}(\lambda^5)$  have to be included in phenomenological applications. This has been carried out by generalizing the above mentioned Wolfenstein parameterization to the Wolfenstein-Buras parameterization<sup>31,32</sup> by including  $\mathcal{O}(\lambda^4)$  and  $\mathcal{O}(\lambda^5)$  terms, e.g.,

$$V_{\text{CKM}} = \begin{pmatrix} 1 - \frac{1}{2}\lambda^2 - \frac{1}{8}\lambda^4 & \lambda + \mathcal{O}(\lambda^7) & A\lambda^3(\rho - i\eta) \\ -\lambda + \frac{1}{2}A^2\lambda^5[1 - 2(\rho + i\eta)] & 1 - \frac{1}{2}\lambda^2 - \frac{1}{8}\lambda^4(1 + 4A^2) & A\lambda^2 + \mathcal{O}(\lambda^8) \\ A\lambda^3(1 - \bar{\rho} - i\bar{\eta}) & -A\lambda^2 + \frac{1}{2}A\lambda^4[1 - 2(\rho + i\eta)] & 1 - \frac{1}{2}A^2\lambda^4 \end{pmatrix}, \quad (7)$$

where

$$\bar{\rho} \simeq \rho(1 - \frac{\lambda^2}{2}) + \mathcal{O}(\lambda^4), \quad \bar{\eta} = \eta(1 - \frac{\lambda^2}{2}) + \mathcal{O}(\lambda^4). \quad (8)$$

By definition the expression for  $V_{ub}$  remains unchanged relative to the original Wolfenstein parameterization, given in Eq. (6), and the corrections to  $V_{us}$  and  $V_{cb}$  appear only at  $\mathcal{O}(\lambda^7)$  and  $\mathcal{O}(\lambda^8)$  respectively. The advantage of this generalization of the Wolfenstein parameterization is the absence of relevant corrections to  $V_{us}$ ,  $V_{cd}$ ,  $V_{ub}$  and  $V_{cb}$  and an elegant change in  $V_{td}$ , however it may be noted that the constraints of unitarity are not explicit.

Another popular parameterization, the ‘standard parameterization’ advocated by Chau, Keung<sup>33</sup>, adopted by Particle Data Group (PDG)<sup>25</sup>, is given by

$$V_{\text{CKM}} = R_{23}(\theta_{23}, 0) R_{13}(\theta_{13}, -\delta) R_{12}(\theta_{12}, 0) \\ = \begin{pmatrix} c_{12}c_{13} & s_{12}c_{13} & s_{13}e^{-i\delta} \\ -s_{12}c_{23} - c_{12}s_{23}s_{13}e^{i\delta} & c_{12}c_{23} - s_{12}s_{23}s_{13}e^{i\delta} & s_{23}c_{13} \\ s_{12}s_{23} - c_{12}c_{23}s_{13}e^{i\delta} & -c_{12}s_{23} - s_{12}c_{23}s_{13}e^{i\delta} & c_{23}c_{13} \end{pmatrix}, \quad (9)$$

with  $c_{ij} = \cos\theta_{ij}$  and  $s_{ij} = \sin\theta_{ij}$ . The angles  $\theta_{12}$ ,  $\theta_{23}$  and  $\theta_{13}$  can be chosen to lie in the first quadrant. The parameter  $\delta$  is the CP violating phase which may vary in the range  $0 \leq \delta \leq 2\pi$ . However, measurements of CP violation in K decays force it to be in the range  $0 < \delta < \pi$  as the sign of the relevant hadronic parameter is fixed. The relationship of the mixing angles and the CP violating phase with the

6 *Manmohan Gupta, Gulsheen Ahuja*

Wolfenstein parameters,  $\lambda, A, \rho$  and  $\eta$  is given by

$$s_{12} = \lambda, \quad s_{23} = A\lambda^2, \quad \rho = \frac{s_{13}}{s_{12}s_{23}}\cos\delta, \quad \eta = \frac{s_{13}}{s_{12}s_{23}}\sin\delta. \quad (10)$$

It may be mentioned that in the present era of precision measurements this parameterization is found to be very useful for numerical evaluations. Noting that  $c_{13}$  being almost close to unity, one can consider the three mixing angles  $\theta_{12}, \theta_{23}$  and  $\theta_{13}$  respectively being represented by the three elements of the mixing matrix,  $V_{us}, V_{cb}$  and  $V_{ub}$ , measurable at tree level. Therefore, whenever one has to consider issues related to New Physics, the use of this parameterization is recommended as the CKM matrix can be easily constructed by making use of the measured values of the above mentioned mixing matrix elements and the CP violating phase  $\delta$ . Also, for phenomenological analyses wherein emphasis is on unitarity it becomes more convenient to use this representation wherein the unitarity is built-in.

Another important parameterization discussed in the literature is the Fritzsch-Xing parameterization<sup>34,35</sup> given by

$$V_{\text{CKM}} = \begin{pmatrix} s_u s_d c + c_u c_d e^{-i\phi} & s_u c_d c + c_u s_d e^{-i\phi} & s_u s \\ c_u s_d c - s_u c_d e^{-i\phi} & c_u c_d c + s_u s_d e^{-i\phi} & c_u s \\ -s_d s & -c_d s & c \end{pmatrix}, \quad (11)$$

where  $s_u = \sin\theta_u$ ,  $s_d = \cos\theta_d$ ,  $c = \cos\theta$ . It may be mentioned that in contrast to the other parameterizations, there is no phase in the third row and the third column of the mixing matrix, thus the CP violating phase resides only in the  $2 \times 2$  submatrix involving light quarks  $u, d, s$  and  $c$ . Fritzsch and Xing recommend the use of this parameterization for the study of flavor mixing and CP violating phenomena.

### 2.1. Unitarity and unitarity triangles in the quark sector

After having looked at some of the parameterizations of the quark mixing matrix, we discuss its unitarity which is the only powerful constraint, imposed by the SM itself, on the quark mixing matrix. It may be noted that unitarity and unitarity triangles have played a crucial role in understanding the implications of CKM phenomenology. The unitarity triangles, in particular, have also played an important role in establishing the CKM paradigm as well as the fact that a single CP violating phase  $\delta$  is largely responsible for understanding the CP violation in the K and B sector. In this context, several well known groups<sup>25–28</sup> have been periodically updating their analyses which have played crucial role in affecting refinements of the CKM paradigm. It is outside the scope of the present review to delve into the details of their analyses, however, we would like to look into some of the aspects of the unitarity triangles which have facilitated understanding of fermion mixing phenomena and its relation to the fermion mass matrices.

Unitarity of the CKM matrix implies nine relations, three in terms of normalization conditions also referred to as ‘weak unitarity conditions’, and the other six are usually expressed through unitarity triangles in the complex plane. Because of

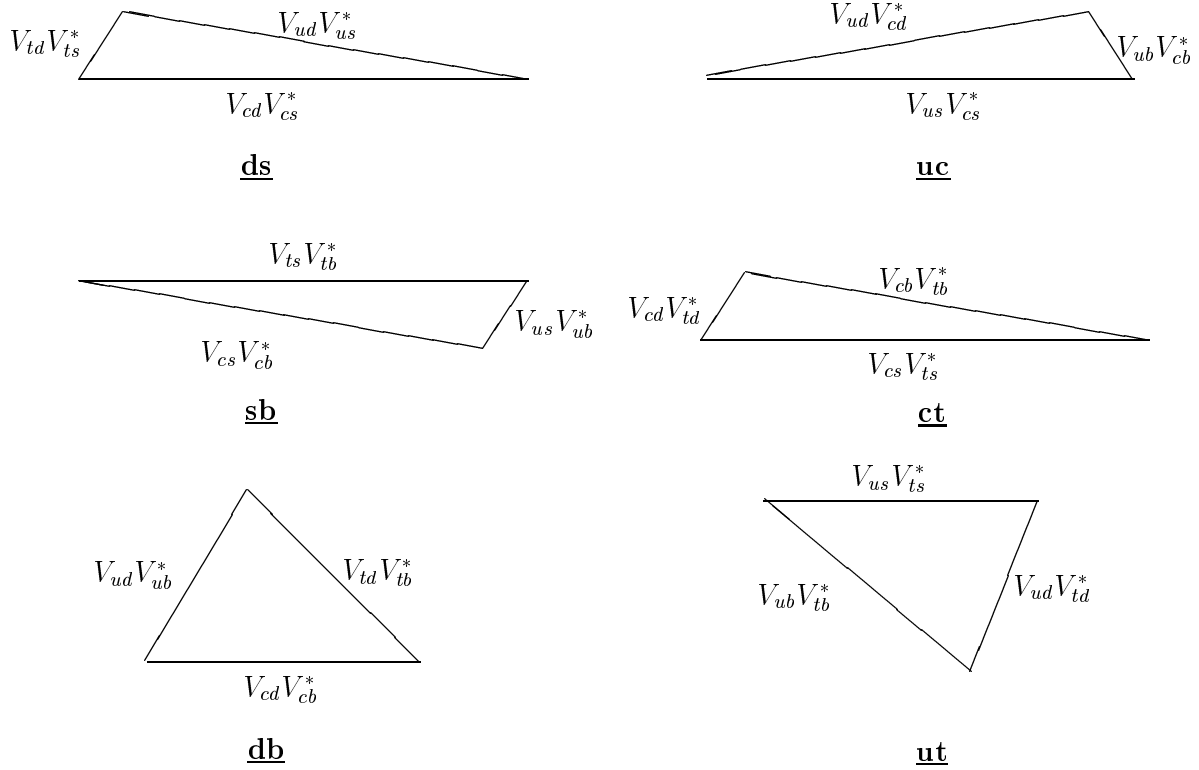


Fig. 1. The six unitarity triangles in the quark sector. The symbols **ds** etc. indicate the pair of rows or columns, whose orthogonality the triangle depicts. The magnitudes of the sides are not to scale.

the strong hierarchical nature of the CKM matrix elements as well as the limitations imposed by the present level of measurements, it is difficult to study the implications of normalization relations, therefore, the six non-diagonal relations are used to study the implications of unitarity on CKM phenomenology. These six non-diagonal relations can be expressed through six independent unitarity triangles in the complex plane and can be defined as

$$\sum_{\alpha=d,s,b} V_{i\alpha} V_{j\alpha}^* = \delta_{ij}, \quad (12)$$

$$\sum_{i=u,c,t} V_{i\alpha} V_{i\beta}^* = \delta_{\alpha\beta}, \quad (13)$$

where Latin indices run over the up type quarks ( $u, c, t$ ) and Greek ones run over the down type quarks ( $d, s, b$ ). The six unitarity triangles in the complex plane can

8 *Manmohan Gupta, Gulsheen Ahuja*

be expressed as

$$uc \quad V_{ud}V_{cd}^* + V_{us}V_{cs}^* + V_{ub}V_{cb}^* = 0, \quad (14)$$

$$db \quad V_{ud}V_{ub}^* + V_{cd}V_{cb}^* + V_{td}V_{tb}^* = 0, \quad (15)$$

$$ds \quad V_{ud}V_{us}^* + V_{cd}V_{cs}^* + V_{td}V_{ts}^* = 0, \quad (16)$$

$$sb \quad V_{us}V_{ub}^* + V_{cs}V_{cb}^* + V_{ts}V_{tb}^* = 0, \quad (17)$$

$$ut \quad V_{ud}V_{td}^* + V_{us}V_{ts}^* + V_{ub}V_{tb}^* = 0, \quad (18)$$

$$ct \quad V_{cd}V_{td}^* + V_{cs}V_{ts}^* + V_{cb}V_{tb}^* = 0, \quad (19)$$

where the letters  $uc$  etc. represent the corresponding unitarity triangle. These triangles are schematically shown in Fig. 1.

## 2.2. Unitarity and CP violation in the quark sector

In the context of CP violation, phenomenologically there is an important parameter known as the Jarlskog's rephasing invariant parameter and denoted as  $J^{29}$ . The significance of  $J$  lies in the fact that all the CP violating effects in the Standard Model (SM) are proportional to it. Also,  $J$  is a universal quantity in the sense that it does not depend on the specific parameterization of the CKM matrix, therefore it is rephasing invariant. Because of the above mentioned reasons,  $J$  is of much interest for the study of CP violation in the CKM phenomenology. Further, the parameter  $J$  is related to area of any of the unitarity triangle as

$$|J| = 2 \times \text{Area of any of the unitarity triangle.} \quad (20)$$

In terms of the elements of the CKM matrix,  $J$  can be written in a form that is explicitly parameterization independent, e.g.,

$$\text{Im} (V_{i\alpha} V_{j\beta} V_{i\beta}^* V_{j\alpha}^*) = J \sum_{k,\gamma} (\varepsilon_{ijk} \varepsilon_{\alpha\beta\gamma}) , \quad (21)$$

in which each Latin subscript ( $i, j, k$ ) runs over the up-type quarks ( $u, c, t$ ) and each Greek subscript ( $\alpha, \beta, \gamma$ ) runs over the down-type quarks ( $d, s, b$ ). Thus knowing the elements of the CKM matrix,  $J$  can be easily evaluated. Further, in the standard parameterization  $J$  is given as

$$J = s_{12}s_{23}s_{13}c_{12}c_{23}c_{13}^2 \sin \delta, \quad (22)$$

with  $c_{ij} = \cos \theta_{ij}$  and  $s_{ij} = \sin \theta_{ij}$  for  $i, j = 1, 2, 3$ .  $\theta_{12}$ ,  $\theta_{23}$  and  $\theta_{13}$  are the mixing angles and  $\delta$  is the CP violating phase.

## 3. Unitarity and CKM phenomenological parameters

In the last few years, many important developments have taken place in the context of phenomenology of Cabibbo-Kobayashi-Maskawa (CKM) matrix, both from theoretical as well as experimental point of view. As mentioned earlier, several detailed and extensive phenomenological analyses<sup>25–28</sup> have allowed us to conclude that



the single CKM phase looks to be a viable solution of CP violation not only in the case of K-decays but also in the context of B-decays, at least to the leading order. In this context, unitarity triangles have been widely used to check the CKM paradigm as well as to test the predictions of the SM. To this end, the readers are referred to Ref. 36 wherein the author presents extensive details of several analyses incorporating global analysis tools to determine the CKM parameters in the framework of the Standard Model. In particular, employing Wolfenstein parameterization, global fits comparing the data to theoretical predictions have been carried out and the results obtained by the UTfit<sup>26</sup> group as well as the CKMfitter<sup>27</sup> group have been presented. These two groups employ different techniques, Bayesian approach detailed in Ref. 37 has been followed by the UTfit group and the CKMfitter group employs the recently introduced RangeFit<sup>38</sup> procedure to combine measurements with very different statistical errors and extract the best information. Combining results from these two approaches one can reach at the conclusion that a good overall consistency between the various measurements at 95% C.L. is observed, thus establishing the CKM mechanism as the dominant source of CP violation in B-meson decays.

### 3.1. Implications of unitarity and $\sin 2\beta$ on $V_{ub}$ and $\delta$

It may be noted that most of the present day analyses related to CKM phenomenology, including the one mentioned above<sup>36</sup>, invoke global inputs, wherein the implications of unitarity are not obvious. This is further complicated by the use of the Wolfenstein-Buras parameterization, wherein unitarity of the CKM matrix has to be satisfied order by order making it further complicated to examine its implications. However, recently, an interesting analysis has been carried out<sup>39</sup> wherein the implications of unitarity on CKM phenomenology have been examined explicitly, unlike the other approaches. This analysis employs the PDG representation of the CKM matrix which is more convenient to use in this context as the unitarity is built-in. The analysis<sup>39</sup> investigates the implications of unitarity along with the well measured  $V_{us}$ ,  $V_{cb}$ ,  $\sin 2\beta$  and angle  $\alpha$  of the unitarity triangle on some of the lesser known elements of the CKM matrix such as  $V_{ub}$ ,  $V_{cs}$ ,  $V_{ts}$  and  $V_{td}$ . Using minimal inputs, the possibility of constructing a ‘precise’ CKM matrix has also been explored. It is instructive to discuss some of the essential details of this analysis.

In this context, it may be mentioned that out of the earlier mentioned six unitarity triangles, the triangles  $uc$ ,  $ds$ ,  $sb$  and  $ct$  are highly skewed which means that one side of these is very small as compared to the other two, therefore it is difficult to study their implications<sup>40–42</sup> with the present level of accuracy of the CKM matrix elements. Out of the other two, it is usual to consider the  $db$  triangle expressed as

$$V_{ud}V_{ub}^* + V_{cd}V_{cb}^* + V_{td}V_{tb}^* = 0. \quad (23)$$

The angles of this triangle in terms of the CKM matrix elements, mixing angles and

10 *Manmohan Gupta, Gulsheen Ahuja*

CP violating phase  $\delta$  are expressed as

$$\alpha \equiv \arg \left[ -\frac{V_{td}V_{tb}^*}{V_{ud}V_{ub}^*} \right] = \tan^{-1} \left[ \frac{s_{12}s_{23} \sin \delta}{c_{12}c_{23}s_{13} - s_{12}s_{23} \cos \delta} \right], \quad (24)$$

$$\beta \equiv \arg \left[ -\frac{V_{cd}V_{cb}^*}{V_{td}V_{tb}^*} \right] = \tan^{-1} \left[ \frac{c_{12}s_{12}s_{13} \sin \delta}{c_{23}s_{23}(s_{12}^2 - c_{12}^2s_{13}^2) - c_{12}s_{12}s_{13}(c_{23}^2 - s_{23}^2) \cos \delta} \right] \quad (25)$$

$$\gamma \equiv \arg \left[ -\frac{V_{ud}V_{ub}^*}{V_{cd}V_{cb}^*} \right] = \tan^{-1} \left[ \frac{s_{12}c_{23} \sin \delta}{c_{12}s_{23}s_{13} + s_{12}c_{23} \cos \delta} \right]. \quad (26)$$

To obtain information about the CP violating phase  $\delta$  from the experimentally well determined angle  $\beta$  one can express Eq. (25) as

$$\tan \frac{\delta}{2} = \frac{A - \sqrt{A^2 - (B^2 - A^2C^2)\tan^2\beta}}{(B + AC)\tan \beta}, \quad (27)$$

where  $A = c_{12}s_{12}s_{13}$ ,  $B = c_{23}s_{23}(s_{12}^2 - c_{12}^2s_{13}^2)$  and  $C = c_{23}^2 - s_{23}^2$ . Using  $s_{12}^2 \gg c_{12}^2s_{13}^2$  and  $s_{23}^2 \ll c_{23}^2$ , the above relation can be re-expressed as

$$\delta = -\beta + \sin^{-1} \left( \frac{s_{12}s_{23}}{c_{12}s_{13}} \sin \beta \right), \quad (28)$$

which can also be written as

$$\frac{\sin(\delta + \beta)}{\sin \beta} = \frac{s_{12}s_{23}}{c_{12}s_{13}}. \quad (29)$$

From Eq. (26), one can easily show that  $\gamma = \delta$  with an error of around 2%, therefore, using the closure property of the angles of the triangle,  $\alpha + \beta + \gamma = \pi$ , the above equation can be written as

$$s_{13} = \frac{s_{12}s_{23} \sin \beta}{c_{12} \sin \alpha}, \quad (30)$$

which can also be derived from Eq. (24) by using the closure property of the triangle. Eq. (29) can be used to provide a lower bound on  $s_{13}$ , e.g.,

$$s_{13} \geq \frac{s_{12}s_{23}}{c_{12}} \sin \beta. \quad (31)$$

On examining unitarity based Eq. (27), it can be noted that  $\delta$  is dependent on  $V_{us}$ ,  $V_{cb}$ , angle  $\beta$  as well as it involves  $V_{ub}$ . Using this equation, the authors have plotted the CP violating phase  $\delta$  versus  $V_{ub}$ , presented in Fig. 2. Also included in the figure is the then<sup>43</sup> experimentally measured  $\delta = (63.0 + 15.0 - 12.0)^\circ$  shown by horizontal dashed lines, inclusive of results of various global analyses. The solid central line depicts  $\delta$  obtained by using the mean values of  $V_{us}$ ,  $V_{cb}$  and  $\sin 2\beta$  whereas the outer lines correspond to the  $1\sigma$  ranges of these inputs.

From the figure one finds that for values of  $V_{ub} > 0.00355$ , the central value of  $\delta$  shows a smooth decline as well as the range of  $\delta$  gets narrower and narrower with increasing  $V_{ub}$ , however for  $V_{ub} < 0.00355$  it seems that there is a sharp broadening of the  $\delta$  range, with no restriction on  $\delta$  when  $V_{ub} < 0.0035$ . It may be noted that

as per the data given by PDG 2006<sup>43</sup>, from the graph one finds that the  $1\sigma$  range of the inclusive value of  $V_{ub}$  restricts  $\delta$  to  $23^\circ - 39^\circ$ , whereas the mean value of the exclusive value does not constrain  $\delta$ , however the upper limit of the  $1\sigma$  range of the exclusive value provides only a lower bound  $\delta > 38^\circ$ . Therefore, it was emphasized that the precisely known  $\sin 2\beta$ , for the inclusive value of  $V_{ub}$  implies a narrow range for  $\delta$ , whereas for the exclusive value of  $V_{ub}$  it implies only a lower bound on  $\delta$ . It may be noted that the above mentioned conclusions remain largely valid even when the recent data pertaining to CKM matrix elements is included.

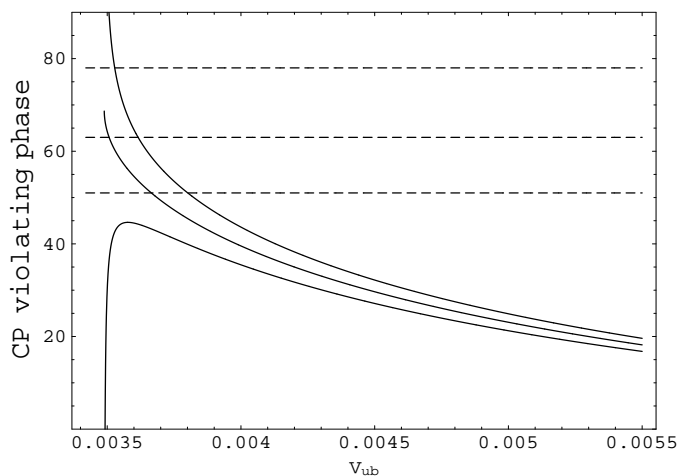


Fig. 2. Plot showing variation of  $V_{ub}$  versus CP violating phase  $\delta$ , obtained by using Eq. (27). The central solid line corresponds to mean value of input parameters, whereas the other 2 lines correspond to  $1\sigma$  variations.

The conclusion about  $V_{ub}$  can be sharpened further, e.g., using Eq. (31) one can easily obtain the following rigorous lower bound on  $V_{ub}$ ,

$$V_{ub} \geq 0.0035. \quad (32)$$

It may be noted that this bound is independent of the value of  $\delta$  as well as contamination of NP in the measurement of  $\delta$ . Predictions regarding  $V_{ub}$  have been refined further by incorporating angle  $\alpha$  of the unitarity triangle, measured from  $B \rightarrow \pi\pi$  and  $B \rightarrow \rho\rho$  decays. Using its then known value<sup>44</sup>, from Eq. (30) one obtains

$$V_{ub} = 0.0035 \pm 0.0002. \quad (33)$$

Interestingly, this precise value of  $V_{ub}$  is a consequence of unitarity and the precisely measured elements  $V_{us}$ ,  $V_{cb}$  and angles  $\beta$  and  $\alpha$  as well as is in full agreement with the exclusive  $V_{ub}$ . It may also be noted that this value is quite insensitive to a change in the value of angle  $\alpha$ , e.g., even if the mean value of  $\alpha$  changes by more than 20%, still  $V_{ub}$  would register a variation of only a few percent.

The above discussion also underlines the fact that precisely measured  $\sin 2\beta$  does not lead to any well defined conclusion regarding  $\delta$  because of the persistent difference between exclusive and inclusive values of  $V_{ub}$ . Therefore, the unitarity based  $\delta$  can be obtained through the angles  $\alpha$  and  $\beta$  by using the closure property of the angles of the unitarity triangle, e.g.,

$$\delta = 67.8^\circ \pm 7.3^\circ. \quad (34)$$

This unitarity based value of  $\delta$  is compatible with its directly measured value in  $B^\pm \rightarrow DK^\pm$  decays<sup>45</sup> as well as with the one obtained<sup>46</sup> from the  $B \rightarrow \pi\pi$  and  $B \rightarrow \pi K$  decays. It may also be mentioned that this value is compatible with the  $\delta$  bound given by exclusive  $V_{ub}$ , as obtained from Fig. 2, however does not agree with the  $\delta$  range obtained for inclusive  $V_{ub}$ .

After having found  $V_{ub}$  and  $\delta$  from unitarity, the authors have constructed the entire CKM matrix which is obtained at  $1\sigma$  C.L. as follows

$$\begin{pmatrix} 0.9738 - 0.9745 & 0.2244 - 0.2272 & 0.0033 - 0.0036 \\ 0.2243 - 0.2270 & 0.9730 - 0.9736 & 0.0409 - 0.0423 \\ 0.0082 - 0.0091 & 0.0401 - 0.0415 & 0.9990 - 0.9991 \end{pmatrix}. \quad (35)$$

It may be mentioned that this matrix is free from contamination by NP to the extent that the measured values of angles  $\alpha$  and  $\beta$  are free from NP effects. The matrix reveals that the ranges of CKM elements obtained here are quite compatible with those obtained by global analyses<sup>25–28</sup>. This perhaps indicates that unitarity plays a key role even in the case of global analyses.

Making use of the above mentioned CKM matrix, the authors have also calculated the ratio  $\frac{V_{ts}}{V_{td}}$  which comes out to be  $4.69 \pm 0.23$ , having an excellent overlap with  $4.7 \pm 0.4$ , found from precision measurements of  $\Delta M_{B_s}$ <sup>47</sup>. The measured value of the ratio  $\frac{V_{ts}}{V_{td}}$  can be considered as an over constraining check on the above unitarity based predictions.

The above discussion leads to the conclusion that a further precision in the measurement of  $\sin 2\beta$ , needless to say, would have far reaching implications for CKM phenomenology, particularly for CP violating phase  $\delta$  and  $V_{ub}$ . In this context, measurements of several other CKM parameters are also reaching at the precision level, making it essential to examine their implications for the CKM paradigm. In the following, we briefly discuss some of the analyses which have explored these issues.

### 3.2. *Implications of precision measurements for CKM paradigm*

As already emphasized, precise measurements of  $\sin 2\beta$  as well as of the Cabibbo-Kobayashi-Maskawa (CKM) matrix<sup>1,3</sup> elements  $V_{us}, V_{cb}, V_{ud}$  and several other parameters have been carried out. Similarly, a good deal of data has been collected for a large number of flavor changing neutral current processes involving  $b \rightarrow d$  and  $b \rightarrow s$  transitions and several CP violating asymmetries have also been studied in

detail<sup>48</sup>. Based on these efforts, one may now conclude that the larger picture of CKM paradigm appears to be well confirmed.

In line with the precision measurements regarding CKM parameters, several recent developments have also taken place on the theoretical front concerning the calculations of hadronic factors. In particular, improvements have taken place in the lattice QCD calculations of hadronic factors in the case of  $K - \bar{K}$  and the  $B_d - \bar{B}_d$  mixings along with contribution of the long distance effects in the  $K - \bar{K}$  system. To this end, the new lattice QCD calculations of the hadronic matrix element  $B_K$ , relevant for the determination of  $\epsilon_K$ , constrain it to an accuracy of  $(4 - 6)\%$ <sup>49</sup>. Also, a correction of  $(5 - 10)\%$ <sup>50</sup> in the determination of  $\epsilon_K$  has now been advocated by incorporating the long distance contribution related to the ratio  $K \rightarrow \pi\pi$  decay amplitudes in the  $\Delta I = 1/2$  channel leading to the introduction of an overall multiplicative factor  $\kappa_\epsilon \sim 0.92$ , omitted from the earlier CKM phenomenological analyses.

Triggered by these theoretical improvements, recently Buras and Guadagnoli<sup>51</sup> as well as Lunghi and Soni<sup>52</sup> have investigated the implications of these for the CKM phenomenology. In particular, Ref. 51 points out that the CP violation in  $B_d - \bar{B}_d$  mixing evaluated by considering the measured ratio  $\Delta m_d/\Delta m_s$ , the recent value of the non-perturbative parameter  $B_K$  and the additional effective suppression factor  $\kappa_\epsilon$  may be insufficient to describe the measured value of  $\epsilon_K$  within the Standard Model (SM). In other words, the above mentioned theoretical improvements tend to lower the SM prediction for  $\epsilon_K$  if the amount of CP violation in the  $B_d$  system, quantified by  $\sin 2\beta$  from  $B_d^0 \rightarrow \psi K_s$  decay, is used as an input. From this, they supposedly obtain a hint for a possible inconsistency between the size of CP violation in the  $K - \bar{K}$  and/or  $B_d - \bar{B}_d$  systems. A closer look at their analysis reveals that in case one considers the absence of an additional CP violating phase in the  $B_d$  system, the value of  $\epsilon_K$  then comes out to be almost 20% below its measured value, hinting at New Physics (NP) in the  $K - \bar{K}$  mixing. On the other hand, if absence of an additional CP violating phase in the  $K - \bar{K}$  system is considered, then this implies  $\sin 2\beta$  coming out be 10-20% larger.

The analysis by Ref. 52 also explores the possibility of the presence of NP in the  $K - \bar{K}$  and  $B_d - \bar{B}_d$  systems as well as in the  $b \rightarrow s$  penguin transitions. In particular, they attempt to predict the value of  $\sin 2\beta$  keeping in mind the role played by the parameter  $V_{ub}$ , e.g., without the inclusion of  $V_{ub}$  the value of  $\sin 2\beta$  comes out to be  $0.87 \pm 0.09$ , whereas on including  $V_{ub}$  the value of  $\sin 2\beta$  becomes  $0.75 \pm 0.04$ . These predicted values of  $\sin 2\beta$  point towards possible inconsistencies with the directly measured value through the gold-plated  $B_d^0 \rightarrow \psi K_s$  decay and also by the penguin-dominated modes leading the authors to conclude that one has to give a re-look at the CKM paradigm. To summarize the findings of the two above mentioned analyses<sup>51,52</sup>, one can conclude that both the analyses supposedly incorporate the presence of NP to reconcile the value of the parameter  $\sin 2\beta$  with the  $K - \bar{K}$  and the  $B_d - \bar{B}_d$  mixings.

However, in a recent analysis by Ahuja *et al.*<sup>53</sup>, attempts have been made to look at the above mentioned conclusions from a different perspective. In this context, one finds that the CKM matrix elements measured at tree level and those which can be constrained by unitarity can be considered to be essentially free from NP effects. Similarly, the ratio  $\Delta m_d/\Delta m_s$  is also considered to be largely free from the effects of NP<sup>25</sup>. Also, regarding the angle  $\alpha$  of the unitarity triangle, for the case of its prediction through the  $B \rightarrow \rho\rho$  decay the effects of the penguin diagrams are considered to be relatively small<sup>25,54–57</sup>. The implications of these NP free CKM parameters have been examined<sup>53</sup> on the parameters  $\sin 2\beta$ ,  $V_{td}$ ,  $\epsilon_K$ , etc.. Employing the PDG representation of the CKM mixing matrix and incorporating the constraints of unitarity, for  $c_{13} \cong 0.9999$  implying  $V_{us} \cong s_{12}$  and  $V_{cb} \cong s_{23}$  up to third place of decimal, the authors consider  $V_{us} \cong V_{cd}$ ,  $V_{ts} \cong V_{cb}$  and  $V_{tb} \cong 1$ .

It may be noted that the CP asymmetry parameter  $\sin 2\beta$  is generally determined from the asymmetry measurement of the  $B_d^0 \rightarrow \psi K_s$  decay. However, as already mentioned, the analyses by Refs. 51 and 52 point towards the possibility of NP due to a new phase in the  $B_o - \bar{B}_o$  mixing. It may also be noted here that information about  $\beta$  can also be obtained from a measurement of element  $V_{td}$  from  $B_o - \bar{B}_o$  mixing, however this cannot be considered free from NP as its evaluation involves loop processes. Also, in near future, the possibility of measurement of the third row elements of the CKM matrix through the tree level decays is not very promising. Therefore, the analysis by Ref. 53 attempts to determine  $\sin 2\beta$  from unitarity and quantities free from NP effects, essential details of this have been summarized here.

Using the  $db$  unitarity triangle, the authors make use of the law of sines to avoid the involvement of  $V_{td}$  in the evaluation of angle  $\beta$  through Eq. (25), re-expressed as

$$\beta = \sin^{-1} \left( \frac{V_{ud}V_{ub}^*}{V_{cd}V_{cb}^* \sin \alpha} \right). \quad (36)$$

Using the PDG 2010 values<sup>25</sup> of the angle  $\alpha$  and the CKM matrix elements, the authors obtain

$$\beta = (23.94 \pm 2.95)^\circ, \quad (37)$$

implying

$$\sin 2\beta = 0.742 \pm 0.103. \quad (38)$$

This value of  $\sin 2\beta$  seems to be free from contamination of NP and is inclusive of its recent experimental range  $0.673 \pm 0.023$ <sup>25</sup>. Further, making use of the closure property of the angles of the unitarity triangle and using the angle  $\alpha$  and the above mentioned value of  $\beta$ , the angle  $\delta$  has been obtained as

$$\delta = 67.1^\circ \pm 5.3^\circ. \quad (39)$$

Again, one finds that this unitarity based value of  $\delta$  is unaffected by NP in the  $B - \bar{B}$  mixing as well as is compatible with the directly measured value,  $(73_{-25}^{+22})^\circ$ , in  $B^\pm \rightarrow DK^\pm$  decays<sup>25</sup> and by many other global analyses<sup>26–28</sup>.

The CKM matrix element  $V_{td}$ , calculated usually from  $B_o - \bar{B}_o$  mixing which is a loop dominated process and therefore not considered to be NP free has also been obtained free from NP effects. Using the PDG values of angle  $\alpha$ , the CKM matrix elements, the above determined value of angle  $\delta \sim \gamma$  and considering  $V_{tb} \cong 1$ , one gets

$$V_{td} = (8.69 \pm 0.61) \times 10^{-3}. \quad (40)$$

It may be noted that this prediction of  $V_{td}$  is based on unitarity and is through CKM parameters essentially free from NP effects.

After having checked that the parameter  $\sin 2\beta$  and CKM matrix element  $V_{td}$  do not require any additional NP inputs, the authors<sup>53</sup> have examined the calculation of  $\epsilon_K$ , defining CP violation in the  $K - \bar{K}$  system. To this end, the recent expression of the CP violating parameter  $\epsilon_K$  has been used which modified by incorporating the factor  $\kappa_\epsilon$  now becomes

$$|\epsilon_K| = \kappa_\epsilon \frac{G_F^2 F_K^2 m_K m_W^2}{6\sqrt{2}\pi^2 \Delta m_k} B_K \text{Im}\lambda_t [\text{Re}\lambda_c(\eta_1 S_0(x_c) - \eta_3 S_0(x_c, x_t)) - \text{Re}\lambda_t \eta_2 S_0(x_t)], \quad (41)$$

where  $\eta_1, \eta_2, \eta_3$  are the perturbative QCD corrections,  $S_0(x_i)$  are Inami-Lim functions,  $x_i = m_i^2/M_W^2$ , and  $\lambda_i = V_{id}V_{is}^*$ ,  $i = c, t$ . In terms of the mixing angles and the phase  $\delta$ , the quantities  $\text{Im}\lambda_t$ ,  $\text{Re}\lambda_t$  and  $\text{Re}\lambda_c$  can be expressed as

$$\text{Im}\lambda_t = s_{23}s_{13}c_{23}\sin\delta, \quad (42)$$

$$\text{Re}\lambda_t = s_{23}s_{13}c_{23}(c_{12}^2 - s_{12}^2)\cos\delta - s_{12}c_{12}(s_{23}^2 - c_{23}^2s_{13}^2), \quad (43)$$

$$\text{Re}\lambda_c = s_{23}s_{13}c_{23}(s_{12}^2 - c_{12}^2)\cos\delta - s_{12}c_{12}(c_{23}^2 - s_{23}^2s_{13}^2). \quad (44)$$

The implications of  $\epsilon_K$  on the CP violating phase  $\delta$  for both the exclusive and inclusive values of CKM matrix element  $V_{ub}$  have been investigated. In Figs. 3 and 4, the plots of phase  $\delta$  versus the parameter  $\epsilon_K$  have been presented. From the graphs, one finds different constraints on phase  $\delta$  for the exclusive and inclusive values of  $V_{ub}$ , e.g.,

$$\text{for exclusive value of } V_{ub}, \quad \delta = (52 - 147)^\circ, \quad (45)$$

$$\text{for inclusive value of } V_{ub}, \quad \delta = (44 - 72)^\circ, \quad (132 - 155)^\circ.$$

It is interesting to note that the above mentioned ranges of the CP violating phase  $\delta$  come out to be compatible with the experimentally determined range of angle  $\delta$ . One can therefore conclude that the recent improvements in the lattice calculations of hadronic parameters, as well as precision measurements of CKM parameters do not seem to provide any significant clues regarding the possibility of existence of NP, as far as compatibility of the CP violating phase  $\delta$  is concerned. If at all effects of NP are present, they are at only a few percent level.

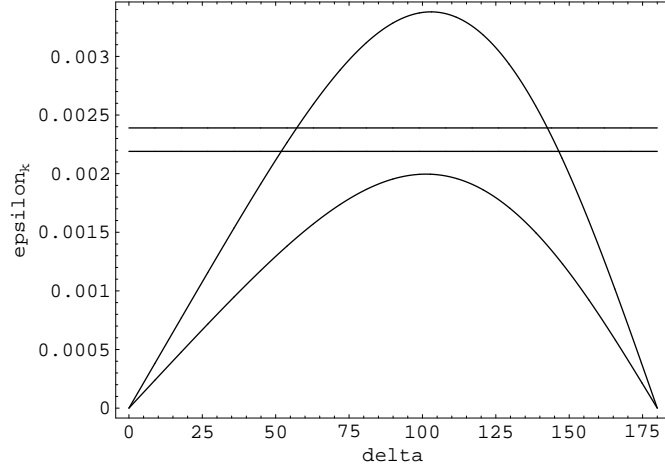


Fig. 3. CP violating phase  $\delta$  versus  $\epsilon_k$  using exclusive value of  $V_{ub}$

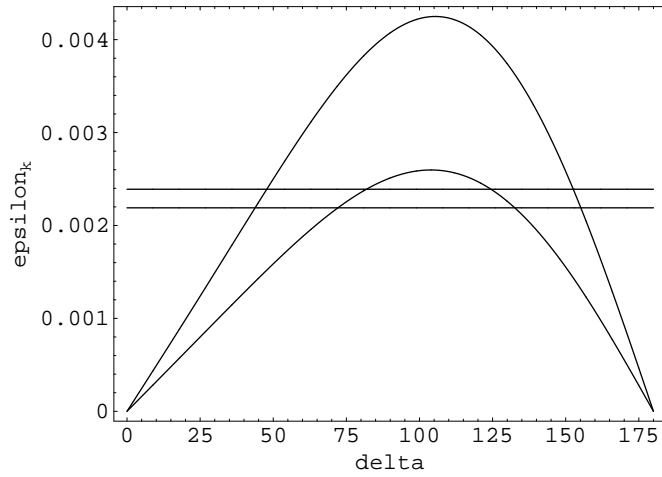


Fig. 4. CP violating phase  $\delta$  versus  $\epsilon_k$  using inclusive value of  $V_{ub}$

#### 4. Unitarity and unitarity triangles in the leptonic sector

At present, one of the key issues in the context of neutrino oscillation phenomenology is to explore the existence of CP violation in the leptonic sector. After having explored the implications of Jarlskog's rephasing invariant parameter  $J$ , unitarity and unitarity triangles, which facilitate the understanding of several features of CKM phenomenology, it becomes interesting to discuss similar attempts in the case



of phenomenology of the Pontecorvo-Maki-Nakagawa-Sakata (PMNS) matrix<sup>58–61</sup>. To this end, several attempts<sup>62–64</sup> have been made to explore the existence of the corresponding unitarity triangle in the leptonic sector. For example, Farzan and Smirnov<sup>62</sup> have explored the construction of leptonic unitarity triangle for finding possible clues to the existence of CP violation in the leptonic sector. In particular, considering the ‘ $e.\mu$ ’ triangle, for  $U_{e3}$  ( $\equiv s_{13}$ ) values in the range 0.09 – 0.22 they have examined the detailed implications of different values of Dirac-like CP violating phase in the leptonic sector  $\delta_l$  on the possible accuracy required in the measurement of various oscillation probabilities. Further, recently Bjorken *et al.*<sup>63</sup>, by considering a modified tri-bimaximal scenario, have not only presented a very useful parameterization of the PMNS matrix but have also proposed a unitarity triangle, referred to as ‘ $\nu_2.\nu_3$ ’, which could be leptonic analogue of the much talked about  $db$  triangle in the quark sector. Furthermore, by considering different values of  $U_{e3}$ , suggested by various theoretical models, in the parameterization of the PMNS matrix given by Bjorken *et al.*<sup>63</sup>, Ahuja and Gupta<sup>64</sup> have explored in detail the probability of finding a non zero value of  $J_l$ , the Jarlskog’s rephasing invariant parameter in the leptonic sector and the related Dirac-like CP violating phase  $\delta_l$ .

It may be noted that the analyses, mentioned above, were carried out before the recent T2K<sup>9</sup>, MINOS<sup>10</sup>, DAYA BAY<sup>11</sup> and RENO<sup>12</sup> observations regarding the mixing angle  $s_{13}$ , suggesting its not so ‘small’ value. These observations have given a big impetus to the sharpening of the implications of the neutrino oscillations, in particular the non zero value of angle  $s_{13}$  implies the possibility of CP violation in the leptonic sector. Recently, keeping in view these latest observations, Ahuja<sup>65</sup> has explored the possibility of existence of CP violation in the leptonic sector through the ‘ $\nu_1.\nu_3$ ’ leptonic unitarity triangle.

It may be mentioned that while the present manuscript was being prepared, we came across a very recent review article by Branco *et al.*<sup>66</sup>, wherein several topics on CP violation in the leptonic sector have been reviewed. However, in the present case, we have made an attempt to emphasize those points which have not been discussed in detail in their review<sup>66</sup>. In the sequel, we would like to present some of the details of the works by Ahuja *et al.*, Refs. 64 and 65. In the absence of information regarding mixing angle  $s_{13}$ , Ref. 64 have made use of the parameterization of the PMNS matrix in the modified tribimaximal scenario and carried out the analysis, whereas Ref. 65 incorporates the latest information regarding  $s_{13}$  to explore the likelihood of CP violation in the leptonic sector.

Before presenting the details of these analyses, we first begin with the neutrino mixing phenomenon, often expressed in terms of a  $3 \times 3$  neutrino mixing Pontecorvo-Maki-Nakagawa-Sakata (PMNS) matrix<sup>58–61</sup> given by

$$\begin{pmatrix} \nu_e \\ \nu_\mu \\ \nu_\tau \end{pmatrix} = \begin{pmatrix} U_{e1} & U_{e2} & U_{e3} \\ U_{\mu 1} & U_{\mu 2} & U_{\mu 3} \\ U_{\tau 1} & U_{\tau 2} & U_{\tau 3} \end{pmatrix} \begin{pmatrix} \nu_1 \\ \nu_2 \\ \nu_3 \end{pmatrix}, \quad (46)$$

where  $\nu_e, \nu_\mu, \nu_\tau$  are the flavor eigenstates and  $\nu_1, \nu_2, \nu_3$  are the mass eigenstates.

Following Particle Data Group (PDG)<sup>25</sup> representation, wherein the unitarity is built-in, involving three angles  $\theta_{12}$ ,  $\theta_{23}$ ,  $\theta_{13}$  and the Dirac-like CP violating phase  $\delta_l$  as well as the two Majorana phases  $\alpha_1$ ,  $\alpha_2$ , the PMNS matrix  $U$  can be written as

$$U = \begin{pmatrix} c_{12}c_{13} & s_{12}c_{13} & s_{13}e^{-i\delta_l} \\ -s_{12}c_{23} - c_{12}s_{23}s_{13}e^{i\delta_l} & c_{12}c_{23} - s_{12}s_{23}s_{13}e^{i\delta_l} & s_{23}c_{13} \\ s_{12}s_{23} - c_{12}c_{23}s_{13}e^{i\delta_l} & -c_{12}s_{23} - s_{12}c_{23}s_{13}e^{i\delta_l} & c_{23}c_{13} \end{pmatrix} \begin{pmatrix} e^{i\alpha_1/2} & 0 & 0 \\ 0 & e^{i\alpha_2/2} & 0 \\ 0 & 0 & 1 \end{pmatrix}, \quad (47)$$

with  $c_{ij} = \cos \theta_{ij}$  and  $s_{ij} = \sin \theta_{ij}$  for  $i, j = 1, 2, 3$ . The Majorana phases  $\alpha_1$  and  $\alpha_2$  do not play any role in neutrino oscillations and henceforth would be dropped from the discussion. Further, in this representation,  $|U_{e3}| \equiv s_{13}$ , therefore, while discussing the magnitude of the PMNS matrix elements,  $U_{e3}$  and  $s_{13}$  would be used interchangeably.

Unitarity of the PMNS matrix implies nine relations, three in terms of normalization conditions, the other six can be defined as

$$\sum_{i=1,2,3} U_{\alpha i} U_{\beta i}^* = \delta_{\alpha\beta} \quad (\alpha \neq \beta), \quad (48)$$

$$\sum_{\alpha=e,\mu,\tau} U_{\alpha i} U_{\alpha j}^* = \delta_{ij} \quad (i \neq j), \quad (49)$$

where Latin indices run over the mass eigenstates (1, 2, 3) and Greek ones run over the flavor eigenstates ( $e, \mu, \tau$ ). These six non-diagonal relations can be expressed through six independent unitarity triangles in the complex plane, shown in Fig. 5 and can also be expressed as

$$e.\mu \quad U_{e1}U_{\mu 1}^* + U_{e2}U_{\mu 2}^* + U_{e3}U_{\mu 3}^* = 0, \quad (50)$$

$$e.\tau \quad U_{e1}U_{\tau 1}^* + U_{e2}U_{\tau 2}^* + U_{e3}U_{\tau 3}^* = 0, \quad (51)$$

$$\mu.\tau \quad U_{\mu 1}U_{\tau 1}^* + U_{\mu 2}U_{\tau 2}^* + U_{\mu 3}U_{\tau 3}^* = 0, \quad (52)$$

$$\nu 1.\nu 2 \quad U_{e1}U_{e 2}^* + U_{\mu 1}U_{\mu 2}^* + U_{\tau 1}U_{\tau 2}^* = 0, \quad (53)$$

$$\nu 1.\nu 3 \quad U_{e1}U_{e 3}^* + U_{\mu 1}U_{\mu 3}^* + U_{\tau 1}U_{\tau 3}^* = 0, \quad (54)$$

$$\nu 2.\nu 3 \quad U_{e2}U_{e 3}^* + U_{\mu 2}U_{\mu 3}^* + U_{\tau 2}U_{\tau 3}^* = 0, \quad (55)$$

where the letters ‘ $e.\mu$ ’ etc. represent the corresponding unitarity triangle.

Similar to the case of quarks, all the six unitarity triangles shown in Fig. 5 are equal in area and can be used to evaluate the CP violating parameters in the leptonic sector namely the Jarlskog’s rephasing invariant parameter in the leptonic sector  $J_l$  and the related Dirac-like CP violating phase  $\delta_l$ . The parameter  $J_l$  is related to area of any of the unitarity triangle as

$$|J_l| = 2 \times \text{Area of any of the unitarity triangle} \quad (56)$$

and yields information about the phase  $\delta_l$  through the relation

$$J_l = s_{12}s_{23}s_{13}c_{12}c_{23}c_{13}^2 \sin \delta_l. \quad (57)$$

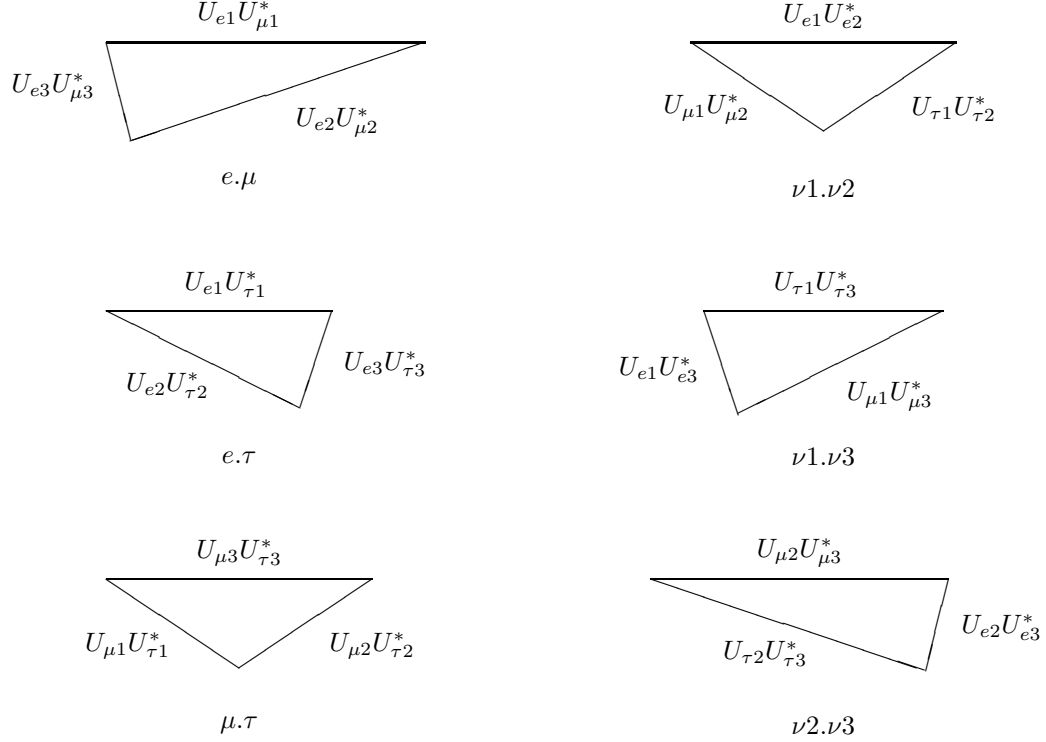


Fig. 5. The six unitarity triangles in the leptonic sector.

Similar to Eq. (21) for the case of quarks,  $J_l$  can also be defined through the relation

$$\text{Im} (U_{\alpha i} U_{\beta j} U_{\alpha j}^* U_{\beta i}^*) = J_l \sum_{\gamma} \varepsilon_{\alpha \beta \gamma} \sum_k \varepsilon_{ijk} , \quad (58)$$

where the Latin subscripts  $(i, j, k)$  and the Greek subscripts  $(\alpha, \beta, \gamma)$  run respectively over  $(1, 2, 3)$  and  $(e, \mu, \tau)$ . It may be noted that  $J_l$  can also be expressed in terms of the moduli of four independent matrix elements of  $U$  as follows

$$J_l^2 = |U_{\alpha i}|^2 |U_{\beta j}|^2 |U_{\alpha j}|^2 |U_{\beta i}|^2 - \frac{1}{4} \left( 1 + |U_{\alpha i}|^2 |U_{\beta j}|^2 + |U_{\alpha j}|^2 |U_{\beta i}|^2 - |U_{\alpha i}|^2 - |U_{\beta j}|^2 - |U_{\alpha j}|^2 - |U_{\beta i}|^2 \right)^2 , \quad (59)$$

in which  $\alpha \neq \beta$  running over  $(e, \mu, \tau)$  and  $i \neq j$  running over  $(1, 2, 3)$ . Therefore, the information about leptonic CP violation can in principle be extracted from the measured moduli of the flavor mixing matrix elements.

#### 4.1. *Leptonic unitarity triangle in the modified tri-bimaximal scenario*

As mentioned earlier, a parameterization of the PMNS matrix in the modified tri-bimaximal scenario has been formulated by Bjorken *et al.*<sup>63</sup>. Making use of this modified tri-bimaximal scenario, Ref. 64 have made an attempt to explore the possibility of the construction of the leptonic unitarity triangle as well as the existence of CP violation in the leptonic sector. To facilitate the discussion as well as understanding of this scenario, we first reproduce here some of the essential details of Ref. 63.

The tri-bimaximal scenario<sup>67–73</sup> and its further generalization can be understood by beginning with the PDG representation of the PMNS matrix. The representation, in terms of the three rotations and Dirac-like CP violating phase  $\delta_l$ , can be expressed as

$$U = \begin{pmatrix} 1 & 0 & 0 \\ 0 & \cos\theta_{23} & \sin\theta_{23} \\ 0 & -\sin\theta_{23} & \cos\theta_{23} \end{pmatrix} \begin{pmatrix} \cos\theta_{13} & 0 & \sin\theta_{13}e^{i\delta_l} \\ 0 & 1 & 0 \\ -\sin\theta_{13}e^{-i\delta_l} & 0 & \cos\theta_{13} \end{pmatrix} \begin{pmatrix} \cos\theta_{12} & \sin\theta_{12} & 0 \\ -\sin\theta_{12} & \cos\theta_{12} & 0 \\ 0 & 0 & 1 \end{pmatrix}. \quad (60)$$

The atmospheric neutrino experiments<sup>74</sup> along with the data from K2K<sup>75</sup> and CHOOZ<sup>76</sup> experiments give the following values of  $U_{e3}$  and  $U_{\mu3}$  at  $1\sigma$  C.L.

$$|U_{e3}|^2 \lesssim 0.013, \quad |U_{\mu3}|^2 = 0.50 \pm 0.11. \quad (61)$$

Using unitarity, one obtains

$$|U_{e3}|^2 \approx 0, \quad |U_{\mu3}| \approx |U_{\tau3}| \approx \frac{1}{\sqrt{2}}. \quad (62)$$

The state  $\nu_3$  in terms of the flavor eigenstates  $\nu_\mu$  and  $\nu_\tau$ , to a good approximation, can be written as

$$\nu_3 = \frac{1}{\sqrt{2}}(\nu_\mu - \nu_\tau). \quad (63)$$

This approximation along with unitarity yields the approximate  $\nu_\mu - \nu_\tau$  symmetry, expressed as

$$|U_{\mu2}| \approx |U_{\tau2}|, \quad |U_{\mu1}| \approx |U_{\tau1}|. \quad (64)$$

The above equation, along with the solar neutrino data at  $1\sigma$  C.L., e.g.,

$$|U_{e2}|^2 = 0.31 \pm 0.04 \quad (65)$$

implies

$$|U_{e2}| \approx |U_{\mu2}| \approx |U_{\tau2}| \approx \frac{1}{\sqrt{3}}. \quad (66)$$

Without the loss of generality, with appropriate phases, the state  $\nu_2$  can be written as

$$\nu_2 = \frac{1}{\sqrt{3}}(\nu_e + \nu_\mu + \nu_\tau). \quad (67)$$

Again using unitarity of the PMNS matrix and the Eqs. (63) and (67), the state  $\nu_1$  is given by

$$\nu_1 = \frac{1}{\sqrt{6}}(2\nu_e - \nu_\tau - \nu_\mu). \quad (68)$$

Eqs. (63), (67) and (68) together define the tri-bimaximal mixing texture<sup>67–73</sup>, depicted as

$$U_{tbm} = \begin{pmatrix} \sqrt{\frac{2}{3}} & \frac{1}{\sqrt{3}} & 0 \\ -\frac{1}{\sqrt{6}} & \frac{1}{\sqrt{3}} & -\frac{1}{\sqrt{2}} \\ -\frac{1}{\sqrt{6}} & \frac{1}{\sqrt{3}} & \frac{1}{\sqrt{2}} \end{pmatrix}. \quad (69)$$

The current situation for neutrino physics and the PMNS matrix appears analogous to the earlier situation for  $B$  physics and the CKM matrix, in which the leading approximation to the matrix was established experimentally, long before its smallest elements were determined. In that case, the Wolfenstein parameterization<sup>30</sup> had become widely adopted. Motivated by the phenomenological success of tri-bimaximal mixing and considering it as a starting point, Bjorken *et al.*<sup>63</sup> have proposed a simple approximation for the PMNS mixing in the leptonic sector. The proposal can be expressed as

$$U \simeq \begin{pmatrix} \frac{2}{\sqrt{6}} & \frac{1}{\sqrt{3}} & 0 \\ -\frac{1}{\sqrt{6}} & \frac{1}{\sqrt{3}} & \frac{1}{\sqrt{2}} \\ -\frac{1}{\sqrt{6}} & \frac{1}{\sqrt{3}} & -\frac{1}{\sqrt{2}} \end{pmatrix} \begin{pmatrix} C & 0 & \sqrt{\frac{3}{2}}U_{e3} \\ 0 & 1 & 0 \\ -\sqrt{\frac{3}{2}}U_{e3}^* & 0 & C \end{pmatrix} \quad (70)$$

$$= \begin{pmatrix} \frac{2}{\sqrt{6}}C & \frac{1}{\sqrt{3}} & U_{e3} \\ -\frac{1}{\sqrt{6}}C - \frac{\sqrt{3}}{2}U_{e3}^* & \frac{1}{\sqrt{3}} & \frac{1}{\sqrt{2}}C - \frac{1}{2}U_{e3} \\ -\frac{1}{\sqrt{6}}C + \frac{\sqrt{3}}{2}U_{e3}^* & \frac{1}{\sqrt{3}} & -\frac{1}{\sqrt{2}}C - \frac{1}{2}U_{e3} \end{pmatrix}, \quad (71)$$

where

$$C = \sqrt{1 - \frac{3}{2}|U_{e3}|^2} \simeq 1. \quad (72)$$

Dropping terms of order  $|U_{e3}|^2$  Eq. (71) can be approximated as

$$U \simeq \begin{pmatrix} \frac{2}{\sqrt{6}} & \frac{1}{\sqrt{3}} & U_{e3} \\ -\frac{1}{\sqrt{6}} - \frac{\sqrt{3}}{2}U_{e3}^* & \frac{1}{\sqrt{3}} & \frac{1}{\sqrt{2}} - \frac{1}{2}U_{e3} \\ -\frac{1}{\sqrt{6}} + \frac{\sqrt{3}}{2}U_{e3}^* & \frac{1}{\sqrt{3}} & -\frac{1}{\sqrt{2}} - \frac{1}{2}U_{e3} \end{pmatrix}. \quad (73)$$

This parameterization is important in the sense that it does not involve the three mixing angles, instead it enables one to directly deal with the complex parameter  $U_{e3}$  of the mixing matrix. Therefore, in this parameterization of the PMNS matrix, the matrix can easily be constructed in case one has knowledge regarding the value of the matrix element  $U_{e3}$ .

Coming to the analysis by Ref. 64, since it was carried out before the recent announcements regarding the measurement of  $U_{e3}$ , therefore for the purpose of construction of PMNS matrix a few representative values of  $U_{e3}$  which broadly agree with those considered by Farzan and Smirnov<sup>62</sup> were chosen. In this regard, theoretical models<sup>77</sup> suggest  $U_{e3}$  taking values around 0.05, 0.10 and 0.15 which can be used for the construction of the magnitudes of the PMNS matrix elements. It may be added that the present limits on  $U_{e3}$  are well within its range considered here. To have realistic estimates of the elements of the PMNS matrix, following Farzan and Smirnov<sup>62</sup>, modest errors to the mixing elements considered by Bjorken *et al.*<sup>63</sup> can be attached. To this end, Ref. 64 associate 5% errors with the elements  $U_{e1}$ ,  $U_{e2}$ ,  $U_{\mu 2}$  and  $U_{\tau 2}$  of the matrix given in Eq. (73) and for  $U_{e3}$  values 0.05, 0.10 and 0.15 have been taken and considered 10% variations to these. The matrices corresponding to  $U_{e3}$  values  $0.05 \pm 0.005$ ,  $0.10 \pm 0.01$  and  $0.15 \pm 0.015$  are respectively as follows

$$U = \begin{pmatrix} 0.8165 \pm 0.0408 & 0.5774 \pm 0.0289 & 0.05 \pm 0.005 \\ 0.4516 \pm 0.0022 & 0.5774 \pm 0.0289 & 0.6821 \pm 0.0034 \\ 0.3649 \pm 0.0018 & 0.5774 \pm 0.0289 & 0.7321 \pm 0.0037 \end{pmatrix}, \quad (74)$$

$$U = \begin{pmatrix} 0.8165 \pm 0.0408 & 0.5774 \pm 0.0289 & 0.1 \pm 0.01 \\ 0.4948 \pm 0.0049 & 0.5774 \pm 0.0289 & 0.6571 \pm 0.0066 \\ 0.3216 \pm 0.0032 & 0.5774 \pm 0.0289 & 0.7571 \pm 0.0076 \end{pmatrix}, \quad (75)$$

$$U = \begin{pmatrix} 0.8165 \pm 0.0408 & 0.5774 \pm 0.0289 & 0.15 \pm 0.015 \\ 0.5382 \pm 0.0081 & 0.5774 \pm 0.0289 & 0.6321 \pm 0.0095 \\ 0.2783 \pm 0.0042 & 0.5774 \pm 0.0289 & 0.7821 \pm 0.0117 \end{pmatrix}, \quad (76)$$

wherein the magnitudes of the elements have been given, as is usual.

Construction of the  $db$  unitarity triangle in the quark sector immediately provides a clue for exploring the probability of non zero Dirac-like CP violating phase  $\delta_l$  in the leptonic sector, even when leptonic mixing matrix is approximately known. Out of the six triangles defined by Eqs. (50)-(55), Bjorken *et al.*<sup>63</sup> have considered the  $\nu_2\nu_3$  triangle, depicted by Eq. (55), which is the leptonic analogue of the  $db$  triangle of the quark sector. This triangle can immediately be constructed in the scenario considered by Bjorken *et al.*<sup>63</sup> in case one uses some values of  $U_{e3}$  to construct the PMNS matrix.

To this end, considering the elements of the above matrices appearing in the  $\nu_2\nu_3$  triangle, given in Eq. (55), to be Gaussian one can obtain the corresponding respective values of the Jarlskog's rephasing invariant parameter in the leptonic sector  $J_l$  as

$$J_l = 0.009 \pm 0.003, \quad (77)$$

$$J_l = 0.017 \pm 0.006, \quad (78)$$

$$J_l = 0.023 \pm 0.009. \quad (79)$$

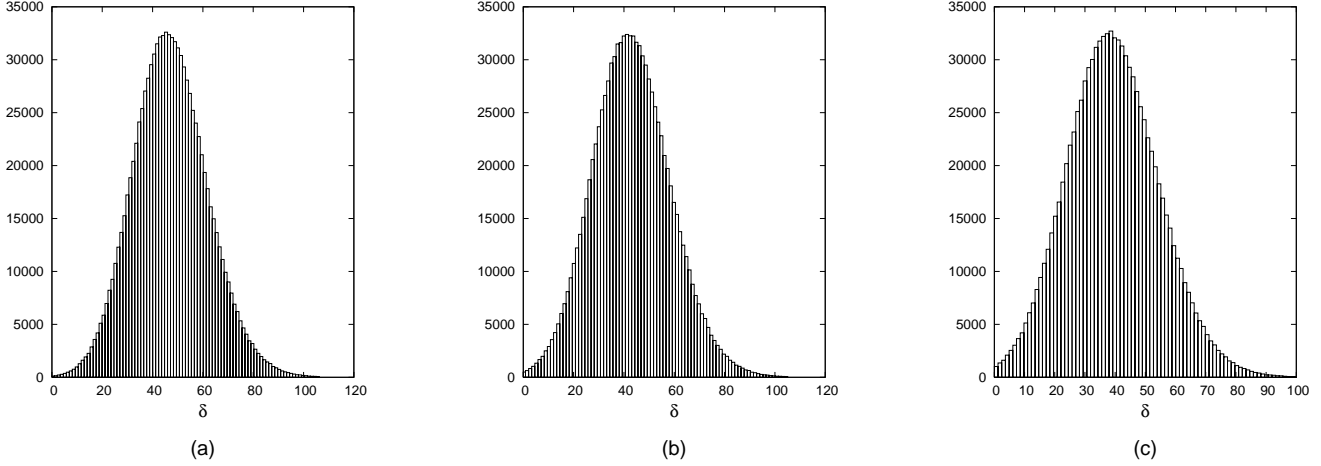


Fig. 6. Histogram of  $\delta_l$  plotted by considering ' $\nu_2, \nu_3$ ' triangle in the modified tri-bimaximal scenario for (a)  $U_{e3} = 0.05 \pm 0.005$  (b)  $U_{e3} = 0.1 \pm 0.01$  (c)  $U_{e3} = 0.15 \pm 0.015$ .

Using these values of  $J_l$  and by considering various elements of Eq. (57) to be Gaussian, one can find the corresponding distributions of  $\delta_l$ . Using these distributions, shown in Fig. 6, the  $\delta_l$  values corresponding to  $U_{e3}$  values  $0.05 \pm 0.005$ ,  $0.10 \pm 0.01$  and  $0.15 \pm 0.015$  are respectively as follows

$$\delta_l \simeq 47^\circ \pm 15^\circ, \quad (80)$$

$$\delta_l \simeq 43^\circ \pm 15^\circ, \quad (81)$$

$$\delta_l \simeq 39^\circ \pm 15^\circ. \quad (82)$$

It is interesting to note that the Dirac-like CP violating phase  $\delta_l$  comes out to be around  $43^\circ$  and is not much sensitive to  $U_{e3}$  in the range  $0.05 - 0.15$ . Further, the above calculated values of  $\delta_l$ , indicating a  $2.5\sigma$  deviation from  $0^\circ$ , in the modified tri-bimaximal scenario for different values of  $U_{e3}$ , are in line with the suggestion by several authors<sup>78–80</sup>, about the expected CP violation in the leptonic sector. Further, it is interesting to note that this analysis carried out purely on phenomenological inputs is very much in agreement with several analyses based on expected outputs from different experimental scenarios<sup>62,78,81–83</sup>.

#### 4.2. Leptonic CP violation after the measurement of mixing angle

$s_{13}$

As mentioned earlier, the recent T2K<sup>9</sup>, MINOS<sup>10</sup>, DAYA BAY<sup>11</sup> and RENO<sup>12</sup> observations regarding the mixing angle  $s_{13}$  immediately provide a clue for exploring the possibility of existence of CP violation in the leptonic sector. In the

context of neutrino oscillation phenomenology, the last few years have seen impressive advances in fixing the neutrino mass and mixing parameters through solar<sup>84–90</sup>, atmospheric<sup>74</sup>, reactor (CHOOZ<sup>76</sup>, KamLAND<sup>91</sup>) and accelerator (K2K<sup>75</sup>, MINOS<sup>10,92</sup>) neutrino experiments. Adopting the three neutrino framework, several authors<sup>91,93–95</sup> have presented updated information regarding these parameters obtained by carrying out detailed global analyses. In particular, incorporating the above mentioned developments regarding the angle  $s_{13}$ , Fogli *et al.*<sup>95</sup> have carried out a global three neutrino oscillation analysis, yielding

$$\Delta m_{21}^2 = 7.58_{-0.26}^{+0.22} \times 10^{-5} \text{ eV}^2, \quad |\Delta m_{31}^2| = 2.35_{-0.21}^{+0.12} \times 10^{-3} \text{ eV}^2, \quad (83)$$

$$\sin^2 \theta_{12} = 0.312_{-0.016}^{+0.017}, \quad \sin^2 \theta_{23} = 0.42_{-0.03}^{+0.08}, \quad \sin^2 \theta_{13} = 0.025 \pm 0.007. \quad (84)$$

In analogy with the quark mixing phenomenon, the above value of  $s_{13}$  suggests likelihood of CP violation in the leptonic sector. A comparison of the mixing angles in the leptonic sector with those in the quark sector point out that the CP violation could, in fact, be considerably large in this case. This possibility, in turn, can have deep phenomenological implications. As is well known, the two CP violating Majorana phases do not play any role in the case of neutrino oscillations, therefore any hint regarding the value of Dirac-like CP violating phase in the leptonic sector  $\delta_l$  will go a long way in the formulation of proposals on observation of CP violation in the Long BaseLine (LBL) experiments<sup>10,75,96</sup>. In the absence of any hints from the data regarding leptonic CP violation, keeping in mind the parallelism between the neutrino mixing and the quark mixing, an analysis of the quark mixing phenomena could provide some viable clues regarding this issue in the leptonic sector.

It may be noted that in the context of fermion mixing phenomena, the Pontecorvo-Maki-Nakagawa-Sakata (PMNS)<sup>58–61</sup> and the Cabibbo-Kobayashi-Maskawa (CKM)<sup>1,3</sup> matrices have similar parametric structure. Also, regarding the three mixing angles corresponding to the quark and leptonic sector, it is interesting to note that in both the cases the mixing angle  $s_{13}$  is smaller as compared to the other two. Taking note of these similarities of features, using the analogy of the quark mixing case Ref. 65 have made an attempt to find the possibility of the existence of CP violation in the leptonic sector. Parallel to the leptonic sector wherein only the three mixing angles or correspondingly the magnitudes of the three elements of the mixing matrix are known, the author has first considered a similar situation in the quark sector and examined whether one can deduce any viable information regarding the existence of CP violation in the quark mixing phenomena. Employing the Particle Data Group (PDG) representation<sup>25</sup> of the CKM matrix and making use of the fact the mixing angle  $s_{13}$  ( $\equiv V_{ub}$ ) is small in comparison to both  $s_{12}$  ( $\equiv V_{us}$ ) and  $s_{23}$  ( $\equiv V_{cb}$ ) the approximate magnitudes of the elements of the quark mixing matrix have been constructed, e.g.,

$$V_{\text{CKM}} = \begin{pmatrix} 0.97431 \pm 0.00021 & 0.2252 \pm 0.0009 & 0.00389 \pm 0.00044 \\ 0.2250 \pm 0.0009 & 0.97351 \pm 0.00021 & 0.0406 \pm 0.0013 \\ 0.00914 \pm 0.00029 & 0.0396 \pm 0.0013 & 0.999168 \pm 0.000053 \end{pmatrix}. \quad (85)$$



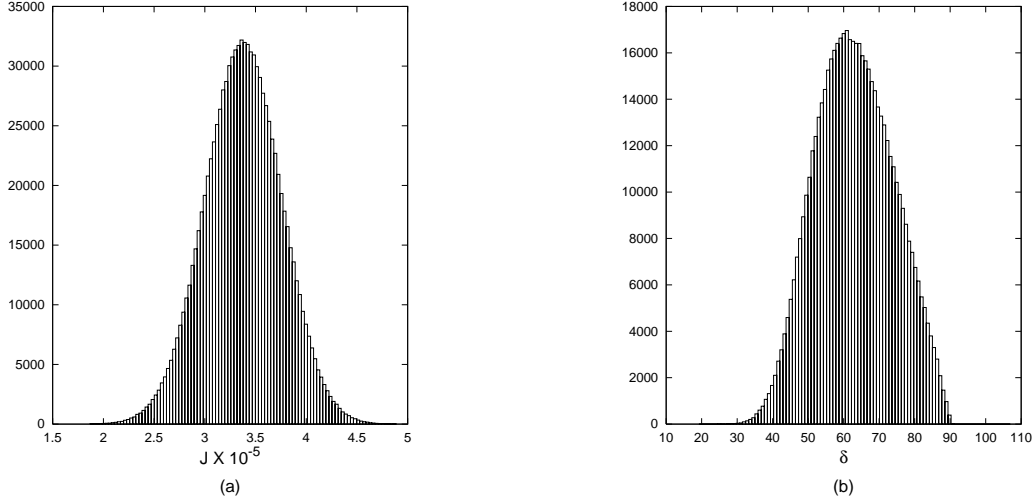


Fig. 7. Histogram of  $J$  and  $\delta$  for ‘ $db$ ’ triangle in the case of quarks

The above matrix is in fairly good agreement with the one given by PDG<sup>25</sup>.

Making use of the above matrix and the usually considered ‘ $db$ ’ unitarity triangle in the quark sector, the Jarlskog’s rephasing invariant parameter  $J$  has been constructed using the magnitudes of the elements of the CKM matrix. From the histogram of  $J$ , shown in Fig. 7(a), one finds

$$J = (3.36 \pm 0.38) \times 10^{-5}, \quad (86)$$

the corresponding histogram of  $\delta$ , shown in Fig. 7(b), yields

$$\delta = 62.60^\circ \pm 10.98^\circ. \quad (87)$$

Interestingly, the above mentioned  $J$  and  $\delta$  values are compatible with those given by PDG 2010<sup>25</sup>.

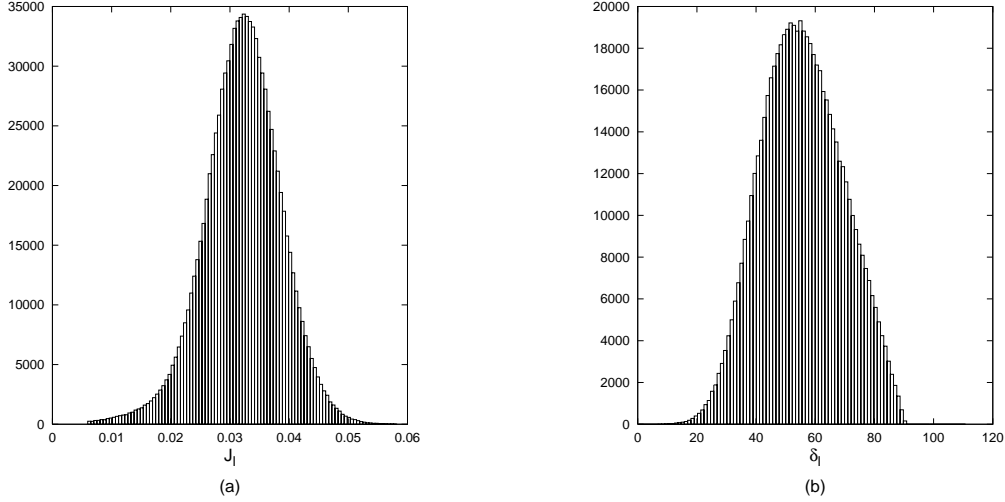
For the case of existence of CP violation in the leptonic sector, analogous to the construction of the CKM matrix presented in Eq. (85) and using the inputs given in Eq. (84), the approximate magnitudes of the elements of the PMNS matrix have been given as

$$U = \begin{pmatrix} 0.8190 \pm 0.0105 & 0.5516 \pm 0.0151 & 0.1581 \pm 0.0221 \\ 0.4254 \pm 0.0315 & 0.6317 \pm 0.0442 & 0.6399 \pm 0.0610 \\ 0.3620 \pm 0.0358 & 0.5376 \pm 0.0516 & 0.7520 \pm 0.0519 \end{pmatrix}. \quad (88)$$

It is interesting to note that this mixing matrix is compatible with those given by Refs. 97–100.

Analogous to the ‘ $db$ ’ triangle in the quark sector, considering the ‘ $\nu_1.\nu_3$ ’ unitarity triangle, expressed as

$$U_{e1}U_{e3}^* + U_{\mu1}U_{\mu3}^* + U_{\tau1}U_{\tau3}^* = 0, \quad (89)$$

Fig. 8. Histogram of  $J_l$  and  $\delta_l$  for ' $\nu_1, \nu_3$ ' triangle in the case of neutrinos

and using the matrix given in Eq. (88), the Jarlskog's rephasing invariant parameter in the leptonic sector  $J_l$  comes out to be

$$J_l = 0.0318 \pm 0.0065, \quad (90)$$

corresponding distribution plotted in Fig. 8(a). Also, the corresponding phase  $\delta_l$  from the histogram given in Fig. 8(b) is given by

$$\delta_l = 54.98^\circ \pm 13.81^\circ. \quad (91)$$

Interestingly, this likely value of the phase  $\delta_l$  has a good overlap with several phenomenological analyses<sup>62,64,78–83</sup>.

## 5. Fermion mass matrices

Coming to the issue of fermion masses, as is well known, along with fermion mixings, these provide a good opportunity to hunt for physics beyond the SM. In view of the relationship of fermion mixing phenomena with that of fermion mass matrices, understanding flavor physics essentially implies formulating fermion mass matrices. As mentioned earlier, the lack of a viable approach from the 'top down' perspective brings up the need for formulating fermion mass matrices from a 'bottom up' approach. In this context, initially several *ansätze*<sup>34,35,101,102</sup> were suggested for quark mass matrices. One of the successful *ansätze* incorporating the 'texture zero' approach was initiated by Fritzsch<sup>34,35</sup>. A particular texture structure is said to be texture  $n$  zero, if it has  $n$  number of non-trivial zeros, for example, if the sum of the number of diagonal zeros and half the number of the symmetrically placed off diagonal zeros is  $n$ .

Further, related to the Fritzsch *ansätze*, Branco *et al.*<sup>103</sup> have formulated mass matrices in the Nearest-Neighbour Interaction (NNI) basis. In particular, it has been shown that in the SM, starting with arbitrary Yukawa couplings, it is possible to find a weak basis where the quark mass matrices have the NNI form. It has also been shown that NNI textures for the quark mass matrices can be obtained through the introduction of an Abelian family symmetry. In the context of two Higgs doublet extension of the SM, the authors point out that the NNI form for the quark mass matrices can be obtained through the introduction of a  $Z_4$  symmetry. The authors also point out<sup>104</sup> that the NNI scheme, with small deviations from hermiticity, can correctly reproduce the experimentally allowed values for quark masses and CKM mixings. In the present review, our emphasis will be essentially on the texture zero formulation of mass matrices, related to the Fritzsch *ansätze*.

### 5.1. Quark mass matrices

The mass matrices, having their origin in the Higgs fermion couplings, are arbitrary in the SM, therefore the number of free parameters available with a general mass matrix is larger than the physical observables. For example, if no restrictions are imposed, there are 36 real free parameters in the two  $3 \times 3$  general complex mass matrices,  $M_U$  and  $M_D$ , which in the quark sector need to describe ten physical observables, i.e., six quark masses, three mixing angles and one CP violating phase. Similarly, in the leptonic sector, physical observables described by lepton mass matrices are six lepton masses, three mixing angles and one CP violating phase for Dirac neutrinos (two additional phases in case neutrinos are Majorana particles). Therefore, to develop viable phenomenological fermion mass matrices one has to limit the number of free parameters in the mass matrices.

In this context, it is well known that in the SM and its extensions wherein the right handed fields in the Lagrangian are SU(2) singlets, without loss of generality, the mass matrices can be considered as hermitian<sup>21</sup>. This immediately brings down the number of real free parameters from 36 to 18, which however, is still a large number compared to the number of observables. To this end, Weinberg<sup>105</sup> implicitly and Fritzsch<sup>34,35</sup> explicitly initiated the idea of texture specific mass matrices which on the one hand imparted predictability to mass matrices while on the other hand, it paved the way for the phenomenology of texture specific mass matrices. To define the various texture specific cases, we present the typical Fritzsch-like texture specific hermitian quark mass matrices, e.g.,

$$M_U = \begin{pmatrix} 0 & A_U & 0 \\ A_U^* & D_U & B_U \\ 0 & B_U^* & C_U \end{pmatrix}, \quad M_D = \begin{pmatrix} 0 & A_D & 0 \\ A_D^* & D_D & B_D \\ 0 & B_D^* & C_D \end{pmatrix}, \quad (92)$$

where  $M_U$  and  $M_D$  correspond to up and down mass matrices respectively. It may be noted that each of the above matrix is texture 2 zero type with  $A_i = |A_i|e^{i\alpha_i}$  and  $B_i = |B_i|e^{i\beta_i}$ , where  $i = U, D$ .

The texture 6 zero Fritzsch mass matrices can be obtained from the above mentioned matrices by taking both  $D_U$  and  $D_D$  to be zero, which reduces the matrices  $M_U$  and  $M_D$  each to texture 3 zero type. This Fritzsch *ansätze*<sup>34,35</sup> as well as some other *ansätze*<sup>101,102</sup> were ruled out because of the large value predicted by these for  $|V_{cb}|$  due to the high ‘t’ quark mass, in disagreement with the experimental data. Further, a few other texture 6 zero mass matrices were analyzed by Ramond, Roberts and Ross<sup>106</sup> revealing that these matrices were again ruled out because of the large predicted value of  $|V_{cb}|$ . They also explored the question of connection between phenomenological quark mass matrices considered at low energies and the possible mass patterns at the GUT scale and showed that the texture structure of mass matrices is maintained as we come down from GUT scale to  $M_Z$  scale. This important conclusion also leads to the fact that the texture zeros of fermion mass matrices can be considered as phenomenological zeros, thereby implying that at all energy scales the corresponding matrix elements are sufficiently suppressed in comparison with their neighboring counterparts. This, therefore, opens the possibility of considering lesser number of texture zeros.

Besides Ramond, Roberts and Ross<sup>106</sup>, several authors<sup>21,107–110</sup> have explored the texture 5 zero quark mass matrices. Fritzsch-like texture 5 zero matrices can be obtained by taking either  $D_U = 0$  and  $D_D \neq 0$  or  $D_U \neq 0$  and  $D_D = 0$  in Eq. (92), thereby giving rise to two possible cases of texture 5 zero mass matrices pertaining to either  $M_U$  or  $M_D$  being texture 3 zero type while the other being texture 2 zero type. These analyses reveal that texture 5 zero mass matrices although not ruled out unambiguously yet are not able to reproduce the entire range of data.

As an extension of texture 5 zero mass matrices, several authors<sup>21,111–115</sup> carried out the study of the implications of the Fritzsch-like texture 4 zero mass matrices. It may be noted that Fritzsch-like texture 4 zero mass matrices can be obtained by considering both  $M_U$  and  $M_D$ , with non zero  $D_i$  ( $i = U, D$ ) in Eq. (92), to be texture 2 zero type. Although from the above mentioned analyses one finds that texture 4 zero mass matrices were able to accommodate the quark mixing data quite well, however it may be noted that these analyses assumed ‘strong hierarchy’, to be defined later, of the elements of the mass matrices as well as explored only their limited domains. Further, in the absence of any precise information about CP violating phase  $\delta$ ,  $\sin 2\beta$  and related parameters, adequate attention was not given to the phases of the mass matrices.

Recent refinements in quark mixing data as well as information about the CP violating phase motivated several authors<sup>116–125</sup> to have a re-look at the compatibility of Fritzsch-like texture 4 zero mass matrices with the quark mixing data. In particular, using assumption of ‘strong hierarchy’ of the elements of the mass matrix defined as  $D_i < |B_i| < C_i$ , ( $i = U, D$ ), having its motivation in the hierarchy of the quark mixing angles several attempts<sup>116–121</sup> were made to predict the value of precisely known parameter  $\sin 2\beta$ . Unfortunately, the value of  $\sin 2\beta$  predicted by these analyses came out to be in quite disagreement with its precisely known value. A somewhat detailed and comprehensive analyses of texture 4 zero quark mass ma-

trices was carried out by Xing and Zhang<sup>123</sup>, in particular they attempted to find the parameter space available to the elements of mass matrices. Their analysis has also given valuable clues about the phase structure of the mass matrices, in particular for the strong hierarchy case they conclude that only one of the two phase parameters plays a dominant role. Subsequently, attempts have also been made by Verma *et al.*<sup>124,125</sup> to update and broaden the scope of the analysis carried out by Xing and Zhang<sup>123</sup>, in particular regarding the structural features of the mass matrices having implications for the value of parameter  $\sin 2\beta$  and the CP violating phase  $\delta$ . Further, recently, an exhaustive analysis of texture 6 and 5 zero non Fritzsch-like texture specific mass matrices have also been carried out<sup>126</sup> leading to some interesting conclusions. In view of the large parameter space available for fitting the data and very large number of possibilities of non Fritzsch-like texture 4 zero mass matrices, an exhaustive analysis in this regard is yet to be carried out. In the sequel, we briefly discuss the analyses of Refs. 124-126 regarding the texture specific mass matrices.

#### 5.1.1. Relationship of quark mass matrices and mixing matrix

Before detailing the analyses of texture specific mass matrices, for the sake of completeness, we present essentials regarding the relationship between the quark mass matrices and the CKM mixing matrix. In the SM, the quark mass terms for three generations of quarks can be expressed as

$$\bar{q}_{U_L} M_U q_{U_R} + \bar{q}_{D_L} M_D q_{D_R}, \quad (93)$$

where  $q_{U_{L(R)}}$  and  $q_{D_{L(R)}}$  are the left handed (right handed) quark fields for the up sector ( $u, c, t$ ) and down sector ( $d, s, b$ ) respectively.  $M_U$  and  $M_D$  are the mass matrices for the up and the down sector of quarks. In order to re-express above equation in terms of the physical quark fields, one can diagonalize the mass matrices by the following bi-unitary transformations

$$V_{U_L}^\dagger M_U V_{U_R} = M_U^{diag} \equiv \text{Diag}(m_u, m_c, m_t), \quad (94)$$

$$V_{D_L}^\dagger M_D V_{D_R} = M_D^{diag} \equiv \text{Diag}(m_d, m_s, m_b), \quad (95)$$

where  $M_{U,D}^{diag}$  are real and diagonal, while  $V_{U_L}$  and  $V_{U_R}$  etc. are complex unitary matrices. The quantities  $m_u, m_d$ , etc. denote the eigenvalues of the mass matrices, i.e. the physical quark masses. Using Eqs. (94) and (95), one can rewrite (93) as

$$\bar{q}_{U_L} V_{U_L} M_U^{diag} V_{U_R}^\dagger q_{U_R} + \bar{q}_{D_L} V_{D_L} M_D^{diag} V_{D_R}^\dagger q_{D_R}, \quad (96)$$

which can be re-expressed in terms of physical quark fields as

$$\bar{q}_{U_L}^{phys} M_U^{diag} q_{U_R}^{phys} + \bar{q}_{D_L}^{phys} M_D^{diag} q_{D_R}^{phys}, \quad (97)$$

where  $q_{U_L}^{phys} = V_{U_L}^\dagger q_{U_L}$  and  $q_{D_L}^{phys} = V_{D_L}^\dagger q_{D_L}$  and so on.

The mismatch of diagonalizations of up and down quark mass matrices leads to the quark mixing matrix  $V_{\text{CKM}}$ , referred to as the Cabibbo-Kobayashi-Maskawa (CKM)<sup>1,3</sup> matrix given as

$$V_{\text{CKM}} = V_{U_L}^\dagger V_{D_L}. \quad (98)$$

The CKM matrix expresses the relationship between quark mass eigenstates  $d, s, b$  which participate in the strong  $q-q$  and  $q-\bar{q}$  interactions and the interaction eigenstates or flavor eigenstates  $d', s', b'$  which participate in the weak interactions and are the linear combinations of mass eigenstates, e.g.,

$$\begin{pmatrix} d' \\ s' \\ b' \end{pmatrix} = \begin{pmatrix} V_{ud} & V_{us} & V_{ub} \\ V_{cd} & V_{cs} & V_{cb} \\ V_{td} & V_{ts} & V_{tb} \end{pmatrix} \begin{pmatrix} d \\ s \\ b \end{pmatrix}, \quad (99)$$

where  $V_{ud}$ ,  $V_{us}$ , etc. describe the transition of  $u$  to  $d$ ,  $u$  to  $s$  respectively, and so on.

In view of the relationship of the mixing matrix with the mass matrix, a knowledge of the CKM matrix elements would have important implications for the mass matrices. The most commonly used parameterization of the quark mixing matrix, the standard parameterization given by Particle Data Group (PDG)<sup>25</sup>, has already been presented in Eq. (9). Keeping in mind the ever increasing precision in the measurement of CKM phenomenological parameters, it is desirable to keep updating the analyses of the mass matrices for their compatibility with the mixing data.

### 5.1.2. Texture 6 zero quark mass matrices

To begin with, we first consider texture 6 zero Fritzsch quark mass matrices given by

$$M_U = \begin{pmatrix} 0 & A_U & 0 \\ A_U^* & 0 & B_U \\ 0 & B_U^* & C_U \end{pmatrix}, \quad M_D = \begin{pmatrix} 0 & A_D & 0 \\ A_D^* & 0 & B_D \\ 0 & B_D^* & C_D \end{pmatrix}, \quad (100)$$

where  $M_U$  and  $M_D$  correspond to up and down mass matrices respectively. The non Fritzsch-like mass matrices differ from the above mentioned Fritzsch-like mass matrices in regard to the position of ‘zeros’ in the structure of the mass matrices. One can get non Fritzsch-like mass matrices by shifting the position of  $C_i$  ( $i = U, D$ ) on the diagonal as well as by shifting the position of zeros among the non diagonal elements. For example, a non Fritzsch-like texture 3 zero matrix is obtained if (1,1) element is non zero, the other diagonal elements are zero leaving the non diagonal elements unchanged, with (1,1) referring to the element corresponding to the first row and first column of the matrix. Similarly, by considering (1,2) and (2,1) element to be zero and (1,3) and (3,1) element to be non zero, without disturbing other elements, we again get texture 3 zero non Fritzsch-like mass matrix. This results into a total of 20 different possible texture patterns, out of which 8 are easily ruled out by imposing the following conditions

$$\text{Trace } M_{U,D} \neq 0 \quad \text{and} \quad \text{Det } M_{U,D} \neq 0, \quad (101)$$

Table 1. Twelve possibilities of texture 3 zero hermitian mass matrices categorized into two classes I and II.

	Class I	Class II
a	$\begin{pmatrix} 0 & Ae^{i\alpha} & 0 \\ Ae^{-i\alpha} & 0 & Be^{i\beta} \\ 0 & Be^{-i\beta} & C \end{pmatrix}$	$\begin{pmatrix} 0 & Ae^{i\alpha} & 0 \\ Ae^{-i\alpha} & D & 0 \\ 0 & 0 & C \end{pmatrix}$
b	$\begin{pmatrix} 0 & 0 & Ae^{i\alpha} \\ 0 & C & Be^{i\beta} \\ Ae^{-i\alpha} & B^{-i\beta} & 0 \end{pmatrix}$	$\begin{pmatrix} 0 & 0 & Ae^{i\alpha} \\ 0 & C & 0 \\ Ae^{-i\alpha} & 0 & D \end{pmatrix}$
c	$\begin{pmatrix} 0 & Ae^{i\alpha} & Be^{i\beta} \\ Ae^{-i\alpha} & 0 & 0 \\ Be^{-i\beta} & 0 & C \end{pmatrix}$	$\begin{pmatrix} D & Ae^{i\alpha} & 0 \\ Ae^{-i\alpha} & 0 & 0 \\ 0 & 0 & C \end{pmatrix}$
d	$\begin{pmatrix} C & Be^{i\beta} & 0 \\ Be^{-i\beta} & 0 & Ae^{i\alpha} \\ 0 & Ae^{-i\alpha} & 0 \end{pmatrix}$	$\begin{pmatrix} C & 0 & 0 \\ 0 & D & Ae^{i\alpha} \\ 0 & Ae^{-i\alpha} & 0 \end{pmatrix}$
e	$\begin{pmatrix} 0 & Be^{i\beta} & Ae^{i\alpha} \\ Be^{-i\beta} & C & 0 \\ Ae^{-i\alpha} & 0 & 0 \end{pmatrix}$	$\begin{pmatrix} D & 0 & Ae^{i\alpha} \\ 0 & C & 0 \\ Ae^{-i\alpha} & 0 & 0 \end{pmatrix}$
f	$\begin{pmatrix} C & 0 & Be^{i\beta} \\ 0 & 0 & Ae^{i\alpha} \\ Be^{-i\beta} & Ae^{-i\alpha} & 0 \end{pmatrix}$	$\begin{pmatrix} C & 0 & 0 \\ 0 & 0 & Ae^{i\alpha} \\ 0 & Ae^{-i\alpha} & D \end{pmatrix}$

corresponding to non zero, non degenerate quark masses.

These possible patterns of texture specific mass matrices can be limited further by considering the constraints imposed by diagonalization procedure of mass matrices in up and down sector to obtain CKM matrix, details of diagonalization can be looked up in Refs. 127 and 128. An essential step in this process is to consider the invariants trace  $M$ , trace  $M^2$  and determinant  $M$  which yield the relations involving elements of mass matrices and mass eigenvalues  $m_1$ ,  $-m_2$  and  $m_3$ <sup>21,128</sup>, taking the second eigenvalue as  $-m_2$  facilitates the diagonalization procedure without affecting the consequences<sup>21</sup>. Following Ref. 126, it is interesting to note that the 12 possible textures break into two classes as shown in Table 1 depending upon the equations these matrices satisfy. For example, six matrices of class I, mentioned in Table 1, satisfy the following equations

$$C = m_1 - m_2 + m_3, \quad A^2 + B^2 = m_1 m_2 + m_2 m_3 - m_1 m_3, \quad A^2 C = m_1 m_2 m_3. \quad (102)$$

Similarly, in case of class II all six matrices satisfy the following equations

$$C + D = m_1 - m_2 + m_3, \quad A^2 - CD = m_1 m_2 + m_2 m_3 - m_1 m_3, \quad A^2 C = m_1 m_2 m_3. \quad (103)$$

The subscripts U and D have not been used as these are valid for both kind of mass matrices.

The matrices  $M_U$  and  $M_D$  each can correspond to any of the 12 possibilities, therefore yielding 144 possible combinations which in principle can yield 144 quark mixing matrices. These 144 combinations can be put into 4 different categories, e.g., if  $M_U$  is any of the 6 matrices from class I, then  $M_D$  can be either from class I or class II yielding 2 categories of 36 matrices each. Similarly, we obtain 2 more categories

of 36 matrices each when  $M_U$  is from class II and  $M_D$  is either from class I or class II. The 36 combinations in each category further can be shown to be reduced to groups of six combinations of mass matrices, each yielding same CKM matrix. For example, six of the 36 combinations belonging to first category, when both up and down sectors mass matrices are of the form  $M_{U_i}$  and  $M_{D_i}$  ( $i = a, b, c, d, e, f$ ), yield the same CKM matrices. Similarly, the remaining 30 matrices in category one yield five groups of six matrices each corresponding to five independent mixing matrices. A similar simplification can be achieved in other three categories.

Keeping in mind the hierarchical nature of the CKM matrix, an analytical analysis of categories as mentioned above yields only 4 groups of  $M_{U_i}$  and  $M_{D_i}$  corresponding to 6 combinations each of which yield 4 CKM matrices. To illustrate this point one can consider first matrix  $M_U$  to be of type (a) from class I and similarly  $M_D$  to be of type (b) from the same class. The corresponding CKM matrix is expressed as

$$V_{\text{CKM}} = \begin{pmatrix} V_{ud} & V_{us} & V_{ub} \\ V_{cd} & V_{cs} & V_{cb} \\ V_{td} & V_{ts} & V_{tb} \end{pmatrix} \quad (104)$$

$$= \begin{bmatrix} -e^{i(\alpha_U - \alpha_D)} & \left(\sqrt{\frac{m_d}{m_s}}\right)e^{i(\alpha_U - \alpha_D)} & \sqrt{\frac{m_u}{m_c}}e^{i\beta_D} \\ \sqrt{\frac{m_u}{m_c}}e^{i(\alpha_U - \alpha_D)} + \sqrt{\frac{m_d}{m_b}}e^{i\beta_D} - \sqrt{\frac{m_s}{m_b}}e^{i\beta_D} - \sqrt{\frac{m_c}{m_t}}e^{i\beta_U} & e^{-i\beta_D} & \\ \sqrt{\frac{m_d}{m_s}}e^{-i\beta_U} & -1 & \sqrt{\frac{m_s}{m_b}}e^{-i\beta_U} + \sqrt{\frac{m_c}{m_t}}e^{-i\beta_D} \end{bmatrix}, \quad (105)$$

where  $\alpha_i$  and  $\beta_i$ ,  $i = U, D$  are related to the phases of the elements  $A_i$  and  $B_i$  of the mass matrices given in Eq. (100). From the above structure of CKM matrix one can easily find out that off diagonal elements, e.g.,  $|V_{cb}|$  and  $|V_{ts}|$  are of the order of unity whereas diagonal elements  $|V_{cs}|$  and  $|V_{tb}|$  are smaller than unity which is in complete contrast to the structure of CKM matrix. In a similar manner, one can conclude that remaining indistinguishable combinations also lead to such non-physical mixing matrices. In case we apply the above criteria, interestingly we are left with only four groups of mass matrices as mentioned in Table 2. Thus the problem of exploring the compatibility of 144 phenomenological allowed texture 6 zero combinations with the recent low energy data is reduced only to an examination of 4 groups each having 6 combinations of mass matrices corresponding to the same CKM matrix.

The compatibility of these 4 groups of texture 6 zero mass matrices with the quark mixing data has been examined in Ref. 126. Considering the quark masses and mass ratios at  $M_z$  scale(GeV)<sup>129</sup>,

$$m_u = 0.002 - 0.003, m_c = 0.6 - 0.7, m_t = 169.5 - 175.5, \quad (106)$$

$$m_d = 0.0037 - 0.0052, m_s = 0.072 - 0.097, m_b = 2.8 - 3.0, \quad (107)$$



Table 2. Predicted values of  $|V_{cb}|$ ,  $\sin 2\beta$ ,  $\delta$  and  $J$  for 4 independent texture 6 zero combinations where  $i = a, b, c, d, e, f$ .

$M_U$	$M_D$	$ V_{cb} $	$\sin 2\beta$	$\delta^\circ$	$J \times 10^{-5}$
$I_i$	$I_i$	0.09-0.24	0.48-0.57	78-100	12-76
$II_i$	$II_i$	0	not defined	not defined	0
$I_i$	$II_i$	0.055-0.065	0.48-0.55	74-90	4.7-5.3
$II_i$	$I_i$	0.15-0.18	0.50-0.54	80-95	32-44

$$m_u/m_d = 0.51 - 0.60, m_s/m_d = 18.1 - 19.7. \quad (108)$$

and by giving full variation to phases  $\phi_1$  and  $\phi_2$ , some of the CKM parameters have been reproduced and compared with the following data,

$$|V_{us}| = 0.2236 - 0.2274, |V_{cb}| = 0.0401 - 0.0423, \quad (109)$$

$$\sin 2\beta = 0.656 - 0.706, \quad J = (2.85 - 3.24) \times 10^{-5}, \quad \delta = 45^\circ - 107^\circ. \quad (110)$$

From Table 2 one can immediately find that all possible combinations of texture 6 zero are ruled out as these are not able to reproduce the CKM element  $|V_{cb}|$ . Thus, none of the texture 6 zero combinations, Fritzsch-like as well as non Fritzsch-like, is found to be compatible with the recent quark mixing data, ruling out the existence of these mass matrices.

### 5.1.3. Texture 5 zero quark mass matrices

As already mentioned, several authors<sup>21,106–110</sup> have explored the case of texture 5 zero quark mass matrices, however, recently a detailed and comprehensive analysis of all possible, Fritzsch-like as well as non Fritzsch-like texture 5 zero mass matrices has been carried out<sup>126</sup>. A brief discussion of this analysis is perhaps in order. As mentioned earlier, texture 5 zero mass matrices can be obtained by either considering  $M_U$  being 2 zero and  $M_D$  being 3 zero type or vice versa. Texture 3 zero possibilities have already been enumerated and after taking into consideration the conditions mentioned in Eq. (101) one can check that there are 18 possible texture 2 zero patterns. These textures further break into three classes detailed in Table 3. It can be easily shown that while constructing the CKM matrix, the element  $F$  in type ‘a’ matrix of class V is much smaller than the other elements of considered mass matrix, therefore it can be considered as a very small perturbation on corresponding texture 3 zero pattern. Similar conclusion can be drawn for other matrices of the same class as well as it can be shown that matrices of class IV also reduce to texture 3 zero patterns. Therefore, one can conclude that the matrices in class IV and V effectively reduce to the corresponding 3 zero patterns, leaving only one, class III of texture 2 zero matrices, that needs to be explored for texture 5 zero combinations. All matrices of this class satisfy the following equation

$$C+D = m_1-m_2+m_3, \quad A^2+B^2-CD = m_1m_2+m_2m_3-m_1m_3, \quad A^2C = m_1m_2m_3. \quad (111)$$

Table 3. Texture 2 zero possibilities categorized into three classes III, IV and V.

	Class III	Class IV	Class V
a	$\begin{pmatrix} 0 & Ae^{i\alpha} & 0 \\ Ae^{-i\alpha} & D & Be^{i\beta} \\ 0 & Be^{-i\beta} & C \end{pmatrix}$	$\begin{pmatrix} D & Ae^{i\alpha} & 0 \\ Ae^{-i\alpha} & 0 & Be^{i\beta} \\ 0 & Be^{-i\beta} & C \end{pmatrix}$	$\begin{pmatrix} 0 & Ae^{i\alpha} & Fe^{i\gamma} \\ Ae^{-i\alpha} & 0 & Be^{i\beta} \\ Fe^{-i\gamma} & Be^{-i\beta} & C \end{pmatrix}$
b	$\begin{pmatrix} 0 & 0 & Ae^{i\alpha} \\ 0 & C & Be^{i\beta} \\ Ae^{-i\alpha} & Be^{-i\beta} & D \end{pmatrix}$	$\begin{pmatrix} D & 0 & Ae^{i\alpha} \\ 0 & C & Be^{i\beta} \\ Ae^{-i\alpha} & Be^{-i\beta} & 0 \end{pmatrix}$	$\begin{pmatrix} 0 & Fe^{i\gamma} & Ae^{i\alpha} \\ Fe^{-i\gamma} & C & Be^{i\beta} \\ Ae^{-i\alpha} & Be^{-i\beta} & 0 \end{pmatrix}$
c	$\begin{pmatrix} D & Ae^{i\alpha} & Be^{i\beta} \\ Ae^{-i\alpha} & 0 & 0 \\ Be^{-i\beta} & 0 & C \end{pmatrix}$	$\begin{pmatrix} 0 & Ae^{i\alpha} & Be^{i\beta} \\ Ae^{-i\alpha} & D & 0 \\ Be^{-i\beta} & 0 & C \end{pmatrix}$	$\begin{pmatrix} 0 & Ae^{i\alpha} & Be^{i\beta} \\ Ae^{-i\alpha} & 0 & Fe^{i\gamma} \\ Be^{-i\beta} & Fe^{-i\gamma} & C \end{pmatrix}$
d	$\begin{pmatrix} C & Be^{i\beta} & 0 \\ Be^{-i\beta} & D & Ae^{i\alpha} \\ 0 & Ae^{-i\alpha} & 0 \end{pmatrix}$	$\begin{pmatrix} C & Be^{i\beta} & 0 \\ Be^{-i\beta} & 0 & Ae^{i\alpha} \\ 0 & Ae^{-i\alpha} & D \end{pmatrix}$	$\begin{pmatrix} C & Be^{i\beta} & Fe^{i\gamma} \\ Be^{-i\beta} & 0 & Ae^{i\alpha} \\ Fe^{-i\gamma} & Ae^{-i\alpha} & 0 \end{pmatrix}$
e	$\begin{pmatrix} D & Be^{i\beta} & Ae^{i\alpha} \\ Be^{-i\beta} & C & 0 \\ Ae^{-i\alpha} & 0 & 0 \end{pmatrix}$	$\begin{pmatrix} 0 & Be^{i\beta} & Ae^{i\alpha} \\ Be^{-i\beta} & C & 0 \\ Ae^{-i\alpha} & 0 & D \end{pmatrix}$	$\begin{pmatrix} 0 & Be^{i\beta} & Ae^{i\alpha} \\ Be^{-i\beta} & C & Fe^{i\gamma} \\ Ae^{-i\alpha} & Fe^{-i\gamma} & 0 \end{pmatrix}$
f	$\begin{pmatrix} C & 0 & Be^{i\beta} \\ 0 & 0 & Ae^{i\alpha} \\ Be^{-i\beta} & Ae^{-i\alpha} & D \end{pmatrix}$	$\begin{pmatrix} C & 0 & Be^{i\beta} \\ 0 & D & Ae^{i\alpha} \\ Be^{-i\beta} & Ae^{-i\alpha} & 0 \end{pmatrix}$	$\begin{pmatrix} C & Fe^{i\gamma} & Be^{i\beta} \\ Fe^{-i\gamma} & 0 & Ae^{i\alpha} \\ Be^{i\beta} & Ae^{-i\alpha} & 0 \end{pmatrix}$

Table 4. Texture 5 zero combinations and their corresponding predicted values pertaining to  $|V_{cb}|$ ,  $|V_{ub}|$ ,  $\sin 2\beta$ ,  $\delta$  and  $J$ .

$M_U$	$M_D$	$ V_{cb} $	$ V_{ub} $	$\sin 2\beta$	$\delta^\circ$	$J \times 10^{-5}$
$I_i$	$III_i$	0.09-0.28	0.005-0.02	0.44-0.60	60-100	10-110
$II_i$	$III_i$	0.14-0.26	0.008-0.02	0.46-0.59	65-93	0.27-0.97
$III_i$	$I_i$	0.0401-0.0423	0.0032-0.0041	0.656-0.701	55-100	2.4-3.8
$III_i$	$II_i$	0.06-0.29	0.003-0.02	0.51-0.54	45-88	4.8-110

Considering class III of texture 2 zero mass matrices along with different patterns of class I and II of texture 3 zero mass matrices we find a total of 144 possibilities of texture 5 zero mass matrices, in sharp contrast to the case if we had considered class IV and V also yielding 432 possibilities. Keeping in mind the hierarchy of CKM matrix, out of 144 cases, one is again left with only 4 groups of texture 5 zero mass matrices detailed in Table 4. A general look at the table immediately reveals that as compared to texture 6 zero case  $|V_{cb}|$  predictions are quite different. However, interestingly only in one case  $|V_{cb}|$  as well as other CKM elements are found to be compatible with their experimentally measured values. Interestingly, this possibility corresponds to the usual Fritzsch-like texture 5 zero mass matrix where  $M_U$  is of texture 2 zero and  $M_D$  is of texture 3 zero type. It may be noted that the possibility corresponding to  $M_U$  being texture 3 zero and  $M_D$  being texture 2 zero is not viable which is due to the fact that pertaining to this case the hierarchy of elements of mass matrices comes out to be very strong, therefore making it difficult to fit the data.

Further, Ref. 126 notes that agreement pertaining to texture 5 zero case mentioned above is valid only when Leutwyler<sup>129</sup> quark masses are used. This agreement gets ruled out in case one uses the latest quark masses proposed by Xing *et al.*<sup>130</sup>. This can be understood from a study of the dependence of the elements

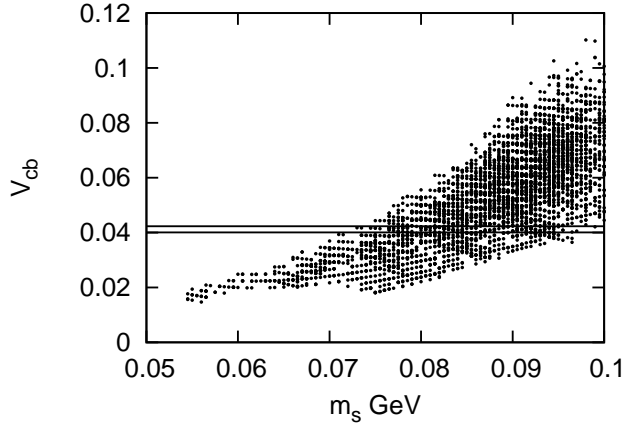


Fig. 9. Plot showing the allowed range of  $|V_{cb}|$  versus  $m_s$

$|V_{cb}|$  and  $|V_{ub}|$  on the mass  $m_s$ . For example, by giving full variation to all other parameters within their allowed ranges, Fig. 9 depicts the plot showing the allowed range of  $|V_{cb}|$  versus  $m_s$ . From the figure, it immediately becomes clear that when  $m_s$  is lower than 0.075, then one is not able to obtain  $|V_{cb}|$  in the allowed range, thereby leading to the conclusion that viability of texture 5 zero Fritzsch-like case is very much dependent on light quark masses used.

#### 5.1.4. Texture 4 zero quark mass matrices

Fritzsch-like texture 4 zero quark mass matrices are known to be compatible with specific models of GUTs<sup>21,122</sup>, Abelian family symmetries<sup>131</sup>, as well as describe the quark mixing data quite well. In the present work our emphasis will be to discuss the attempts<sup>124,125</sup> pertaining to the compatibility of these mass matrices with the precisely measured parameter  $\sin 2\beta$ , the issue whether one can consider ‘weakly’ hierarchical mass matrices to reproduce ‘strongly’ hierarchical mixing angles and the parameter space available to their elements in explaining the quark mixing data. Also, it may be mentioned that we have not discussed non Fritzsch-like texture 4 zero mass matrices as the texture two zero possibilities, presented in Table 3, result into 324 texture 4 zero possibilities making it a difficult and an elaborate task, yet to be carried out.

It may be noted that keeping in mind that the parameter  $\sin 2\beta$  provides vital clues to the structural features of texture specific mass matrices, comprising of hierarchy and phases of the elements of the mass matrices, several authors<sup>116–124</sup> have explored its implications for these. In particular, using assumption of ‘strong hierarchy’ of the elements of the mass matrix, having its motivation in the hierarchy of the quark mixing angles, the following leading order relationships between the

various elements of the mixing matrix and quark masses have been obtained in Refs. 116 -121,

$$\left| \frac{V_{ub}}{V_{cb}} \right| = \sqrt{\frac{m_u}{m_c}}, \quad \left| \frac{V_{td}}{V_{ts}} \right| = \sqrt{\frac{m_d}{m_s}}, \quad |V_{us}| = \left| \sqrt{\frac{m_d}{m_s}} e^{i\phi} - \sqrt{\frac{m_u}{m_c}} \right|. \quad (112)$$

Following Particle Data Group (PDG)<sup>25</sup> definition, these further give the expression for  $\beta$  in the ‘strong hierarchy’ case, e.g.,

$$\beta \equiv \arg \left[ -\frac{V_{cd}V_{cb}^*}{V_{td}V_{tb}^*} \right] = \arg \left[ 1 - \sqrt{\frac{m_u m_s}{m_c m_d}} e^{-i\phi} \right]. \quad (113)$$

Unfortunately, the value of  $\sin 2\beta$  predicted by the above formula is in quite disagreement with its present precisely known value. In particular, with the present values of input quark masses and by giving full variation to phase  $\phi$ , the maximum value of  $\sin 2\beta$  comes out to be 0.5, which is in sharp conflict with its present PDG 2010 value  $0.673 \pm 0.023$ <sup>25</sup>. However, recently a detailed and comprehensive analysis by Verma *et al.* has been carried out<sup>124</sup> wherein this conflict seems to have been resolved.

To begin with, the authors<sup>124,125</sup> define the ‘weak’ and ‘strong’ hierarchy of the elements of the mass matrices. For example, in case  $D_i < |B_i| < C_i$  it would lead to a strongly hierarchical mass matrix whereas a weaker hierarchy of the mass matrix implies  $D_i \lesssim |B_i| \lesssim C_i$ . It may also be added that for the purpose of numerical work, the ratio  $D_i/C_i \sim 0.01$  characterizes strong hierarchy whereas  $D_i/C_i \gtrsim 0.2$  implies weak hierarchy of the elements of the mass matrices. This can be understood by expressing these parameters in terms of the quark masses, in particular  $D_U/C_U \sim 0.01$  implies  $C_U \sim m_t$  and  $D_D/C_D \sim 0.01$  leads to  $C_D \sim m_b$ .

The mass matrices  $M_U$  and  $M_D$  can be exactly diagonalized. To facilitate the understanding of modification of the formula of  $\sin 2\beta$  given in Eq. (113), we present some essential details. The texture 4 zero hermitian mass matrix  $M_i$  ( $i = U, D$ ) can be expressed as

$$M_i = Q_i M_i^r P_i \quad (114)$$

or

$$M_i^r = Q_i^\dagger M_i P_i^\dagger, \quad (115)$$

where  $M_i^r$  is a real symmetric matrix with real eigenvalues and  $Q_i$  and  $P_i$  are diagonal phase matrices. The matrix  $M_i^r$  can be diagonalized by the orthogonal transformation, e.g.,

$$M_i^{\text{diag}} = O_i^T M_i^r O_i, \quad (116)$$

where

$$M_i^{\text{diag}} = \text{diag}(m_1, -m_2, m_3), \quad (117)$$

the subscripts 1, 2 and 3 referring respectively to  $u, c$  and  $t$  for the up sector as well as  $d, s$  and  $b$  for the down sector. Using the invariants,  $\text{tr} M_i^r$ ,  $\text{tr} M_i^{r^2}$  and  $\det M_i^r$ ,

the values of the elements of the mass matrices  $A_i$ ,  $B_i$  and  $C_i$ , in terms of the free parameter  $D_i$  and the quark masses are given as

$$C_i = (m_1 - m_2 + m_3 - D_i), \quad (118)$$

$$|A_i| = (m_1 m_2 m_3 / C_i)^{1/2}, \quad (119)$$

$$|B_i| = [(m_3 - m_2 - D_i)(m_3 + m_1 - D_i)(m_2 - m_1 + D_i) / C_i]^{1/2}. \quad (120)$$

The exact diagonalizing transformation  $O_i$  is expressed as

$$O_i = \begin{pmatrix} \pm \sqrt{\frac{m_2 m_3 (C_i - m_1)}{(m_3 - m_1)(m_2 + m_1) C_i}} \pm \sqrt{\frac{m_1 m_3 (C_i + m_2)}{C_i (m_2 + m_1)(m_3 + m_2)}} \pm \sqrt{\frac{m_1 m_2 (m_3 - C_i)}{C_i (m_3 + m_2)(m_3 - m_1)}} \\ \pm \sqrt{\frac{m_1 (C_i - m_1)}{(m_3 - m_1)(m_2 + m_1)}} \mp \sqrt{\frac{m_2 (C_i + m_2)}{(m_3 + m_2)(m_2 + m_1)}} \pm \sqrt{\frac{m_3 (m_3 - C_i)}{(m_3 + m_2)(m_3 - m_1)}} \\ \mp \sqrt{\frac{m_1 (m_3 - C_i)(C_i + m_2)}{C_i (m_3 - m_1)(m_2 + m_1)}} \pm \sqrt{\frac{m_2 (C_i - m_1)(m_3 - C_i)}{C_i (m_3 + m_2)(m_2 + m_1)}} \pm \sqrt{\frac{m_3 (C_i - m_1)(C_i + m_2)}{C_i (m_3 + m_2)(m_3 - m_1)}} \end{pmatrix}. \quad (121)$$

It may be noted that while finding the diagonalizing transformation  $O_i$ , one has the freedom to choose several equivalent possibilities of phases. Similarly, while normalizing the diagonalized matrix to quark masses, one again has the freedom to choose the phases for the quark masses. This is due to the fact that the diagonalizing transformations of  $M_U$  and  $M_D$  occur in a particular manner in the weak charge current interactions of quarks to give the CKM mixing matrix. As is usual, the phase of  $m_2$  has been chosen to be negative facilitating the diagonalization process as well as the construction of the CKM matrix. This is one of the possibilities considered by Xing and Zhang<sup>123</sup>, the others are related and are all equivalent, these only redefining the phases  $\phi_1$  and  $\phi_2$  which in any case are arbitrary. In the work being discussed, the authors have chosen the possibility

$$O_i = \begin{pmatrix} O_i(11) & O_i(12) & O_i(13) \\ O_i(21) & -O_i(22) & O_i(23) \\ -O_i(31) & O_i(32) & O_i(33) \end{pmatrix}. \quad (122)$$

As already mentioned, the CKM mixing matrix can be obtained using  $O_{U(D)}$  through the relation  $V_{\text{CKM}} = O_U^T (P_U P_D^\dagger) O_D$ . Explicitly, the elements of the CKM mixing matrix can be expressed as

$$V_{lm} = O_{1l}^U O_{1m}^D e^{-i\phi_1} + O_{2l}^U O_{2m}^D + O_{3l}^U O_{3m}^D e^{i\phi_2}, \quad (123)$$

where the subscripts  $l$  and  $m$  run respectively over  $u, c, t$  and  $d, s, b$  and  $\phi_1 = \alpha_U - \alpha_D$ ,  $\phi_2 = \beta_U - \beta_D$ .

To evaluate the parameter  $\sin 2\beta$ , the elements  $V_{cd}$ ,  $V_{cb}$ ,  $V_{td}$  and  $V_{tb}$  are required

38 *Manmohan Gupta, Gulsheen Ahuja*

to be known. Using the above equation, these elements can be easily found, e.g.,

$$\begin{aligned}
 V_{cd} = & \sqrt{\frac{m_u m_t (-D_u + m_u + m_t)}{C_u (m_u + m_c)(m_c + m_t)}} \sqrt{\frac{m_s m_b (-D_d + m_b - m_s)}{C_d (m_b - m_d)(m_s + m_d)}} e^{-i\phi_1} \\
 & - \sqrt{\frac{m_c (-D_u + m_u + m_t)}{(m_u + m_c)(m_c + m_t)}} \sqrt{\frac{m_d (-D_d + m_b - m_s)}{(m_b - m_d)(m_s + m_d)}} \\
 & - \sqrt{\frac{m_c (-D_u + m_t - m_c)(D_u - m_u + m_c)}{C_u (m_u + m_c)(m_t + m_c)}} \times \\
 & \sqrt{\frac{m_d (D_d - m_d + m_s)(-D_d + m_d + m_b)}{C_d (m_b - m_d)(m_s + m_d)}} e^{i\phi_2}.
 \end{aligned} \tag{124}$$

In case one uses the above complicated expression for  $V_{cd}$  as well as similar expressions of the other elements to evaluate  $\sin 2\beta$ , one can find that these would yield a long and complicated formula from which it would be difficult to understand the implications on the phases and other parameters of the mass matrices. To derive a simple and informative formula, one needs to first rewrite the diagonalizing transformation  $O_i$  keeping in mind  $m_3 \gg m_2 \gg m_1$  and the element of the mass matrix  $C_i \gg m_1$ , which is always valid without any dependence on the hierarchy of the elements of the mass matrices. It may be mentioned that this approximation induces less than a fraction of a percentage error in the numerical results. The structure of  $O_i$  can be simplified and expressed as

$$O_i = \begin{pmatrix} 1 & \zeta_{1i} \sqrt{\frac{m_1}{m_2}} \frac{\zeta_{2i}}{\zeta_{3i}} \sqrt{\frac{m_1 m_2}{m_3^2}} \\ \zeta_{3i} \sqrt{\frac{m_1}{m_2}} & -\zeta_{1i} \zeta_{3i} & \zeta_{2i} \\ -\zeta_{1i} \zeta_{2i} \sqrt{\frac{m_1}{m_2}} & \zeta_{2i} & \zeta_{1i} \zeta_{3i} \end{pmatrix}, \tag{125}$$

where the three parameters  $\zeta_{1i}$ ,  $\zeta_{2i}$ ,  $\zeta_{3i}$ , with  $i$  denoting  $U$  and  $D$  are given by

$$\zeta_{1i} = \sqrt{1 + \frac{m_2}{C_i}}, \quad \zeta_{2i} = \sqrt{1 - \frac{C_i}{m_3}}, \quad \zeta_{3i} = \sqrt{\frac{C_i}{m_3}}. \tag{126}$$

Making use of this equation, along with relation (123), the following elements needed to evaluate  $\beta$  are obtained as

$$V_{cd} = \zeta_{1U} \sqrt{\frac{m_u}{m_c}} e^{-i\phi_1} - \sqrt{\frac{m_d}{m_s}} [\zeta_{1U} \zeta_{3U} \zeta_{3D} + \zeta_{2U} \zeta_{1D} \zeta_{2D} e^{i\phi_2}], \tag{127}$$

$$V_{cb} = \frac{\zeta_{1U} \zeta_{2D}}{\zeta_{3D}} \sqrt{\frac{m_u m_d m_s}{m_c m_b^2}} e^{-i\phi_1} - [\zeta_{1U} \zeta_{3U} \zeta_{2D} - \zeta_{2U} \zeta_{1D} \zeta_{3D} e^{i\phi_2}], \tag{128}$$

$$V_{td} = \frac{\zeta_{2U}}{\zeta_{3U}} \sqrt{\frac{m_u m_c}{m_t^2}} e^{-i\phi_1} + \sqrt{\frac{m_d}{m_s}} [\zeta_{2U} \zeta_{3D} - \zeta_{1U} \zeta_{3U} \zeta_{1D} \zeta_{2D} e^{i\phi_2}], \tag{129}$$

$$V_{tb} = \frac{\zeta_{2U}\zeta_{2D}}{\zeta_{3U}\zeta_{3D}} \sqrt{\frac{m_u m_c m_d m_s}{m_t^2 m_b^2}} e^{-i\phi_1} + [\zeta_{2U}\zeta_{2D} + \zeta_{1U}\zeta_{3U}\zeta_{1D}\zeta_{3D} e^{i\phi_2}]. \quad (130)$$

A general look on the above elements clearly shows that the above relations are not only more compact but also more useful to view the dependence of these CKM matrix elements on the quark masses and phases. Using these elements, after some non trivial algebra, one arrives at the following expression of  $\beta$ , wherein its dependence on the quark masses and the elements of the quark mass matrices is visible in a simple and clear manner, e.g.,

$$\beta \equiv \arg \left[ -\frac{V_{cd}V_{cb}^*}{V_{td}V_{tb}^*} \right] = \arg \left[ \left( 1 - \sqrt{\frac{m_u m_s}{m_c m_d}} e^{-i(\phi_1 + \phi_2)} \right) \left( \frac{1 - r_2 e^{i\phi_2}}{1 - r_1 e^{i\phi_2}} \right) \right], \quad (131)$$

where the parameters  $r_1$  and  $r_2$  can be expressed in terms of the quark masses and the elements of the quark mass matrices via the relations,

$$r_1 = \frac{\zeta_{1U}\zeta_{3U}\zeta_{1D}\zeta_{2D}}{\zeta_{2U}\zeta_{3D}} \quad \text{and} \quad r_2 = \frac{\zeta_{1U}\zeta_{3U}\zeta_{2D}}{\zeta_{2U}\zeta_{1D}\zeta_{3D}}. \quad (132)$$

The relationship given in Eq. (131) is an ‘exact’ formula emanating from texture 4 zero mass matrices, incorporating both the phases. This formula has several interesting aspects. Apart from clearly underlying the dependence of small quark masses and the phases  $\phi_1$  and  $\phi_2$ , it also clearly establishes the modification of the earlier formula. It is very easy to check that the earlier formula can be easily deduced from the present one by using the strong hierarchy assumption which essentially translates to  $\zeta_{1D} \simeq \zeta_{1U} \simeq 1$ , further implying  $r_1 = r_2$  and  $\left( \frac{1 - r_2 e^{i\phi_2}}{1 - r_1 e^{i\phi_2}} \right) = 1$ . The phase of the earlier formula can be obtained by identifying  $\phi_1 + \phi_2$  as  $\phi$ , taking values from 0 to  $2\pi$ .

It also needs to be re-emphasized that while arriving at the above ‘exact’ relationship, the hierarchy of the quark masses, e.g.,  $m_t \gg m_u$  and  $m_b \gg m_d$  has been considered as well as  $m_3 \gg m_2 \gg m_1$  and the element of the mass matrix  $C_i \gg m_1$  have been used, these being valid in both weak and strong hierarchy cases. It may also be added that the formula remains valid for both the weak hierarchy of the elements of the mass matrices as well as for the strong hierarchy assumption. Interestingly, the modification to the earlier formula contributes only when  $\phi_2 \neq 0$ , implying thereby that both the phases of the mass matrices might play an important role in achieving the agreement with data.

In order to investigate the implications of the formula given in Eq. (131) on the structural features of the mass matrices and the CKM parameters, as a first step one can find the range of  $\sin 2\beta$  predicted by the above formula. In this regard, the following ranges of quark masses at the energy scale of  $M_z$  have been adopted by Refs. 124 and 125, e.g.,

$$\begin{aligned} m_u &= 0.8 - 1.8 \text{ MeV}, \quad m_d = 1.7 - 4.2 \text{ MeV}, \quad m_s = 40.0 - 71.0 \text{ MeV}, \\ m_c &= 0.6 - 0.7 \text{ GeV}, \quad m_b = 2.8 - 3.0 \text{ GeV}, \quad m_t = 169.5 - 175.5 \text{ GeV}. \end{aligned} \quad (133)$$

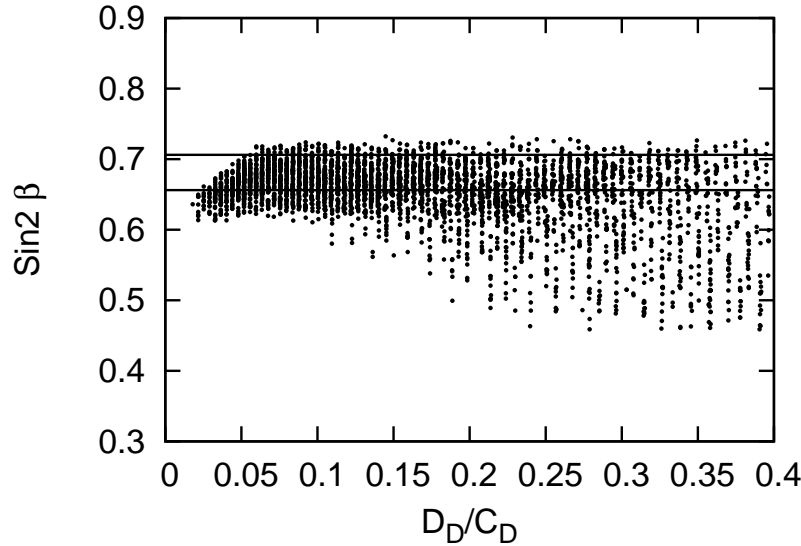


Fig. 10. Plot showing variation of CP violating parameter  $\sin 2\beta$  versus hierarchy characterizing ratio  $D_D/C_D$

With these inputs and the ‘exact’ formula given in Eq. (131), one can evaluate  $\sin 2\beta$  by giving full variation to the phases  $\phi_1$  and  $\phi_2$ , the parameters  $D_U$  and  $D_D$  have been given wide variation in conformity with the natural hierarchy of the elements of the mass matrices, e.g.,  $D_i < C_i$  for  $i = U, D$ . The  $\sin 2\beta$  so evaluated comes out to be

$$\sin 2\beta = 0.4105 - 0.7331. \quad (134)$$

Interestingly, one finds that the above value is inclusive of its experimental range  $0.681 \pm 0.025$ . This clearly indicates that the formula which includes weak hierarchy as well as additional phase factors plays a crucial role in bringing out reconciliation between texture 4 zero mass matrices and the present precise value of  $\sin 2\beta$ .

After having shown the compatibility of texture 4 zero mass matrices with  $\sin 2\beta$ , Ref. 124 examines the constraints imposed on the ratio  $D_i/C_i$  for  $i = U, D$ , characterizing hierarchy, as well as on the phases  $\phi_1$  and  $\phi_2$  of the mass matrices. As a first step, using the relation obtained earlier, one can investigate the role of hierarchy by plotting  $\sin 2\beta$  against the ratio  $D_D/C_D$ , shown in Fig. 10. Several interesting conclusions follow from the graph. It can be easily noted that when  $D_D/C_D < 0.02$ , one is not able to reproduce any point within the  $1\sigma$  range of  $\sin 2\beta$ , even after giving full variation to all the other parameters. It may be of interest to mention that the earlier attempts<sup>116–121</sup> had considered a value of  $D_D/C_D \lesssim 0.02$ , thereby resulting in the incompatibility of texture 4 zero mass matrices with  $\sin 2\beta$ . From the figure it can be easily checked that only for  $D_D/C_D > 0.05$ , full range of  $\sin 2\beta$



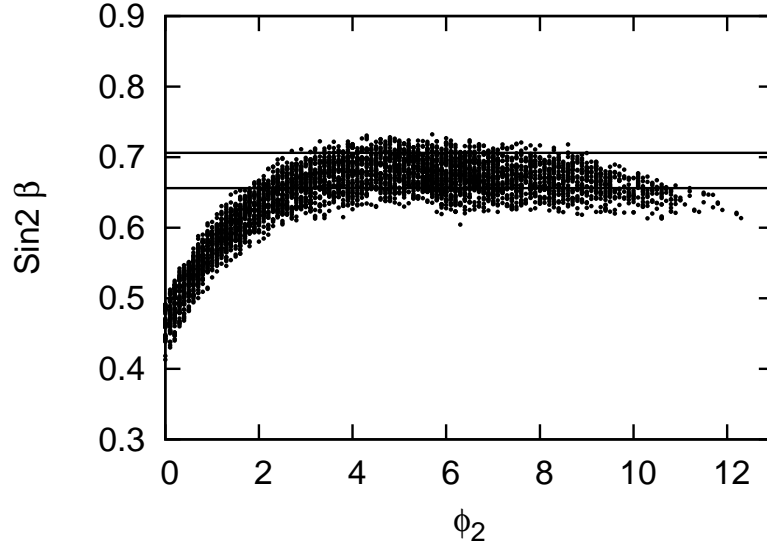


Fig. 11. Plot showing variation of CP violating parameter  $\sin 2\beta$  versus the phase  $\phi_2$

is reproduced. This clearly shows that as one deviates from strong hierarchy characterized by the ratio  $D_D/C_D \sim 0.01$  towards weak hierarchy given by  $D_D/C_D \gtrsim 0.1$ , one is able to reproduce the results. It may be mentioned that although the graph has been plotted for  $D_D/C_D$  up to 0.4, however the same pattern is followed up to  $D_D/C_D \sim 0.6$ , beyond which the basic structure of the mass matrix is changed. It may be added that the corresponding graph of  $D_U/C_U$  is also very much similar. One would also like to emphasize that the agreement between  $\sin 2\beta$  and higher values of  $D_i/C_i$  does not spoil the overall agreement of texture 4 zero mass matrices with the CKM matrix derived earlier. This brings out an extremely important point as the conventional belief was that the hierarchical quark mixing angles can be reproduced only by strong hierarchy mass matrices.

Regarding the phases  $\phi_1$  and  $\phi_2$  of the mass matrices, in Fig. 11 graph of  $\sin 2\beta$  versus angle  $\phi_2$  has been plotted. The graph clearly illustrates the crucial role played by the phase  $\phi_2$  in bringing out agreement of texture 4 zero mass matrices and the precisely known  $\sin 2\beta$ . It is interesting to emphasize that despite giving full variation to other parameters, for  $\phi_2 = 0^\circ$  one is not able to reproduce  $\sin 2\beta$  within the experimental range.

Coming to the issue whether ‘weakly hierarchical’ quark mass matrices are able to reproduce the mixing data which involves strongly hierarchical parameters. In this context, it may be mentioned that in the case of quark mass matrices, usually the elements are assumed to follow ‘strong hierarchy’, whereas there is no such compulsion for the leptonic mass matrices. Therefore, in case one needs to invoke

quark-lepton unification<sup>13</sup>, this issue becomes interesting. This is all the more important as the texture 4 zero mass matrices perhaps provide the simplest parallel structure for quark and lepton mass matrices which are compatible with the low energy data.

Realizing the importance of Fritzsch-like hermitian texture 4 zero mass matrices in the context of quarks, a few years back Xing and Zhang<sup>123</sup> have attempted to find the parameter space of the elements of these mass matrices. Their analysis has provided good deal of information regarding the space available to various parameters as well as have provided valuable insight into the ‘structural features’ of texture 4 zero mass matrices. In this context, it may be noted that the hierarchy of the elements of the mass matrices is largely governed by the (2,2) element of the matrix. In their analysis, attempt has been made to go somewhat beyond the minimal values of this element, corresponding to the ‘strong hierarchy’ case, however in case one has to consider the ‘weak hierarchy’ case as well then there seems a further need to consider a still larger range for this element.

Recently, an interesting analysis has been carried out by Verma *et al.*<sup>125</sup> which updates and broadens the scope of the analysis carried out by Xing and Zhang<sup>123</sup> as well as examines the implications of recent precision measurements on the structural features of texture 4 zero mass matrices. The analysis incorporates the latest values of quark masses and their ratios and full variation has been given to the phases associated with the mass matrices  $\phi_1$  and  $\phi_2$ , the parameters  $D_U$  and  $D_D$  have been given wide variation in conformity with the hierarchy of the elements of the mass matrices e.g.,  $D_i < C_i$  for  $i = U, D$ . The extended range of these parameters allows the calculations for the case of weak hierarchy of the elements of the mass matrices as well.

The key findings of Ref. 125 can be understood from the following figures, reproduced here for the readers’ convenience. In Fig. 12(a),  $C_U/m_t$  versus  $C_D/m_b$  has been plotted revealing that both  $C_U/m_t$  as well as  $C_D/m_b$  take values from  $\sim 0.55 - 0.95$ , which interestingly indicates the ratios being almost proportional. Also, the figure gives interesting clues regarding the role of strong and weak hierarchy. In particular, one finds that in case one restricts to the assumption of strong hierarchy then these ratios take large values around 0.95. However, for the case of weak hierarchy, the ratios  $C_U/m_t$  and  $C_D/m_b$  take much larger number of values, in fact almost the entire range mentioned above, which are compatible with the data.

In Fig. 12(b), the plot of  $\phi_1$  versus  $\phi_2$  has been presented. Interestingly, the present refined inputs limit the ranges of the two phases to  $\phi_1 \sim 76^\circ - 92^\circ$  and  $\phi_2 \sim 1^\circ - 11^\circ$ . Keeping in mind that full variation has been given to the free parameters  $D_U$  and  $D_D$ , corresponding to both strong as well as weak hierarchy cases, it may be noted that the allowed ranges of the two phases come out to be rather narrow. In particular, for the strong hierarchy case one gets  $\phi_2 \sim 10^\circ$ , whereas for the case of weak hierarchy  $\phi_2$  takes almost its entire range mentioned

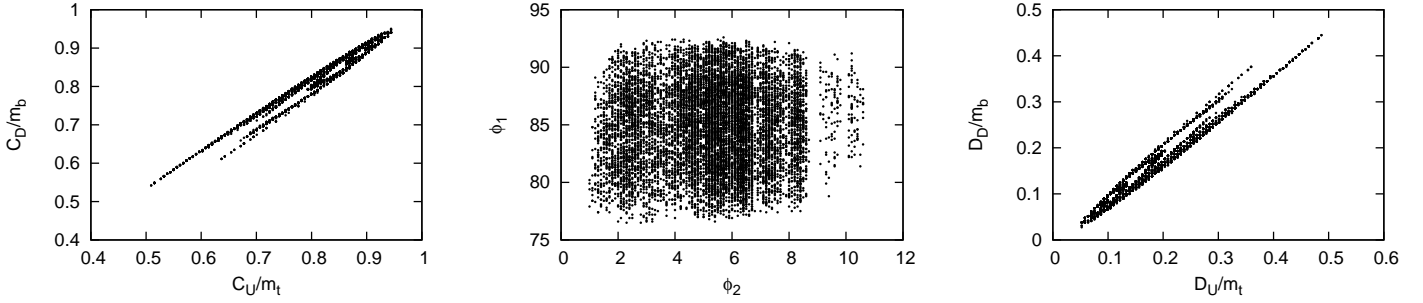


Fig. 12. Plots showing the allowed ranges of (a)  $C_U/m_t$  versus  $C_D/m_b$ , (b)  $\phi_1$  versus  $\phi_2$  and (c)  $D_U/m_t$  versus  $D_D/m_b$

above. Also, the analysis indicates that although  $\phi_1 \gg \phi_2$ , still both the phases are required for fitting the mixing data.

As a next step, in Fig. 12(c)  $D_U/m_t$  versus  $D_D/m_b$  has been given, representing an extended range of the parameters  $D_U$  and  $D_D$ . A closer look at the figure reveals both  $D_U/m_t$  as well as  $D_D/m_b$  take values  $\sim 0.05 - 0.5$ . The lower limit of the range i.e. when the ratios  $D_U/m_t$  and  $D_D/m_b$  are around 0.05 corresponds to strong hierarchy amongst the elements of the mass matrices, whereas when the elements have weak hierarchy then these ratios take a much larger range of values. From this one may conclude that in the case of strongly hierarchical elements of the texture 4 zero mass matrices, one has limited compatibility of these matrices with the quark mixing data, whereas the weakly hierarchical ones indicate the compatibility for much broader range of the elements.

The above discussion can also be understood by the construction of the mass matrices. However, as the phases of the elements of the mass matrices can be separated out, as can be seen from Eq. (115), one needs to consider  $M_i^r$  ( $i = U, D$ ) instead of  $M_i$ . The ranges of the elements of these matrices  $M_U^r$  and  $M_D^r$  are as follows

$$M_U^r = m_t \begin{pmatrix} 0 & 0.000174 - 0.000252 & 0 \\ 0.000174 - 0.000252 & 0.0464 - 0.4870 & 0.2184 - 0.5017 \\ 0 & 0.2184 - 0.5017 & 0.5094 - 0.9500 \end{pmatrix}, \quad (135)$$

$$M_D^r = m_b \begin{pmatrix} 0 & 0.003555 - 0.006154 & 0 \\ 0.003555 - 0.006154 & 0.0276 - 0.4448 & 0.2194 - 0.5044 \\ 0 & 0.2194 - 0.5044 & 0.5418 - 0.9505 \end{pmatrix}. \quad (136)$$

It may be noted that the elements of the mass matrices  $A_i$ ,  $B_i$ ,  $C_i$  and  $D_i$  satisfy the relation  $|B_i|^2 - C_i D_i \simeq m_2 m_3$  for both the strong and the weak hierarchy cases characterized respectively by  $D_i < |B_i| < C_i$  and  $D_i \lesssim |B_i| \lesssim C_i$ . This relation can be numerically checked from the above mentioned mass matrices in Eqs. (135) and (136). The above constraint on the elements of the mass matrices as well as

the ranges of various ratios, particularly in the case of weak hierarchy, provide an interesting possibility for checking the viability of various mass matrices formulated at the GUTs scale or obtained using horizontal symmetries. From a different point of view, this can also provide vital clues to the formulation of mass matrices which are in agreement with the low energy data.

After constructing the mass matrices, the authors have also constructed the corresponding CKM mixing matrix and compared it with the one arrived through global analysis. The CKM mixing matrix obtained by the authors is as follows

$$V_{\text{CKM}} = \begin{pmatrix} 0.9738 - 0.9747 & 0.2236 - 0.2274 & 0.00357 - 0.00429 \\ 0.2234 - 0.2274 & 0.9729 - 0.9739 & 0.0401 - 0.0423 \\ 0.0057 - 0.0114 & 0.0388 - 0.0420 & 0.9991 - 0.9992 \end{pmatrix}. \quad (137)$$

A general look at the matrix reveals that the ranges of CKM elements obtained here are quite compatible with those obtained by recent global analyses<sup>25–28</sup>. The Jarlskog’s rephasing invariant parameter  $J$  has also been evaluated which comes out to be

$$J = (1.807 - 3.977)10^{-5}. \quad (138)$$

Further, using this value of  $J$  one can obtain the following range of the CP violating phase  $\delta$

$$\delta = 28.8.8^\circ - 110.4^\circ. \quad (139)$$

The above mentioned ranges of the parameters  $J$  and the phase  $\delta$  are inclusive of the values given by latest PDG data<sup>25</sup>.

## 5.2. *Lepton mass matrices*

In the leptonic sector, the observation of neutrino oscillations has added another dimension to the issue of fermion masses and mixing. In fact, the pattern of neutrino masses and mixings seems to be vastly different from that of quarks. At present, the available neutrino oscillation data does not throw any light on the neutrino mass hierarchy, which may be normal/ inverted and may even be degenerate. Further, the situation becomes complicated when one realizes that neutrino masses are much smaller than charged fermion masses as well as it is not clear whether neutrinos are Dirac or Majorana particles. The situation becomes more complicated in case one has to understand the quark and neutrino mixing phenomena in a unified manner.

In the literature, several attempts have been made to formulate the phenomenological mass matrices considering charged leptons to be diagonal, usually referred to as the flavor basis case<sup>22</sup>. In case the PMNS matrix is known, then, in principle, the mass matrices for Dirac and Majorana case can be expressed as

$$m_\nu^{\alpha\beta} = \sum_i (U^*)_{\alpha i} m_i (U^\dagger)_{i\beta}. \quad (140)$$

It is clear from the above equation that the elements of the neutrino mass matrix in the flavor basis can be determined in case we have complete knowledge about

the mass eigenvalues as well as the elements of the mixing matrix. In the case of Dirac neutrinos, one would require knowledge of the three mixing angles and one Dirac-like CP violating phase  $\delta_l$ . For Majorana neutrinos, things become more complicated as one needs to have additional information about the two Majorana phases also. It is likely in the near future the precision regarding the measurement of the three mixing angles would increase and also some information about the phase  $\delta_l$  becomes available. Similarly, it is also likely that one may be able to get some clues about the overall scale of neutrino masses. However, extracting information about Majorana phases from neutrinoless double  $\beta$  decay experiments would be a challenging task.

To understand the pattern of neutrino masses and mixings, texture zero approach has been tried with good deal of success<sup>22,132–174</sup>. In the light of quark-lepton unification hypothesis, advocated by Smirnov<sup>13</sup>, in the sequel, parallel to the case of quarks, we would restrict ourselves to the Fritzsch-like as well as non Fritzsch-like texture specific lepton mass matrices. An important attempt to formulate texture specific lepton mass matrices, however in the flavor basis, was carried out by Frampton, Glashow and Marfatia<sup>137</sup>, wherein assuming a complex symmetric Majorana mass matrix and considering seven possible texture 2 zero cases, they carried out the implications of these for the neutrino oscillation data. Further, without considering the flavor basis, for normal hierarchy of neutrino masses, Fukugita, Tanimoto and Yanagida<sup>146</sup> carried out an analysis of Fritzsch-like texture 6 zero mass matrices. Similarly, Zhou and Xing<sup>161</sup> also carried out a systematic analysis of all possible texture 6 zero mass matrices for Majorana neutrinos with an emphasis on normal hierarchy of neutrino masses. Recently,<sup>167,172,173</sup> for all possible hierarchies of neutrino masses, for both Majorana as well as Dirac neutrinos, detailed analyses of Fritzsch-like texture 6, 5 and 4 zero mass matrices was carried out. Further, in view of absence of any theoretical justification for Fritzsch-like mass matrices, recent attempts<sup>174</sup> were made to consider non Fritzsch-like mass matrices for neutrinos. Before we present the essential details of some of these analyses, in the following section, we first present the relation between lepton mass matrices and mixing matrix.

### 5.2.1. Relationship of lepton mass matrices and mixing matrix

The observation of neutrino oscillation phenomenon which essentially implies the flavor conversion of neutrinos is similar to the quark mixing phenomenon. This possibility of flavor conversion was originally examined by B. Pontecorvo and further generalized by Maki, Nakagawa and Sakata<sup>58–61</sup>. The emerging picture that neutrinos are massive and therefore mix has been proved beyond any doubt and provides an unambiguous signal of NP.

In the case of neutrinos, the generation of masses is not straight-forward as they may have either the Dirac masses or the more general Dirac-Majorana masses. A Dirac mass term can be generated by the Higgs mechanism with the standard Higgs

doublet by introducing singlet right handed neutrinos in the SM. In this case, the neutrino mass term can be written as

$$\bar{\nu}_{aL} M_{\nu D} \nu_{aR} + h.c., \quad (141)$$

where  $a = e, \mu, \tau$  and  $\nu_e, \nu_\mu, \nu_\tau$  are the flavor eigenstates.  $M_{\nu D}$  is a complex  $3 \times 3$  Dirac mass matrix. The mass term mentioned above would also be characterized by the same symmetry breaking scale such as that of charged leptons or quarks, therefore, in this case very small masses of neutrinos would be very unnatural from the theory point of view. On the other hand, the neutrino might be a Majorana particle which is defined as is its own anti-particle and is characterized by only two independent particle states of the same mass ( $\nu_L$  and  $\bar{\nu}_R$  or  $\nu_R$  and  $\bar{\nu}_L$ ). A Majorana mass term, which violates both the law of total lepton number conservation and that of individual lepton flavor conservation, can be written either as

$$\frac{1}{2} \bar{\nu}_{aL} M_L \nu_{aR}^c + h.c. \quad \text{or as} \quad \frac{1}{2} \bar{\nu}_{aL}^c M_R \nu_{aR} + h.c., \quad (142)$$

where  $M_L$  and  $M_R$  are complex symmetric matrices.

A simple extension of the SM is to include one right handed neutrino in each of the three lepton families, while the Lagrangian of the electroweak interactions is kept invariant under  $SU(2)_L \times U(1)_Y$  gauge transformations. This can be shown to lead to Dirac-Majorana mass terms which further lead to the famous seesaw mechanism<sup>175–179</sup> for the generation of small neutrino masses, e.g.,

$$M_\nu = -M_{\nu D}^T (M_R)^{-1} M_{\nu D}, \quad (143)$$

where  $M_{\nu D}$  and  $M_R$  are respectively the Dirac neutrino mass matrix and the right handed Majorana neutrino mass matrix. The seesaw mechanism is based on the assumption that, in addition to the standard Higgs mechanism of generation of the Dirac mass term, there exists a beyond the SM mechanism of generation of the right handed Majorana mass term, which changes the lepton number by two and is characterized by a mass  $M \gg m$ . The Dirac mass term mixes the left handed field  $\nu_L$ , the component of a doublet, with a single field  $(\nu^c)_R$ . As a result of this mixing the neutrino acquires Majorana mass, which is much smaller than the masses of leptons or quarks.

Similar to the quark sector, the lepton mass matrices can be diagonalized by bi-unitary transformations and the corresponding mixing matrix obtained, known as Pontecorvo-Maki-Nakagawa-Sakata (PMNS) or lepton mixing matrix<sup>58–61</sup> is given as

$$V_{\text{PMNS}} = V_{l_L}^\dagger V_{\nu_L}. \quad (144)$$

The PMNS matrix expresses the relationship between the neutrino mass eigenstates and the flavor eigenstates, e.g.,

$$\begin{pmatrix} \nu_e \\ \nu_\mu \\ \nu_\tau \end{pmatrix} = \begin{pmatrix} V_{e1} & V_{e2} & V_{e3} \\ V_{\mu 1} & V_{\mu 2} & V_{\mu 3} \\ V_{\tau 1} & V_{\tau 2} & V_{\tau 3} \end{pmatrix} \begin{pmatrix} \nu_1 \\ \nu_2 \\ \nu_3 \end{pmatrix}, \quad (145)$$

where  $\nu_e, \nu_\mu, \nu_\tau$  are the flavor eigenstates,  $\nu_1, \nu_2, \nu_3$  are the mass eigenstates and the  $3 \times 3$  mixing matrix is the leptonic mixing matrix<sup>58–61</sup>. For the case of three Dirac neutrinos, in the standard PDG parameterization<sup>25</sup>, involving three angles  $\theta_{12}, \theta_{23}, \theta_{13}$  and the Dirac-like CP violating phase  $\delta_l$  the mixing matrix has the form

$$V_{\text{PMNS}} = \begin{pmatrix} c_{12}c_{13} & s_{12}c_{13} & s_{13}e^{-i\delta_l} \\ -s_{12}c_{23} - c_{12}s_{23}s_{13}e^{i\delta_l} & c_{12}c_{23} - s_{12}s_{23}s_{13}e^{i\delta_l} & s_{23}c_{13} \\ s_{12}s_{23} - c_{12}c_{23}s_{13}e^{i\delta_l} & -c_{12}s_{23} - s_{12}c_{23}s_{13}e^{i\delta_l} & c_{23}c_{13} \end{pmatrix}, \quad (146)$$

with  $s_{ij} = \sin\theta_{ij}$ ,  $c_{ij} = \cos\theta_{ij}$ . In the case of the Majorana neutrinos, there are extra phases which cannot be removed. Therefore, the above matrix takes the following form

$$\begin{pmatrix} c_{12}c_{13} & s_{12}c_{13} & s_{13}e^{-i\delta_l} \\ -s_{12}c_{23} - c_{12}s_{23}s_{13}e^{i\delta_l} & c_{12}c_{23} - s_{12}s_{23}s_{13}e^{i\delta_l} & s_{23}c_{13} \\ s_{12}s_{23} - c_{12}c_{23}s_{13}e^{i\delta_l} & -c_{12}s_{23} - s_{12}c_{23}s_{13}e^{i\delta_l} & c_{23}c_{13} \end{pmatrix} \begin{pmatrix} e^{i\alpha_1/2} & 0 & 0 \\ 0 & e^{i\alpha_2/2} & 0 \\ 0 & 0 & 1 \end{pmatrix}, \quad (147)$$

where  $\alpha_1$  and  $\alpha_2$  are the Majorana phases which do not play any role in neutrino oscillations.

### 5.2.2. Texture 6 zero lepton mass matrices

Parallel to the case of quarks, there are a total number of 144 possible cases of texture 6 zero mass matrices. In the case of lepton mass matrices, for each of the 144 combinations, there are 6 cases each corresponding to normal/ inverted hierarchy and degenerate scenario of neutrino masses for Majorana neutrinos as well as Dirac neutrinos, leading to a total of 864 cases. Recently, a detailed analysis of these cases was carried out by Mahajan *et al.*<sup>174</sup>, revealing several interesting points. In particular, their investigations for Dirac neutrinos show that there are no viable texture 6 zero lepton mass matrices for normal/ inverted hierarchy as well as degenerate scenario of neutrino masses. For the case of Majorana neutrinos, again all the cases pertaining to inverted hierarchy and degenerate scenario of neutrino masses are ruled out. For normal hierarchy of Majorana neutrinos, the analysis reveals that out of 144, only 16 combinations are compatible with current neutrino oscillation data at  $3\sigma$  C.L.. For a detailed discussion, we refer the readers to Ref. 174.

Keeping in mind the important role played by Fritzsch-like mass matrices in understanding the quark and neutrino mixing phenomenology, in the present work, we would like to present the details regarding this case. Recently, using Fritzsch-like texture 6 zero lepton mass matrices, detailed predictions for cases pertaining to normal/inverted hierarchy as well as degenerate scenario of neutrino masses have been carried out for the case of Majorana neutrinos by Randhawa *et al.*<sup>167</sup> and for Dirac neutrinos by Ahuja *et al.*<sup>173</sup>.

Without getting into the detailed methodology and inputs used in these analyses<sup>167,173</sup>, it is instructive to present some of the discussions leading to key

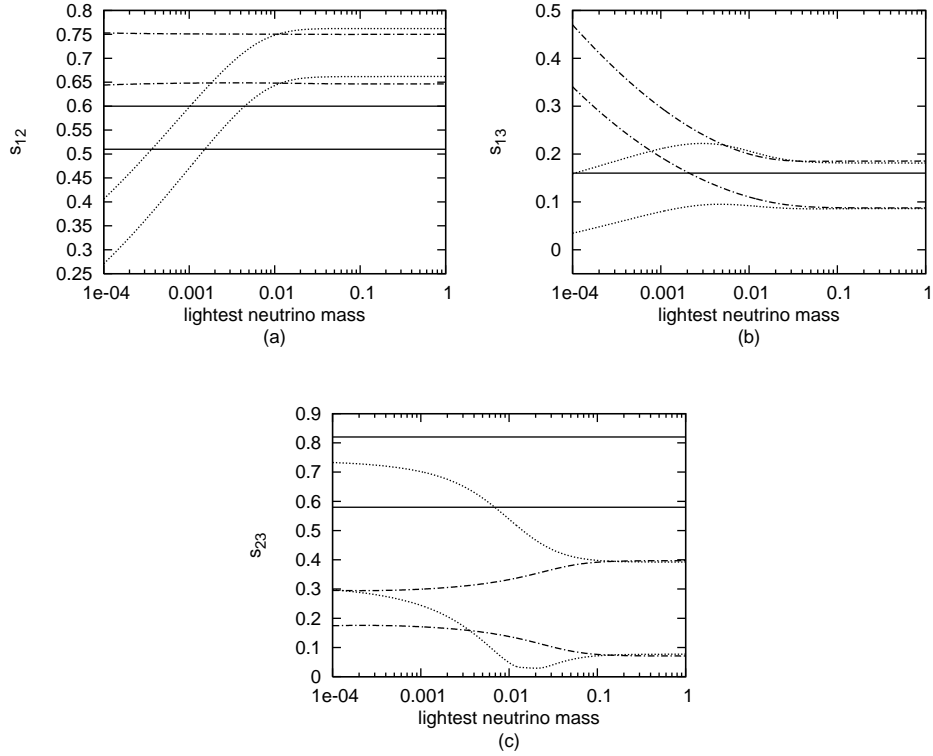


Fig. 13. Plots showing variation of mixing angles  $s_{12}$ ,  $s_{13}$  and  $s_{23}$  with the lightest neutrino mass for texture 6 zero case of Majorana neutrinos. The dotted lines and the dot-dashed lines depict the limits obtained assuming normal and inverted hierarchy respectively, the solid horizontal lines show the  $3\sigma$  limits of the mixing angles.

conclusions. In particular, for both Majorana and Dirac neutrinos, all the cases pertaining to inverted hierarchy and degenerate scenario of neutrino masses seem to be ruled out. For the case of Majorana neutrinos, following Ref. 167, the ruling out of inverted hierarchy can be understood from the graphs shown in Fig. 13, wherein by giving full variations to other parameters, plots of the mixing angles  $s_{12}$ ,  $s_{23}$  and  $s_{13}$  against the lightest neutrino mass have been given. The dotted lines and the dot-dashed lines depict the limits obtained assuming normal and inverted hierarchy respectively, the solid horizontal lines show the  $3\sigma$  limits of the plotted mixing angle. Interestingly, it is clear from Figs. 13(a) and 13(c) that inverted hierarchy is ruled out by the experimental limits on  $s_{12}$  and  $s_{23}$  respectively, however, in the case of Fig. 13(b) inverted hierarchy seems to be allowed for  $m_{\nu_1} \gtrsim 0.001$ . To this end, it may be noted that to rule out inverted hierarchy any single plot of Fig. 13 is sufficient.

Coming to the degenerate scenarios of Majorana neutrinos characterized by either  $m_{\nu_1} \lesssim m_{\nu_2} \sim m_{\nu_3} \sim 0.1$  eV or  $m_{\nu_3} \sim m_{\nu_1} \lesssim m_{\nu_2} \sim 0.1$  eV corresponding



to normal hierarchy and inverted hierarchy respectively. For both these degenerate scenarios Figs. 13(a) and 13(c) can again be used to rule them out at  $3\sigma$  C.L.. It needs to be mentioned that while plotting these figures the range of the lightest neutrino mass is taken to be  $10^{-5} \text{ eV} - 10^{-1} \text{ eV}$ , which includes the neutrino masses corresponding to degenerate scenario, therefore by discussion similar to the one given for ruling out inverted hierarchy, degenerate scenarios of neutrino masses are ruled out as well.

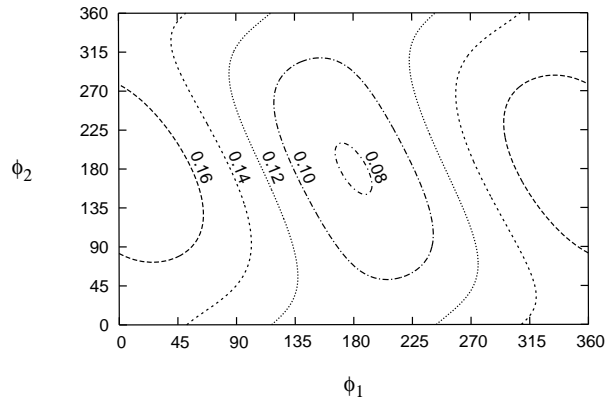


Fig. 14. The contours of  $s_{13}$  in  $\phi_1 - \phi_2$  plane for texture 6 zero matrices for the normal hierarchy case of Majorana neutrinos.

After ruling out the cases pertaining to inverted hierarchy and degenerate scenarios, the authors discuss the normal hierarchy cases. Interestingly, the possibility when charged leptons are in flavor basis is also completely ruled out. For the case of  $M_l$  being texture specific, the viable ranges of neutrino masses, mixing angle  $s_{13}$ , Jarlskog's rephasing invariant parameter in the leptonic sector  $J_l$ , Dirac-like CP violating phase in the leptonic sector  $\delta_l$  and effective neutrino mass  $\langle m_{ee} \rangle$  related to neutrinoless double beta decay  $(\beta\beta)_{0\nu}$  have been evaluated. One finds that the calculated values of parameters  $m_{\nu_1}$ ,  $s_{13}$ ,  $J_l$  and  $\langle m_{ee} \rangle$  are well within the ranges obtained by other similar approaches. It may be added that the predicted lower limit on  $s_{13}$  is in agreement with recent measurements of  $s_{13}$ . Further, a measurement of effective mass  $\langle m_{ee} \rangle$ , through the  $(\beta\beta)_{0\nu}$  decay experiments, would also have implications for these kind of mass matrices. Besides the above mentioned parameters, the implications of  $s_{13}$  on the phases  $\phi_1$  and  $\phi_2$  have also been considered.

To this end, in Fig. 14 the contours for  $s_{13}$  in  $\phi_1 - \phi_2$  plane have been shown. From the figure it is clear that  $s_{13}$  plays an important role in constraining the phases, in particular if lower limit of  $s_{13}$  is on the higher side, then  $\phi_1$  is restricted to I or IV quadrant.

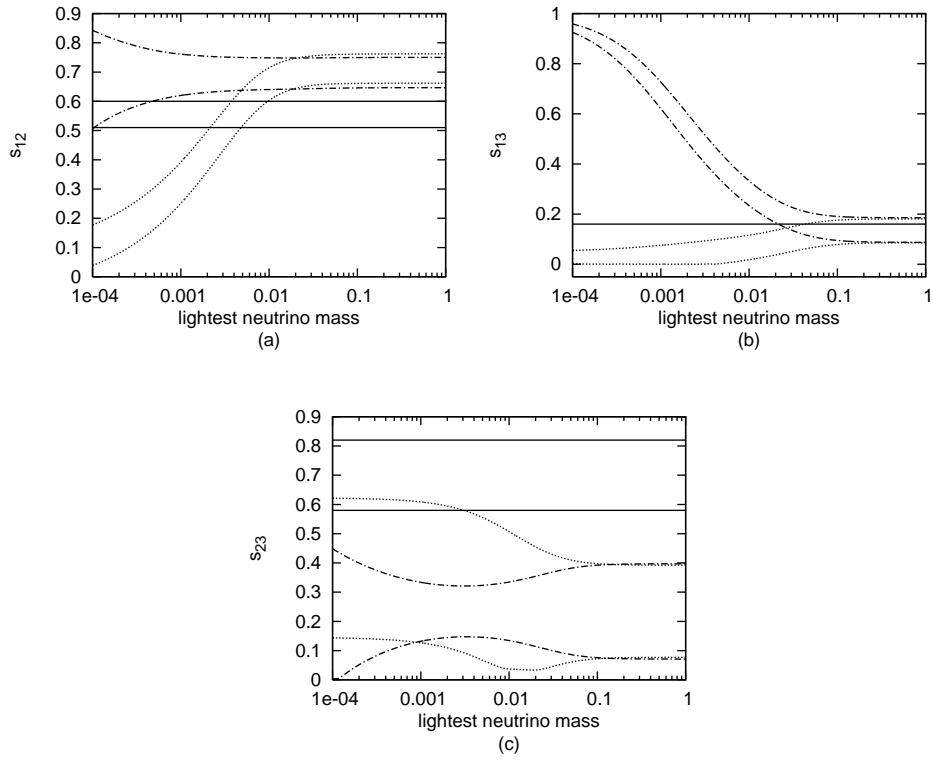


Fig. 15. Plots showing variation of mixing angles  $s_{12}$ ,  $s_{13}$  and  $s_{23}$  with lightest neutrino mass for texture 6 zero case of Dirac neutrinos. The dotted lines and the dot-dashed lines depict the limits obtained assuming normal and inverted hierarchy respectively, the solid horizontal lines show the  $3\sigma$  limits of the mixing angles.

After studying the implications of texture 6 zero neutrino mass matrices on the various hierarchies of neutrino masses for the Majorana neutrinos, it becomes desirable to carry out similar investigations for Dirac neutrinos. As expected, similar to the Majorana case, all the cases pertaining to inverted hierarchy and degenerate scenarios of neutrino masses seem to be ruled out. Parallel to the case of Majorana neutrinos, in Fig. 15, by giving full variations to other parameters, the mixing angles against the lightest neutrino mass have been plotted. The dotted lines and the dot-dashed lines depict the limits obtained assuming normal and inverted hierarchy respectively, the solid horizontal lines show the  $3\sigma$  limits of the plotted mixing angle. A general comparison of these plots with those for Majorana neutrinos, shown in

Fig. 13, suggests that the variation of the mixing angles  $s_{12}$  and  $s_{23}$  with the lightest neutrino mass does not depict much change for the two different types of neutrinos. Also, it is easily evident from the Fig. 15(c) that inverted hierarchy is ruled out by the experimental limits on the mixing angle  $s_{23}$ .

One can easily check that degenerate scenarios characterized by either  $m_{\nu_1} \lesssim m_{\nu_2} \sim m_{\nu_3} \sim 0.1$  eV or  $m_{\nu_3} \sim m_{\nu_1} \lesssim m_{\nu_2} \sim 0.1$  eV are clearly ruled out from Figs. 15(a) and 15(c). This can be understood by noting that around 0.1 eV, the limits obtained assuming normal and inverted hierarchies have no overlap with the experimental limits of angles  $s_{12}$  and  $s_{23}$ .

For the normal hierarchy of neutrino masses, similar to the texture 6 zero mass matrices for Majorana neutrinos, the possibility of charged leptons being in the flavor basis is again completely ruled out. Corresponding to the case when  $M_l$  is considered texture specific, the viable ranges of neutrino masses, mixing angle  $s_{13}$ , Jarlskog's rephasing invariant parameter in the leptonic sector  $J_l$ , Dirac-like CP violating phase in the leptonic sector  $\delta_l$  have again been evaluated. Interestingly, the viable ranges of masses  $m_{\nu_1}$ ,  $m_{\nu_2}$ , and  $m_{\nu_3}$  as well as the range of  $s_{13}$  for Dirac neutrinos are much narrower compared to the Majorana case. Further, compared to the Majorana neutrinos, the upper limit of  $J_l$  now cones out to be considerably lower.

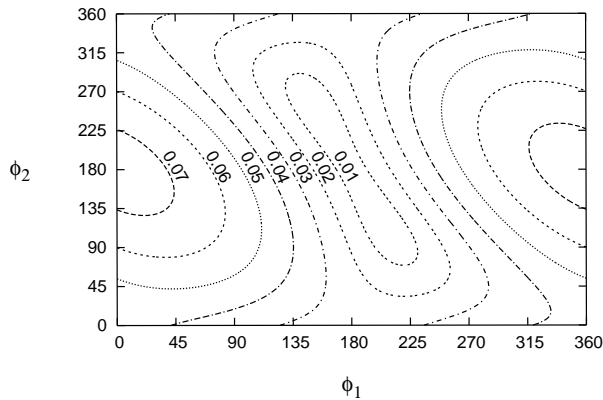


Fig. 16. The contours of  $s_{13}$  in  $\phi_1 - \phi_2$  plane for texture 6 zero matrices for the normal hierarchy case of Dirac neutrinos.

For Dirac neutrinos also, the implications of the mixing angle  $s_{13}$  on the phases

$\phi_1$  and  $\phi_2$  have been examined. In this context, in Fig. 16 the contours for  $s_{13}$  in  $\phi_1 - \phi_2$  plane have been plotted. These contours indicate that the mixing angle  $s_{13}$  constrains both the phases  $\phi_1$  and  $\phi_2$ . For example, if the lower limit of  $s_{13}$  is around 0.07, then  $\phi_1$  lies in either the I or the IV quadrant and  $\phi_2$  lies between  $135^\circ - 225^\circ$ .

### 5.2.3. *Texture 5 zero lepton mass matrices*

Similar to the case of texture 6 zero lepton mass matrices, the implications for different hierarchies in the case of Fritzsch-like and non Fritzsch-like texture 5 zero lepton mass matrices have also been investigated for both Majorana and Dirac neutrinos<sup>167,173,180</sup>. Following Gupta<sup>180</sup>, one finds that for the two types of neutrinos, corresponding to normal/ inverted hierarchy and degenerate scenario of neutrino masses 360 cases each have been considered for carrying out the analysis, making it a total of 2160 cases. For Majorana neutrinos with normal hierarchy of neutrino masses, out of the 360 combinations, 67 are compatible with the neutrino mixing data. Most of the phenomenological implications of combinations of different categories are similar, however, still these can be experimentally distinguished with more precise measurements of  $\theta_{13}$  and  $\theta_{23}$ . Interestingly, degenerate scenario of Majorana neutrinos is completely ruled out by the existing data. In the case of inverted hierarchy, 24 combinations out of 360 are compatible with the neutrino mixing data. For Dirac neutrinos with normal hierarchy of neutrino masses, as compared to Majorana cases, out of 360 only 44 combinations are compatible with neutrino mixing data. Interestingly, 6 combinations out of 44 can accommodate degenerate Dirac neutrinos. For inverted hierarchy, 24 combinations are compatible with the existing data. Again, similar to the discussion presented for the case of texture 6 zero lepton mass matrices, for the case of texture 5 zero matrices also, we would like to present some of the details of the analyses<sup>167,173</sup> carried out for the Fritzsch-like case.

Following Ref. 167, for texture 5 zero cases, we first discuss the case when  $D_l = 0$  and  $D_\nu \neq 0$ . In Fig. 17 the plots of the mixing angles against the lightest neutrino mass for both normal and inverted hierarchy for a particular value of  $D_\nu = \sqrt{m_{\nu_3}}$  have been given. Interestingly, texture 5 zero  $D_l = 0$  case shows a big change in the behaviour of the mixing angles versus the lightest neutrino mass as compared to the texture 6 zero case shown in Fig. 13. A look at Fig. 17(b) clearly shows that inverted hierarchy as well as degenerate scenario corresponding to it are ruled out by the experimental limits on  $s_{13}$ . A closer look at Figs. 17(a) and 17(c) reveals that the region pertaining to inverted hierarchy, depicted by dot-dashed lines, shows an overlap with the experimental limits on  $s_{12}$  and  $s_{23}$  respectively, depicted by solid horizontal lines, around the region when neutrino masses are almost degenerate. This suggests that, for these angles, in case the degenerate scenario is ruled out inverted hierarchy is also ruled out.

Coming to the texture 5 zero  $D_\nu = 0$  and  $D_l \neq 0$  case, interestingly the plots of mixing angles against the lightest neutrino mass are very similar to those in Fig. 13

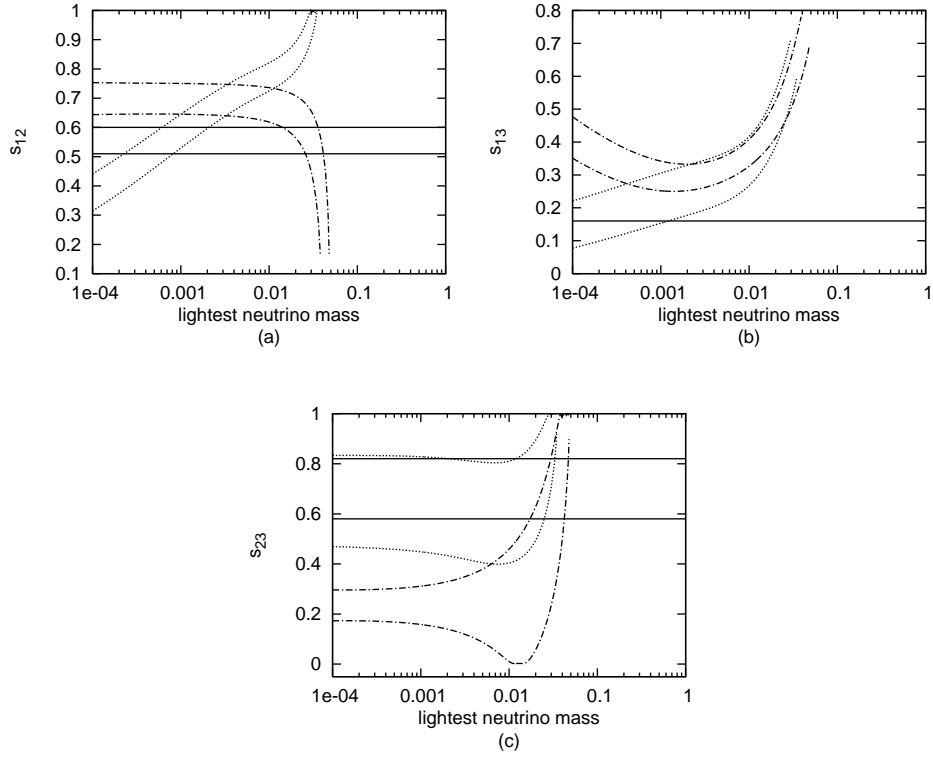


Fig. 17. Plots showing variation of mixing angles  $s_{12}$ ,  $s_{13}$  and  $s_{23}$  with lightest neutrino mass for texture 5 zero  $D_l = 0$  case of Majorana neutrinos, with a value  $D_\nu = \sqrt{m_{\nu_3}}$ . The representations of the curves remain the same as in Fig. 13.

Table 5. Calculated ranges for neutrino mass and mixing parameters obtained by varying  $\phi_1$  and  $\phi_2$  from 0 to  $2\pi$  for the normal hierarchy cases of Majorana neutrinos. All masses are in eV.

Parameter	5 zero $D_l = 0$ ( $M_l$ 3 zero, $M_{\nu D}$ 2 zero)	5 zero $D_\nu = 0$ ( $M_l$ 2 zero, $M_{\nu D}$ 3 zero)
$m_{\nu_1}$	0.00020 - 0.0020	0.0005 - 0.0032
$m_{\nu_2}$	0.0086 - 0.0094	0.0086 - 0.0097
$m_{\nu_3}$	0.0421 - 0.0547	0.0421 - 0.055
$s_{13}$	0.076 - 0.160	0.055 - 0.160
$J_l$	$\sim 0 - 0.025$	$\sim 0 - 0.037$
$\delta_l$	$0^\circ - 50.0^\circ$	$0^\circ - 90.0^\circ$
$\langle m_{ee} \rangle$	0.0029 - 0.0059	0.0028 - 0.0068

pertaining to the texture 6 zero case. By similar arguments, this case is also ruled out for inverted hierarchy as well as for the two degenerate scenarios.

Coming to the normal hierarchy cases, for the two cases of texture 5 zero mass matrices, in Table 5 the viable ranges of neutrino masses, mixing angle  $s_{13}$ , Jarlskog's rephasing invariant parameter in the leptonic sector  $J_l$ , Dirac-like CP vi-

olating phase in the leptonic sector  $\delta_l$  and effective neutrino mass  $\langle m_{ee} \rangle$  related to neutrinoless double beta decay  $(\beta\beta)_{0\nu}$  have been presented. Considering the  $D_l = 0$  case, interestingly, results are obtained for both the possibilities of  $M_l$  having Fritzsche-like structure as well as  $M_l$  being in the flavor basis. When  $M_l$  is assumed to have Fritzsche-like structure, the possibility of  $D_\nu \neq 0$  considerably affects the viable range of  $m_{\nu_1}$  as well as of  $s_{13}$ . The Pontecorvo-Maki-Nakagawa-Sakata (PMNS) mixing matrix<sup>58–61</sup> constructed for this case is as follows

$$U = \begin{pmatrix} 0.7898 - 0.8571 & 0.5035 - 0.5971 & 0.0761 - 0.1600 \\ 0.1845 - 0.4413 & 0.5349 - 0.7459 & 0.5725 - 0.8135 \\ 0.3546 - 0.5615 & 0.3926 - 0.6689 & 0.5652 - 0.8107 \end{pmatrix}. \quad (148)$$

When  $M_l$  is considered in the flavor basis, one gets a very narrow range of masses,  $m_{\nu_1} \sim 0.00063$ ,  $m_{\nu_2} = 0.0086 - 0.0088$  and  $m_{\nu_3} = 0.0534 - 0.0546$ , for which 5 zero matrices are viable. Also for this case, there is a limited overlap of with its recent measurements. In case the value of  $s_{13}$  gets constrained further, then it may have implications for this case.

For the texture 5 zero  $D_\nu = 0$  case, when  $M_l$  is considered in the flavor basis, one does not find any viable solution, however when it has Fritzsche-like structure there are a few important observations. The range of  $m_{\nu_1}$  gets extended as compared to the texture 6 zero case, whereas compared to the texture 5 zero  $D_l = 0$  case, both the lower and upper limits of  $m_{\nu_1}$  have higher values. Interestingly, this case has the widest  $s_{13}$  range among all the cases considered here. The PMNS matrix corresponding to this case does not show any major variation compared to the earlier case, except that the ranges of some of the elements like  $U_{\mu 1}$ ,  $U_{\mu 2}$ ,  $U_{\tau 1}$  and  $U_{\tau 2}$  become little wider. This can be understood when one realizes that  $D_l$  can take much wider variation compared to  $D_\nu$ .

Coming to the case of Dirac neutrinos<sup>173</sup>, we first discuss the texture 5 zero case when  $D_l = 0$  and  $D_\nu \neq 0$ . Again to facilitate comparison with the earlier texture 5 zero  $D_l = 0$  case for Majorana neutrinos, in Fig. 18 the mixing angles against the lightest neutrino mass for both normal and inverted hierarchy for a particular value of  $D_\nu = \sqrt{m_{\nu_3}}$  have been plotted. Interestingly, we find that similar to the texture 6 zero case, the texture 5 zero  $D_l = 0$  case for Dirac neutrinos also shows a big change in the behaviour of  $s_{13}$  versus the lightest neutrino mass as compared to the corresponding case of texture 5 zero matrices shown in Fig. 17. This again suggests that the variation of the other two mixing angles,  $s_{12}$  and  $s_{23}$ , with the lightest neutrinos is not much dependent on the type of neutrinos for the texture 5 zero  $D_l = 0$  case also. The graph of  $s_{13}$  versus the lightest neutrino mass, shown in Fig. 18(b) immediately rules out inverted hierarchy by experimental limits on angle  $s_{13}$ .

For the texture 5 zero  $D_\nu = 0$  and  $D_l \neq 0$  case, similar to the Majorana case, the plots of mixing angles against the lightest neutrino mass are very similar to Fig. 15 pertaining to the texture 6 zero case of Dirac neutrinos. Therefore, arguments similar to the ones for the texture 6 zero case lead us to conclude that both inverted

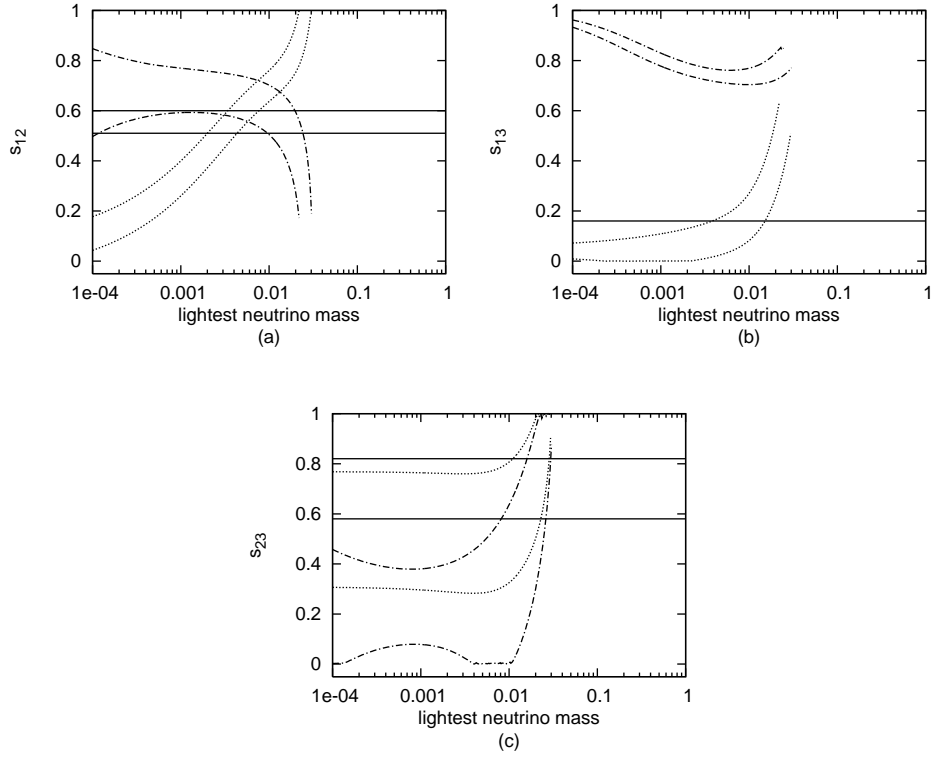


Fig. 18. Plots showing variation of mixing angles  $s_{12}$ ,  $s_{13}$  and  $s_{23}$  with lightest neutrino mass for texture 5 zero  $D_l = 0$  case of Dirac neutrinos, with a value  $D_\nu = \sqrt{m_{\nu_3}}$ . The representations of the curves remain the same as in Fig. 15.

Table 6. Calculated ranges for neutrino mass and mixing parameters obtained by varying  $\phi_1$  and  $\phi_2$  from 0 to  $2\pi$  for the normal hierarchy cases of Dirac neutrinos. All masses are in eV.

Parameter	5 zero $D_l = 0$ ( $M_l$ 3 zero, $M_{\nu D}$ 2 zero)	5 zero $D_\nu = 0$ ( $M_l$ 2 zero, $M_{\nu D}$ 3 zero)
$m_{\nu_1}$	0.00032 - 0.0063	0.0025 - 0.0079
$m_{\nu_2}$	0.0086 - 0.0112	0.0089 - 0.0122
$m_{\nu_3}$	0.0421 - 0.0550	0.0422 - 0.0552
$s_{13}$	0.005 - 0.160	0.0001 - 0.135
$J_l$	$\sim 0$ - 0.027	$\sim 0$ - 0.028
$\delta_l$	$0^\circ$ - $80.2^\circ$	$0^\circ$ - $90.0^\circ$

hierarchy as well as degenerate scenarios of neutrino masses are ruled out for this case as well. It may be mentioned that similarities observed in the mixing angles variation with the lightest neutrino mass for the texture 5 zero  $D_\nu = 0$  and the texture 6 zero cases of both Majorana and Dirac neutrinos can be understood by noting that a very strong hierarchy in the case of charged leptons reduces the texture 5 zero  $D_\nu = 0$  case essentially to the texture 6 zero case only.

Coming to the normal hierarchy cases for the texture 5 zero mass matrices corresponding to Dirac neutrinos, we first consider the  $D_l = 0$  case. Analogous to the corresponding case of Majorana neutrinos, both the possibilities of  $M_l$  having Fritzsch-like structure as well as  $M_l$  being in the flavor basis yield viable ranges for the various phenomenological quantities presented in Table 6. One finds that going from texture 6 zero to texture 5 zero  $D_l = 0$  case, the viable ranges of  $m_{\nu_1}$  and  $m_{\nu_3}$  get much broader. Also, the upper limit of  $s_{13}$  is pushed considerably higher which can be understood by noting that  $s_{13}$  is quite sensitive to variations in  $D_\nu$ . The Pontecorvo-Maki-Nakagawa-Sakata (PMNS) mixing matrix<sup>58–61</sup> obtained for the texture 5 zero  $D_l = 0$  case is given by

$$U = \begin{pmatrix} 0.7897 - 0.8600 & 0.5036 - 0.5998 & 0.0054 - 0.1600 \\ 0.1838 - 0.4748 & 0.4859 - 0.7438 & 0.5726 - 0.8194 \\ 0.3107 - 0.5633 & 0.3974 - 0.6890 & 0.5650 - 0.8142 \end{pmatrix}. \quad (149)$$

For the case of  $M_l$  being in the flavor basis, the range of masses so obtained are  $m_{\nu_1} = 0.0020 - 0.0040$ ,  $m_{\nu_2} = 0.0088 - 0.0100$  and  $m_{\nu_3} = 0.0422 - 0.0548$ . The range of the mixing angle  $s_{13}$  is  $0.0892 - 0.1594$ , indicating that the lower limit of  $s_{13}$  is considerably high which implies that refinements in the measurement of this angle would have consequences for this case of texture 5 zero mass matrices for Dirac neutrinos.

A comparison of the texture 5 zero  $D_l = 0$  case of Dirac neutrino with the corresponding case of Majorana neutrinos, presented in Table 6 indicates that now there is an expansion of the range of  $m_{\nu_1}$ , in particular its upper limit is pushed higher. There is also a significant lowering down of the lower limit of the angle  $s_{13}$  and a considerable increase in the upper limit of the Dirac-like CP violating phase  $\delta_l$  for the Dirac neutrinos as compared to the Majorana neutrinos. This difference in the viable ranges of these quantities could provide clues to neutrinos being Dirac or Majorana.

Considering the texture 5 zero  $D_\nu = 0$  case for Dirac neutrinos, again the possibility of  $M_l$  being in the flavor basis does not yield any results, however the case of  $M_l$  having Fritzsch-like structure reveals several interesting facts. For Dirac neutrinos, a comparison of the texture 5 zero  $D_\nu = 0$  case with the texture 5 zero  $D_l = 0$  case shows both the lower and upper limits of  $m_{\nu_1}$  have higher values. Interestingly, for this case the lower limit of  $s_{13}$  becomes almost 0. Also, it may be noted that for this case one gets a wide range of the Dirac-like CP violating phase  $\delta_l$ . The PMNS matrix corresponding to this case is quite similar to the one presented in Eq. (149), except for somewhat wider ranges of the elements  $U_{e3}$ ,  $U_{\mu 2}$ ,  $U_{\mu 2}$ ,  $U_{\tau 1}$  and  $U_{\tau 2}$ .

#### 5.2.4. Texture 4 zero lepton mass matrices

Like the case of quarks, the number of viable possibilities for the case of texture 4 zero lepton mass matrices is also quite large. Recently, an interesting analysis has been carried out by Branco *et al.*<sup>181</sup> wherein they have classified and analyzed



the texture 4 zero *ansätze* for the charged lepton mass matrix and the neutrino mass matrix with a parallel structure. It has been pointed out that these *ansätze* do have physical implications, since not all the zeros can be obtained simultaneously, just by making weak basis (WB) transformations. Further, it has been shown that these texture 4 zero *ansätze* can be classified in four classes, one of which is not compatible with the experimental data. For the remaining three classes, the authors have presented a summary of predictions pertaining to the lightest neutrino mass and the effective Majorana mass.

Similar, to the discussion presented for the texture 4 zero quark mass matrices, for the case of leptons also we have presented details pertaining to only the Fritzsch-like texture 4 zero mass matrices. Before proceeding further, for ready reference as well as to facilitate subsequent discussions, we would again like to mention that most of the attempts to understand the pattern of neutrino masses and mixings have been carried out using the seesaw mechanism<sup>175–179</sup> given by

$$M_\nu = -M_{\nu D}^T (M_R)^{-1} M_{\nu D}, \quad (150)$$

where  $M_{\nu D}$  and  $M_R$  are respectively the Dirac neutrino mass matrix and the right handed Majorana neutrino mass matrix. Similarly, we would like to reiterate that the predictions are quite different, on the one hand when texture is imposed only on  $M_{\nu D}$  and  $M_R$  and on the other hand when  $M_\nu$  and  $M_{\nu D}$  have the same texture by imposing ‘texture invariant conditions’<sup>22,168</sup>.

We begin by discussing briefly the attempts<sup>22,168,172</sup> made by a few authors regarding the texture 4 zero mass matrices. Assuming normal hierarchy of masses as well as imposing texture 4 zero structure on  $M_{\nu D}$  and charged lepton mass matrices, Xing<sup>22</sup> has not only shown the compatibility of these with neutrino oscillation phenomenology but have also shown the seesaw invariance of these structures under certain conditions. Very recently, for normal hierarchy, Matsuda *et al.*<sup>168</sup> have shown that texture 4 zero lepton mass matrices can accommodate large values of mixing angle  $s_{13}$ . In particular, by imposing texture invariant conditions they have shown that  $M_\nu$  can be texture 2 zero when one assumes Fritzsch-like texture 2 zero structure for  $M_{\nu D}$ ,  $M_R$  as well as for charged lepton mass matrix. Further, for both Majorana and Dirac neutrinos, Ahuja *et al.*<sup>172</sup> have carried out detailed and comprehensive investigation regarding the compatibility of texture 4 zero lepton mass matrices with the normal/inverted hierarchy, degenerate scenario of neutrino masses and have arrived at some very interesting conclusions. In the present work, we have presented essential details of the analysis by Ref. 172.

For the sake of the convenience of the reader as well as for better understanding of the conclusions by Ref. 172, we first define the Fritzsch-like texture 4 zero mass matrices, e.g.,

$$M_l = \begin{pmatrix} 0 & A_l & 0 \\ A_l^* & D_l & B_l \\ 0 & B_l^* & C_l \end{pmatrix}, \quad M_{\nu D} = \begin{pmatrix} 0 & A_\nu & 0 \\ A_\nu^* & D_\nu & B_\nu \\ 0 & B_\nu^* & C_\nu \end{pmatrix}, \quad (151)$$

$M_l$  and  $M_{\nu D}$  respectively corresponding to charged lepton and Dirac neutrino mass matrices. The matrices  $M_l$  and  $M_{\nu D}$  together are referred to as the texture 4 zero mass matrices, each being texture 2 zero type with  $D_l$  and  $D_\nu$  being non zero. Corresponding to these mass matrices, the PMNS matrix for Dirac neutrinos is expressed as

$$U = O_l^\dagger Q_l P_{\nu D} O_{\nu D}, \quad (152)$$

where  $Q_l$ ,  $P_{\nu D}$  are the diagonal phase matrices and  $O_l$ ,  $O_{\nu D}$  correspond to the orthogonal transformations used for diagonalizing the matrices  $M_l$  and  $M_{\nu D}$ . For the two types of neutrinos, the details of diagonalization procedure of the mass matrices and the elements of the PMNS matrices have been presented in Appendices A and B respectively.

The analysis by Ref. 172 incorporates the following inputs at  $3\sigma$  C.L.,

$$\Delta m_{12}^2 = (7.1 - 8.9) \times 10^{-5} \text{ eV}^2, \quad \Delta m_{23}^2 = (2.0 - 3.2) \times 10^{-3} \text{ eV}^2, \quad (153)$$

$$\sin^2 \theta_{12} = 0.24 - 0.40, \quad \sin^2 \theta_{23} = 0.34 - 0.68, \quad \sin^2 \theta_{13} \leq 0.040. \quad (154)$$

For the purpose of calculations, the lightest neutrino mass, the phases  $\phi_1$ ,  $\phi_2$  and the elements of the mass matrices  $D_{l,\nu}$  are considered as free parameters, the other two masses are constrained by  $\Delta m_{12}^2 = m_{\nu_2}^2 - m_{\nu_1}^2$  and  $\Delta m_{23}^2 = m_{\nu_3}^2 - m_{\nu_2}^2$  in the normal hierarchy case and by  $\Delta m_{23}^2 = m_{\nu_2}^2 - m_{\nu_3}^2$  in the inverted hierarchy case. For all the three hierarchies, the explored range of the lightest neutrino mass is  $10^{-8} \text{ eV} - 10^{-1} \text{ eV}$ . In the absence of any constraint on the phases,  $\phi_1$  and  $\phi_2$  have again been given full variation from 0 to  $2\pi$ .

To begin with, the authors consider the inverted hierarchy case for both Majorana and Dirac neutrinos. In this context, it may be mentioned that for both the possibilities texture is imposed only on  $M_{\nu D}$ , with no such restriction on  $M_\nu$  for the Majorana case. For Majorana neutrinos, Figs. 19(a), 19(b) and 19(c) present the plots pertaining to the parameter space corresponding to any of the two mixing angles by constraining the third angle by its values given in Eq. (154) while giving full allowed variation to other parameters. Also included in the figures are blank rectangular regions indicating the experimentally allowed  $3\sigma$  region of the plotted angles. Interestingly, a general look at these figures reveals that the case of inverted hierarchy seems to be ruled out. From Fig. 19(a) showing the plot of angles  $\theta_{12}$  versus  $\theta_{23}$ , one can immediately conclude that the plotted parameter space includes the experimentally allowed range of  $\theta_{23}$ , however it excludes the experimentally allowed range of  $\theta_{12}$ . This clearly indicates that at  $3\sigma$  C.L. inverted hierarchy is not viable. The conclusions arrived above can be further checked from Figs. 19(b) and 19(c) wherein  $\theta_{12}$  versus  $\theta_{13}$  and  $\theta_{23}$  versus  $\theta_{13}$  have been plotted respectively by constraining angles  $\theta_{23}$  and  $\theta_{12}$ . Both the figures indicate that the plotted parameter space does not include simultaneously the experimental bounds of the plotted angles, e.g.,  $\theta_{12}$  in the case of Fig. 19(b) and  $\theta_{13}$  in Fig. 19(c).

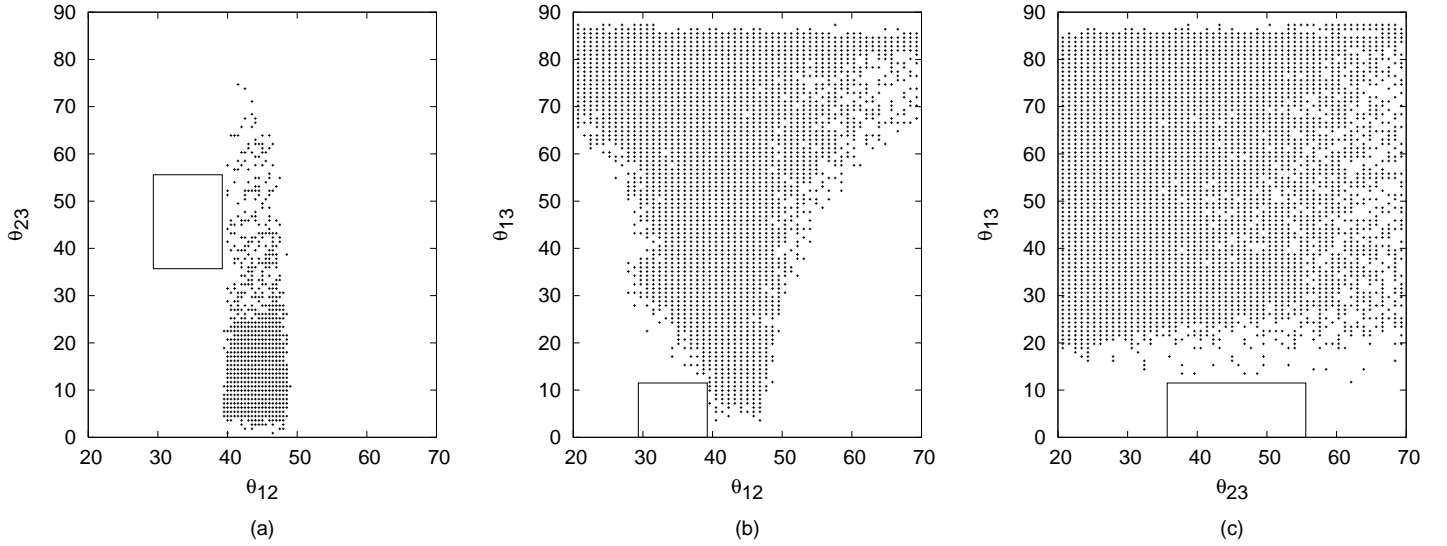


Fig. 19. Plots showing the parameter space corresponding to any of the two mixing angles by constraining the third angle by its experimental limits and giving full allowed variation to other parameters for Majorana neutrinos. The blank rectangular region indicates the experimentally allowed  $3\sigma$  region of the plotted angles.

For Dirac neutrinos, again inverted hierarchy seems to be ruled out using graphs which can be plotted in a manner similar to the Majorana case by constraining one mixing angle by its experimental limits and plotting the parameter space for the other two angles. Again, the plotted parameter space does not overlap with the experimental limits of at least one of the plotted angles, thereby indicating that inverted hierarchy is ruled out at  $3\sigma$  C.L. for Dirac neutrinos as well.

For Majorana or Dirac neutrinos the cases of neutrino masses being degenerate, characterized by either  $m_{\nu_1} \lesssim m_{\nu_2} \sim m_{\nu_3} \lesssim 0.1$  eV or  $m_{\nu_3} \sim m_{\nu_1} \lesssim m_{\nu_2} \lesssim 0.1$  eV corresponding to normal and inverted hierarchy respectively, are again ruled out. Considering degenerate scenario corresponding to inverted hierarchy, Figs. 19 can again be used to rule out degenerate scenario at  $3\sigma$  C.L. for Majorana neutrinos respectively. It needs to be mentioned that while plotting these figures the range of the lightest neutrino mass is taken to be  $10^{-8}$  eV –  $10^{-1}$  eV, which includes the neutrino masses corresponding to degenerate scenario, therefore by discussion similar to the one given for ruling out inverted hierarchy, degenerate scenario of neutrino masses is ruled out as well.

Coming to degenerate scenario corresponding to normal hierarchy, one can easily show that this is ruled out again. To this end, in Fig. 20, by giving full variation to other parameters, the mixing angle  $\theta_{12}$  against the lightest neutrino mass  $m_{\nu_1}$  has been plotted. Fig. 20(a) corresponds to the case of Majorana neutrinos and Fig. 20(b) to the case of Dirac neutrinos. From the figures one can immediately find

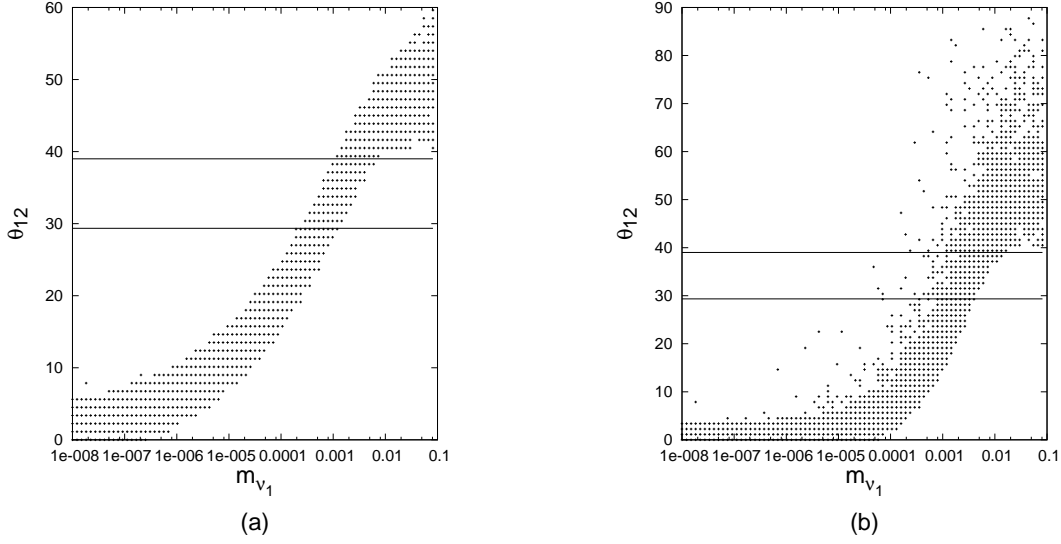


Fig. 20. Plots showing variation of mixing angle  $\theta_{12}$  with lightest neutrino mass  $m_{\nu_1}$  by giving full variation to other parameters for (a) Majorana neutrinos and (b) Dirac neutrinos. The parallel lines indicate the  $3\sigma$  limits of angle  $\theta_{12}$ .

Table 7. Calculated ranges for neutrino mass and mixing parameters for the normal hierarchy case of texture 4 zero lepton mass matrices. All masses are in eV.

	$M_l$ being Fritzsch-like		$M_l$ being in the flavor basis	
	Dirac case	Majorana case	Dirac case	Majorana case
$m_{\nu_1}$	$5.73 \times 10^{-5} - 0.012$	$2.47 \times 10^{-4} - 0.006$	$(1.63 - 6.28) \times 10^{-3}$	$(0.402 - 2.06) \times 10^{-3}$
$m_{\nu_2}$	$0.0084 - 0.0149$	$0.0084 - 0.0108$	$0.0086 - 0.0113$	$0.0084 - 0.0096$
$m_{\nu_3}$	$0.0456 - 0.0577$	$0.0455 - 0.0575$	$0.0446 - 0.0576$	$0.0455 - 0.0573$
$\theta_{12}$	$29.30^\circ - 39.20^\circ$	$29.30^\circ - 39.20^\circ$	$29.30^\circ - 39.20^\circ$	$29.30^\circ - 39.04^\circ$
$\theta_{23}$	$35.70^\circ - 55.60^\circ$	$35.70^\circ - 55.60^\circ$	$35.70^\circ - 55.59^\circ$	$35.70^\circ - 40.15^\circ$
$\theta_{13}$	$0.084^\circ - 11.50^\circ$	$1.14^\circ - 11.50^\circ$	$3.60^\circ - 11.15^\circ$	$8.43^\circ - 11.50^\circ$
$J_l$	$-0.0462 - 0.0448$	$-0.0459 - 0.0463$	$\sim 0$	$\sim 0$
$\delta_l$	$-90^\circ - 90.0^\circ$	$-90^\circ - 90.0^\circ$	$\sim 0$	$\sim 0$
$\langle m_{ee} \rangle$	-	$0.00086 - 0.0173$	-	$0.0032 - 0.0075$

that the values of  $\theta_{12}$  corresponding to  $m_{\nu_1} \lesssim 0.1$  eV lie outside the experimentally allowed range, thereby ruling out degenerate scenario for Majorana as well as Dirac neutrinos at  $3\sigma$  C.L..

It may also be added that in the case when charged leptons are in the flavor basis, one can easily check that inverted hierarchy and degenerate scenarios for the texture 4 zero mass matrices are again ruled out, in agreement with the conclusions of Ref. 171. The results pertaining to this case can easily be derived from the earlier cases.

After ruling out the cases pertaining to inverted hierarchy and degenerate scenarios, the authors then discuss the normal hierarchy cases. For the charged lepton

mass matrix  $M_l$  being Fritzsch-like or in the flavor basis, for Majorana as well as Dirac neutrinos, Table 7 presents the viable ranges of neutrino masses, mixing angles  $\theta_{12}$ ,  $\theta_{23}$  and  $\theta_{13}$ , Jarlskog's rephasing invariant parameter in the leptonic sector  $J_l$ , Dirac-like CP violating phase in the leptonic sector  $\delta_l$  and effective neutrino mass  $\langle m_{ee} \rangle$ . For both Dirac or Majorana neutrinos, the viable range of the lightest neutrino mass  $m_{\nu_1}$  is quite different, in particular the range corresponding to Dirac neutrinos is much wider at both the ends as compared to the Majorana neutrinos. Similar conclusions can be arrived at by studying the implications of the well known mixing angle  $\theta_{12}$  on the lightest neutrino mass  $m_{\nu_1}$  through a closer look at the Figs. 20(a) and 20(b). Therefore, a measurement of  $m_{\nu_1}$  could have important implications for the nature of neutrinos. Somewhat constrained range of  $m_{\nu_2}$  for the Majorana case as compared to the Dirac case is also due to the constrained range of  $m_{\nu_1}$  for the Majorana case. Also, from the table one finds that the lower limit on  $\theta_{13}$  for both the Dirac case and the Majorana case are quite small as compared to the recently measured value of angle  $\theta_{13}$ . It must be noted that the calculated values of  $\langle m_{ee} \rangle$  are much less compared to the present limits of  $\langle m_{ee} \rangle$ <sup>182,183</sup>, therefore, these do not have any implications for the texture 4 zero cases considered here. However, the future experiments with considerably higher sensitivities, aiming to measure  $\langle m_{ee} \rangle \simeq 3.6 \times 10^{-2}$  eV (MOON<sup>184</sup>) and  $\langle m_{ee} \rangle \simeq 2.7 \times 10^{-2}$  eV (CUORE<sup>185</sup>), would have implications on the cases considered here. The different cases of Dirac and Majorana neutrinos do not show any divergence for the ranges of Jarlskog's rephasing invariant parameter.

In Table 7 the results when charged leptons are in the flavor basis which can be easily deduced from the case when  $M_l$  is Fritzsch-like have also been presented. Interestingly, in this case both  $J_l$  and  $\delta_l$  are vanishingly small for the wide range of parameters considered here, which can easily be understood by examining the corresponding mixing matrix. Also, the range of angle  $\theta_{13}$  is much narrower compared to the case when  $M_l$  is Fritzsch-like, particularly for the Majorana case the predicted range is very narrow, however being very much in agreement with the recent measurement of  $\theta_{13}$ . It may also be added that for the Majorana case, the range of  $\theta_{23}$  is compatible only with the lower part of the present admissible range, however for the Dirac case there is no such restriction. These conclusions are broadly in agreement with those of Ref. 171.

Further, the authors have also constructed the Pontecorvo-Maki-Nakagawa-Sakata (PMNS) mixing matrix<sup>58–61</sup> which for Majorana neutrinos is

$$U = \begin{pmatrix} 0.7599 - 0.8701 & 0.4797 - 0.6294 & 0.0199 - 0.1994 \\ 0.1673 - 0.5715 & 0.3948 - 0.7606 & 0.5720 - 0.8224 \\ 0.1854 - 0.5912 & 0.3549 - 0.7363 & 0.5540 - 0.8094 \end{pmatrix}, \quad (155)$$

wherein the magnitude of the matrix elements have been given. Similarly, for Dirac

62 *Manmohan Gupta, Gulsheen Ahuja*

neutrinos, the PMNS matrix is

$$U = \begin{pmatrix} 0.7604 - 0.9213 & 0.3887 - 0.6317 & 0.0015 - 0.1993 \\ 0.1475 - 0.5552 & 0.4049 - 0.8170 & 0.4154 - 0.8244 \\ 0.1830 - 0.6022 & 0.3648 - 0.7441 & 0.5546 - 0.9095 \end{pmatrix}. \quad (156)$$

A general look at the two matrices reveals that the ranges of the matrix elements are more wider in the case of Dirac neutrinos as compared to those in the case of Majorana neutrinos. A comparison of the two matrices shows that the lower limit of the element  $U_{\mu 3}$  show an appreciable difference, which seems to be due to the nature of neutrinos, hence, a further precision of  $U_{\mu 3}$  would have important implications. Also, it may be mentioned that both the above mentioned matrices are fully compatible with a very recent construction of a mixing matrix by Bjorken *et al.*<sup>63</sup> assuming democratic trimaximally mixed  $\nu_2$  mass eigenstate as well as with the one presented by Giunti<sup>98</sup>.

## 6. Textures and general mass matrices

From the previous sections, one finds that texture specific mass matrices are able to accommodate the quark as well as neutrino mixing data. This immediately brings in focus the question whether textures can be derived from more fundamental considerations. In this context, several ideas have been advocated in the literature, e.g., Peccei and Wang<sup>186</sup> have imposed the conditions of naturalness which makes certain elements of the texture specific mass matrices very small relative to the others, indicating that the idea of naturalness is in accordance with the texture *ansätze*. Similarly, Branco and collaborators<sup>181,187,188</sup> have used the facility of weak basis transformations to derive textures. In the sequel, we present the essentials pertaining to these ideas.

### 6.1. Natural mass matrices

Peccei and Wang<sup>186</sup> advocated the concept of natural mass matrices which makes it possible to restrict the arbitrariness in the mass pattern construction, thereby allowing a search for viable GUT patterns more systematically and efficiently. The essential idea consists of avoidance of fine tuning in the elements of the mass matrices so as to reproduce the hierarchical structure of the CKM matrix. To illustrate their idea, Peccei and Wang first discuss the two generation quark case. For this case, the natural mass matrices take the following form

$$\tilde{M}_u \simeq \begin{pmatrix} \alpha'_u \lambda^4 & \alpha_u \lambda^2 \\ \alpha_u \lambda^2 & 1 \end{pmatrix}, \tilde{M}_d \simeq \begin{pmatrix} \alpha'_d \lambda^2 & \alpha_d \lambda \\ \alpha_d \lambda & 1 \end{pmatrix}, \quad (157)$$

where  $\lambda$  is a small parameter of the order of Cabibbo angle and

$$\sin \theta_u = \alpha_u \lambda^2, \quad \alpha'_u - \alpha_u^2 = \xi_{uc}, \quad \sin \theta_d = \alpha_d \lambda, \quad \alpha'_d - \alpha_d^2 = \xi_{ds}, \quad \alpha_d - \alpha_u \lambda \simeq 1. \quad (158)$$

With the parameters  $\alpha$  and  $\alpha'$  of  $O(1)$ , one gets the observed hierarchy (i.e. the  $\xi$ 's being of  $O(1)$ ) without any need for fine tunings. This also illustrates that even if

the element (1,1) is taken to be zero, reducing both  $\tilde{M}_u$  and  $\tilde{M}_d$  to texture 1 zero mass matrices, the matrix will continue to remain natural.

Further, they have also considered natural mass matrices for the three generation case. Again keeping in mind the structure of the CKM matrix, a convenient parameterization of the mass matrices based on a perturbative expansion in ‘ $\lambda$ ’ has been introduced. For  $\theta_{1d} \sim \lambda$ ,  $\theta_{1u} \sim \theta_{2d} \sim \lambda^2$ ,  $\theta_{2u} \sim \theta_{3u} \sim \lambda^4$  and  $\theta_{3d} \sim \lambda^5$  one gets a particular mass pattern, e.g.,

$$\begin{aligned}\tilde{M}_u &\simeq \begin{pmatrix} u_{11}\lambda^7 & u_{12}\lambda^6 & e^{-i\delta_u}u_{13}\lambda^4 \\ u_{12}\lambda^6 & u_{22}\lambda^4 & u_{23}\lambda^4 \\ e^{i\delta_u}u_{13}\lambda^4 & u_{23}\lambda^4 & 1 \end{pmatrix}, \\ \tilde{M}_d &\simeq \begin{pmatrix} d_{11}\lambda^4 & d_{12}\lambda^3 & e^{-i\delta_d}d_{13}\lambda^5 \\ d_{12}\lambda^3 & d_{22}\lambda^2 & d_{23}\lambda^2 \\ e^{i\delta_d}d_{13}\lambda^5 & d_{23}\lambda^2 & 1 \end{pmatrix},\end{aligned}\quad (159)$$

where the real coefficients  $u_{ij}$ ’s,  $d_{ij}$ ’s are functions of the  $O(1)$  parameters. A closer look at the structure reveals that some of the elements of the mass matrices can be considered to be highly suppressed compared with others, again in consonance with the concept of texture specific mass matrices. It may also be mentioned that the elements of a general mass matrix, following the hierarchy

$$(1,1), (1,3), (3,1) \lesssim (1,2), (2,1) \lesssim (2,3), (3,2), (2,2) \lesssim (3,3),$$

can be considered to be natural mass matrices.

## 6.2. Texture and weak basis transformations

The study of viable texture zeros is further complicated by the fact that some sets of these zeroes have by themselves no physical significance. This is due to the fact that these can be obtained starting from arbitrary fermion mass matrices by making appropriate weak basis (WB) transformations under which quark mass matrices change but the gauge currents remain real and diagonal. In this context, several attempts<sup>21,181,187–190</sup> have been made wherein the above freedom is exploited to introduce WB zeros in the fermion mass matrices  $M_u$ ,  $M_d$ . If we consider  $M_u$  and  $M_d$  hermitian mass matrices, then most general WB transformations that leave the mass matrices hermitian is

$$M_d \rightarrow M'_d \equiv W^T M_d W, \quad (160)$$

$$M_u \rightarrow M'_u \equiv W^T M_u W. \quad (161)$$

where  $W$  is arbitrary unitary matrix.

The WB transformations broadly lead to two possibilities for the texture zero fermion mass matrices. In the first possibility, as observed by Branco *et al.*<sup>187,188</sup>, one ends up with texture 3 zero fermion mass matrices  $M_u$ ,  $M_d$  wherein one of the

matrix among these pairs is a texture 2 zero Fritzsch-like hermitian mass matrix given by

$$M_q = \begin{pmatrix} 0 & * & 0 \\ * & * & * \\ 0 & * & * \end{pmatrix}, \quad (162)$$

where  $q = U/D$ , while the other mass matrix is a texture 1 zero hermitian mass matrix of the following form

$$M'_q = \begin{pmatrix} 0 & * & * \\ * & * & * \\ * & * & * \end{pmatrix}. \quad (163)$$

In the second possibility, as observed by Fritzsch and Xing<sup>189,190</sup>, one ends up with texture 2 zero fermion mass matrices, wherein both the fermion mass matrices assume a texture 1 zero hermitian structure of the following form

$$M'_q = \begin{pmatrix} * & * & 0 \\ * & * & * \\ 0 & * & * \end{pmatrix}. \quad (164)$$

In addition, the position of the WB zeros in these mass matrices can be varied by the use of parallel  $S_3$  or permutation transformations<sup>181</sup> on the fermion mass matrices. However, it is known<sup>126</sup> that such permutation transformations generally lead to the re-positioning of the various elements of these mass matrices. For details in this regard, we refer the reader to Ref. 181.

It is important to emphasize here that in the first approach, without any loss of generality, one is able to embed at the most three WB zeros in the fermion mass matrices, whereas the maximum number of such WB zeros that can be introduced using the Fritzsch-Xing approach is only two. Further, one can conclude<sup>21,181,189,190</sup> that the inclusion of an additional texture zero in these approaches, like texture 4 zero Fritzsch-like mass matrices, does have physical implications. One may note that the above two possibilities of WB transformations are equivalent, however the Fritzsch-Xing approach<sup>189,190</sup> not only exhibits parallel texture structure but can also be diagonalized exactly, making the construction of corresponding CKM matrix rather simple. As a result, we would like to discuss the general texture specific fermion mass matrices based on the Fritzsch-Xing approach for investigating the implications of these<sup>180</sup>.

In the leptonic sector there is an extra motivation for introducing texture zeros<sup>181</sup>, namely the fact that without an appeal to theory it is not possible to fully reconstruct the neutrino mass matrix from experimental inputs. This is further reinforced by the fact that if Dirac neutrino and the Majorana mass matrix  $M_D$  and  $M_R$  are assumed to have zero texture structure then the neutrino mass matrix remains seesaw invariant under these transformations. This not only simplifies the analysis of texture specific mass matrices in the leptonic sector, but also



suggests the possibility of quarks and leptons having texture universality. Further, this provides a motivation for exploring the compatibility of texture specific mass matrices with GUT models such as SO(10), etc..

After having observed that the most general mass matrices can be reduced to texture 1 zero hermitian mass matrices given by Eq. (164), it becomes desirable to check the implications of quark and lepton mixing data on such texture specific fermion mass matrices. In particular, if the mass matrices are ‘natural’, it becomes interesting to check the parameter space available to the additional non zero diagonal elements ‘ $e_q$ ’ appearing in the (1,1) positions, as compared to the texture 4 zero Fritzsch-like fermion mass matrices, while fitting the precisely measured CKM elements and other CKM parameters. In the case of leptons, it is easy to check that such mass matrices would be able to explain the neutrino mixing data as well. To this end, in the sequel we shall discuss the attempt by Gupta<sup>180</sup> wherein the texture 2 zero fermion mass matrices with parallel texture structures obtained using the Fritzsch-Xing approach<sup>189,190</sup> have been considered. Following Ref. 180, beginning with the diagonalizing transformation of texture 1 zero hermitian mass matrices, presented in Appendix C, the implications for texture 2 zero natural mass matrices for both quarks and leptons have been discussed below.

### 6.3. Texture 2 zero natural quark mass matrices and CKM matrix

Considering texture 2 zero fermion mass matrices with parallel texture structures obtained using the Fritzsch-Xing approach<sup>189,190</sup>, for  $q = U/D$ , the texture 1 zero hermitian mass matrix can be expressed as

$$M_q = \begin{pmatrix} e_q & a_q & 0 \\ a_q^* & d_q & b_q \\ 0 & b_q^* & c_q \end{pmatrix}, \quad (165)$$

where  $a_q = |a_q|e^{i\alpha_q}$  and  $b_q = |b_q|e^{i\beta_q}$ . One may note that in comparison to Fritzsch-like texture 4 zero mass matrices, now one has an additional element  $e_q$  appearing at the (1,1) positions both in  $M_u$ ,  $M_d$ . To study the implications of this element  $e_q$  one needs to first find the diagonalizing transformation of these matrices, presented in Appendix C, so as to construct the corresponding mixing matrix.

Following Appendix C, in order to deduce the quark mixing matrix, one can easily use the approximations for the elements of the diagonalizing transformations, e.g.,  $m_1 \ll m_2 \ll m_3$  and  $c_q \gg m_1$ , resulting into

$$O_q = \begin{pmatrix} 1 & \sqrt{\frac{(m_1 - e_q)(c_q + m_2)}{c_q m_2}} \frac{m_2}{m_3} \sqrt{\frac{(m_1 - e_q)(m_3 - c_q)}{c_q m_2}} \\ -\sqrt{\frac{c_q(m_1 - e_q)}{m_2 m_3}} & -\sqrt{\frac{(c_q + m_2)}{m_3}} & \sqrt{\frac{(m_3 - c_q)}{m_3}} \\ -\sqrt{\frac{(m_1 - e_q)(m_3 - c_q)(c_q + m_2)}{m_2 m_3 c_q}} & \sqrt{\frac{(m_3 - c_q)}{m_3}} & \sqrt{\frac{(c_q + m_2)}{m_3}} \end{pmatrix}. \quad (166)$$

This can be further simplified to the following form

$$O_q = \begin{pmatrix} 1 & k_{1q}k_{4q} & k_{2q}k_{4q}m_2/k_{3q}m_3 \\ k_{3q}k_{4q} & -k_{1q}k_{3q} & k_{2q} \\ -k_{1q}k_{2q}k_{4q} & k_{2q} & k_{1q}k_{3q} \end{pmatrix}, \quad (167)$$

where the parameters  $k_{1q}$ ,  $k_{2q}$ ,  $k_{3q}$  and  $k_{4q}$  are defined as follows

$$k_{1q} = \sqrt{\frac{c_q + m_2}{c_q}}, \quad k_{2q} = \sqrt{\frac{m_3 - c_q}{m_3}}, \quad k_{3q} = \sqrt{\frac{c_q}{m_3}} = 1 - k_{2q}^2, \quad k_{4q} = \sqrt{\frac{m_1 - e_q}{m_2}}. \quad (168)$$

One can now compute the quark mixing matrix or the CKM matrix through

$$V_{CKM} = O_u^\dagger P_u P_d^\dagger O_d. \quad (169)$$

In general these can be expressed as

$$V_{i\sigma} = O_{1i}^u O_{1\sigma}^d e^{-i\phi_1} + O_{2i}^u O_{2\sigma}^d + O_{3i}^u O_{3\sigma}^d e^{i\phi_2}. \quad (170)$$

Explicitly, the various CKM matrix elements may be re-expressed in terms of the quark mass ratios  $k_{1q}$ ,  $k_{2q}$ ,  $k_{3q}$ ,  $k_{4q}$  and the phases  $\phi_1$  and  $\phi_2$ , e.g.,

$$V_{ud} = e^{-i\phi_1} + k_{4u}k_{4d}[k_{3u}k_{3d} + k_{1u}k_{2u}k_{1d}k_{2d}e^{i\phi_2}], \quad (171)$$

$$V_{us} = k_{1d}k_{4d}e^{-i\phi_1} - k_{4u}[k_{3u}k_{1d}k_{3d} + k_{1u}k_{2u}k_{2d}e^{i\phi_2}], \quad (172)$$

$$V_{ub} = \frac{m_s}{m_b} \frac{k_{2d}k_{4d}}{k_{3d}} e^{-i\phi_1} + k_{4u}[k_{3u}k_{2d} - k_{1u}k_{2u}k_{1d}k_{3d}e^{i\phi_2}], \quad (173)$$

$$V_{cd} = k_{1u}k_{4u}e^{-i\phi_1} - k_{4d}[k_{1u}k_{3u}k_{3d} + k_{2u}k_{1d}k_{2d}e^{i\phi_2}], \quad (174)$$

$$V_{cs} = k_{1u}k_{1d}k_{4u}k_{4d}e^{-i\phi_1} + [k_{1u}k_{3u}k_{1d}k_{3d} + k_{2u}k_{2d}e^{i\phi_2}], \quad (175)$$

$$V_{cb} = \frac{m_s}{m_b} \frac{k_{1u}k_{2d}k_{4u}k_{4d}}{k_{3d}} e^{-i\phi_1} - [k_{1u}k_{3u}k_{2d} - k_{2u}k_{1d}k_{3d}e^{i\phi_2}], \quad (176)$$

$$V_{td} = \frac{m_c}{m_t} \frac{k_{2u}k_{4u}}{k_{3u}} e^{-i\phi_1} + k_{4d}[k_{2u}k_{3d} - k_{1u}k_{3u}k_{1d}k_{2d}e^{i\phi_2}], \quad (177)$$

$$V_{ts} = \frac{m_c}{m_t} \frac{k_{2u}k_{1d}k_{4u}k_{4d}}{k_{3u}} e^{-i\phi_1} - [k_{2u}k_{1d}k_{3d} - k_{1u}k_{3u}k_{2d}e^{i\phi_2}], \quad (178)$$

$$V_{tb} = \frac{m_c}{m_t} \frac{m_s}{m_b} \frac{k_{2u}k_{2d}k_{4u}k_{4d}}{k_{3u}k_{3d}} e^{-i\phi_1} + [k_{2u}k_{2d} + k_{1u}k_{3u}k_{1d}k_{3d}e^{i\phi_2}]. \quad (179)$$

To facilitate the understanding of CKM elements in terms of the quark mass ratios, phases  $\phi_1$ ,  $\phi_2$  and the hierarchy among the elements of the mass matrices, we define

$$\xi_q = \frac{e_q}{m_1} \quad \text{and} \quad \zeta_q = \frac{d_q}{c_q}. \quad (180)$$

Subsequently, the parameters  $k_{1q}$ ,  $k_{2q}$ ,  $k_{3q}$  and  $k_{4q}$  appearing in the diagonalizing transformation  $O_q$  and the elements of the CKM matrix may be rewritten as

$$k_{1q} = \sqrt{1 - \left(\frac{m_2}{m_3}(1 + \zeta_q)\right)}, \quad k_{2q} = \sqrt{\frac{\zeta_q}{1 + \zeta_q}}, \quad (181)$$

$$k_{3q} = 1 - k_{2q}^2 = \sqrt{\frac{1}{1 + \zeta_q}}, \quad k_{4q} = \sqrt{\frac{m_1}{m_2}(1 - \xi_q)}. \quad (182)$$

As a result, the various CKM matrix elements can be expressed in terms of these, e.g.,

$$V_{ud} = e^{-i\phi_1} + \sqrt{\frac{m_u m_d}{m_c m_s}} \sqrt{\frac{(1 - \xi_u)(1 - \xi_d)}{(1 + \zeta_u)(1 + \zeta_d)}} [1 + k_{1u} k_{1d} \sqrt{\zeta_u \zeta_d} e^{i\phi_2}], \quad (183)$$

the others can be written in a similar manner.

It has already been shown in the context of texture 4 zero quark mass matrices that the precisely known parameter  $\sin 2\beta$  gives vital clues for the structural features of mass matrices. It was also mentioned that Verma *et al.*<sup>124</sup> had incorporated certain vital corrections to the formula of  $\sin 2\beta$ , ignored in the earlier attempts of texture 4 zero quark mass matrices, showing unambiguously that both the phases of the mass matrices are essential for compatibility with the quark mixing data. In the context of texture 2 zero natural quark mass matrices, we would like to present the generalization of the formula of  $\sin 2\beta$  given in Ref. 124. It is easy to check that for the natural mass matrices considered here, the parameter  $k_{1q} \approx 1$ . Using the above approximations, the formula of angle  $\beta$  now becomes

$$\beta = \arg \left( 1 - \sqrt{\frac{m_u m_s}{m_c m_d}} \sqrt{\frac{(1 - \xi_u)}{(1 - \xi_d)}} e^{-i(\phi_1 + \phi_2)} \right) + \arg \left( \frac{1 - r_2 e^{i\phi_2}}{1 - r_1 e^{i\phi_2}} \right), \quad (184)$$

where the parameters  $r_1$  and  $r_2$  are defined as

$$r_1 = \frac{1}{\sqrt{\zeta_u/\zeta_d}} \left( 1 + \frac{m_s}{m_b} \frac{(1 + \zeta_d)}{2} \right), \quad (185)$$

and

$$r_2 = \frac{1}{\sqrt{\zeta_u/\zeta_d}} \left( 1 - \frac{m_s}{m_b} \frac{(1 + \zeta_d)}{2} \right). \quad (186)$$

It is interesting to note that the various CKM elements and related parameters can now be expressed entirely in terms of the quark masses, the hierarchy parameters  $\xi_q$ ,  $\zeta_q$  and the phases  $\phi_1$  and  $\phi_2$ . Furthermore the above relations incorporate the ‘next to leading order’ terms and are found to hold remarkably well within an error of less than fraction of a percent, consistent with the present experimental bounds. Apart from clearly underlying the dependence on quark masses and both the phases  $\phi_1$  and  $\phi_2$ , the above formulae clearly depict the corrections induced by the parameters  $e_q$  through the terms  $\xi_u$  and  $\xi_d$  viz-a-viz the corresponding relations obtained from

the texture 4 zero Fritzsch-like quark mass matrices. It is easy to check that the above relations reduce to the corresponding texture 4 zero relations in case  $e_q = 0$  implying vanishing  $\xi_u$  and  $\xi_d$ . Also it is interesting to observe that the relation for  $V_{cb}$  is the same in the texture 2 zero case and the texture 4 zero case. This is justified since the elements  $e_q$  only lead to a mixing among the first and second generations as well as first and third generations and not among the second and the third generations. This is further evident from the minor corrections appearing in the expressions for  $V_{us}$  and  $V_{ub}$  in relations in comparison to their counterparts in texture 4 zero case.

In case one uses the quark masses at  $M_Z$  scale and the values of the quark mixing parameters  $V_{us}$ ,  $V_{cb}$ ,  $V_{ub}$  and  $\sin 2\beta$ , one can make an attempt to study the implications of the additional element  $e_q$  on the quark mixing parameters. The calculations suggest that the parameters  $\xi_u$  and  $\xi_d$  can assume only very small values and also that their parameter space is very limited, this being compatible with the condition of ‘naturalness’ of the mass matrices. One arrives at similar conclusions in case one makes an attempt to study the implications of  $\xi_u$  and  $\xi_d$  on some of the vital CKM parameters such as  $V_{us}$ ,  $V_{cb}$ ,  $V_{ub}$  and  $\sin 2\beta$ . In particular, it is observed that  $\xi_u$  and  $\xi_d$  do not have any pronounced effect on  $V_{us}$ ,  $V_{cb}$  as well as  $\sin 2\beta$ . However, for the case of  $V_{ub}$  one finds that for its inclusive values, the allowed ranges of the parameters  $\xi_u$  and  $\xi_d$  are somewhat limited whereas in case one restrict to exclusive values of  $V_{ub}$  then almost the entire ranges of  $\xi_u$  and  $\xi_d$  are able to reproduce the results.

#### 6.4. *Texture 2 zero lepton mass matrices and PMNS matrix*

Following the case of quarks, it becomes interesting to check whether we arrive at the same conclusions in the case of texture 2 zero lepton mass matrices. For this purpose, one need not look into an extensive analysis, rather it is informative to discuss the effects of additional parameter  $e_\nu$  in the case of leptons. To this end, it is interesting to discuss the attempt by Ref. 180 wherein the compatibility of such texture 2 zero lepton mass matrices for Dirac as well as Majorana neutrinos has been explored. It may be mentioned that while carrying out the diagonalization of these mass matrices, the approximations used in the quarks case do not seem to be valid, therefore the exact diagonalizing transformations given in Eq. (C.6) need to be considered. It may be noted that in case neutrinos are considered to be Dirac-like, the procedure for the calculation of the mixing matrix is essentially the same as that for the case of quarks considered in the previous section. However, if neutrinos are considered to be Majorana-like, one first obtains the light Majorana neutrino mass matrix  $M_\nu$  using the type-I seesaw mechanism,  $M_\nu = -M_{\nu D}^T M_{\nu R}^{-1} M_{\nu D}$ , where  $M_{\nu D}$  and  $M_{\nu R}$  are respectively the Dirac neutrino mass matrix and right handed Majorana neutrino mass matrix. For the case of normal hierarchy of neutrinos characterized by  $m_{\nu_1} < m_{\nu_2} \ll m_{\nu_3}$ , one of the element of the diagonalizing transformation for the

neutrino mass matrix is

$$O_{\nu M}(1,1) = \sqrt{\frac{(e_{\nu M} + \sqrt{m_{\nu M_2}})(\sqrt{m_{\nu M_3}} - e_{\nu M})(e_{\nu M} - \sqrt{m_{\nu M_1}})}{(e_{\nu M} - e_{\nu M})(\sqrt{m_{\nu M_3}} - \sqrt{m_{\nu M_1}})(\sqrt{m_{\nu M_2}} - \sqrt{m_{\nu M_1}})}}, \quad (187)$$

the other elements can be found in a similar manner.

As already mentioned, texture 4 zero Fritzsch-like lepton mass matrices with parallel texture structure for neutrinos and charged leptons are able to accommodate the lepton mixing data quite well, it is therefore expected that the same can also be achieved using texture 2 zero hermitian lepton mass matrices with parallel texture structure. In this context, it becomes interesting to find the viable range for the additional elements  $e_q$ ,  $q = e, \nu$  in these mass matrices, both for the case of Dirac neutrinos as well as for Majorana neutrinos, especially when the condition of ‘naturalness’ is invoked on these mass matrices.

To this end, for the purpose of numerical calculations, using the recent values of the lepton mixing angles as well as neutrino mass square differences as inputs, one can examine the implications of the lepton mixing angle  $(s_{13}^l)^2$  (the superscript  $l$  denotes the ‘lepton’ mixing angle in order to differentiate it from the corresponding ‘quark’ mixing angle) on the (1,1) elements in these matrices for the Dirac neutrinos as well as for the Majorana neutrinos. In the case of Dirac neutrinos, it is observed that the Dirac neutrino masses take the following values

$$m_{\nu D_1} = 2.3 \times 10^{-13} - 9.9 \times 10^{-12} \text{ GeV}, \quad (188)$$

$$m_{\nu D_2} = 8.3 \times 10^{-12} - 1.3 \times 10^{-11} \text{ GeV}, \quad (189)$$

$$m_{\nu D_3} = 4.4 \times 10^{-11} - 5.3 \times 10^{-11} \text{ GeV}. \quad (190)$$

It is interesting to note that the parameter  $e_e$  takes all values between 0 to  $m_e \sim 5 \times 10^{-4}$  GeV, while the parameter  $e_{\nu D}$  takes values between 0 to  $7 \times 10^{-12}$  GeV which is about 70% of the value of the lightest Dirac neutrino mass  $m_{\nu D_1}$ , consistent with the condition of ‘naturalness’ imposed on these mass matrices. It can also be seen that the additional free parameters  $e_e$  and  $e_{\nu D}$  do not show any pronounced effect on the lepton mixing angle  $(s_{13}^l)^2$ . This clearly indicates that provided the condition of ‘naturalness’ is obeyed by these mass matrices, the results obtained using texture 2 zero hermitian lepton mass matrices and those obtained using texture 4 zero Fritzsch-like lepton mass matrices are essentially the same since the additional (1,1) elements  $e_e$  and  $e_{\nu D}$  in the texture 2 zero hermitian lepton mass matrices do not have any pronounced effect on the lepton mixing data.

In a similar manner, for the Majorana neutrinos it is observed that the light Majorana neutrino masses, obtained through the type-I seesaw mechanism, take the following values

$$m_{\nu M_1} = 2.8 \times 10^{-13} - 9.9 \times 10^{-12} \text{ GeV}, \quad (191)$$

70 *Manmohan Gupta, Gulsheen Ahuja*

$$m_{\nu M_2} = 8.3 \times 10^{-12} - 1.3 \times 10^{-11} \text{ GeV}, \quad (192)$$

$$m_{\nu M_3} = 4.4 \times 10^{-11} - 5.3 \times 10^{-11} \text{ GeV}. \quad (193)$$

In this case, the parameter  $e_e$  again takes all values between 0 to  $m_e \sim 5 \times 10^{-4} \text{ GeV}$ , while the parameter  $e_{\nu D}$  takes a maximum value which is about 50% of the value of the square root of the lightest Majorana neutrino mass i.e.  $\sqrt{m_{\nu M_1}}$  consistent with the condition of ‘naturalness’ imposed on these mass matrices. Additionally, in case one assumes that the right handed Majorana neutrino mass matrix elements  $m_R$  are of the order of  $2 \times 10^{14} \text{ GeV}$ , corresponding to the intermediate energy scale<sup>191</sup> in GUTs, then the values of the Dirac neutrino masses predicted in this case are as follows

$$m_{\nu D_1} = 7.6 - 44.5 \text{ GeV}, \quad (194)$$

$$m_{\nu D_2} = 40.9 - 51.6 \text{ GeV}, \quad (195)$$

$$m_{\nu D_3} = 94.5 - 102.8 \text{ GeV}. \quad (196)$$

It is interesting to note that the order of these masses is the same as that of the up sector of quarks, a feature that emerges naturally<sup>191–193</sup> in GUTs like SO(10).

These calculations reveal that even in the case of Majorana neutrinos, both the additional parameters  $e_e$  and  $e_{\nu M}$  have almost no pronounced effect on the lepton mixing data as compared to the texture 4 zero Fritzsch-like lepton mass matrices. In conclusion, we can state that the condition of ‘naturalness’ re-ensures that the results obtained using texture 2 zero lepton mass matrices and those obtained using texture 4 zero Fritzsch-like lepton mass matrices are essentially the same.

## 7. SO(10) and texture specific fermion mass matrices

After having discussed that the phenomenological texture specific mass matrices are able to accommodate the fermion mixing data and further noting that these are also compatible with the ‘naturalness’ condition and weak basis transformations, one may now mention that recently a few authors<sup>135,193–195</sup> have also observed the importance of texture 4 zero Fritzsch-like mass matrices in the context of SO(10). It may be noted that an extensive and detailed review of some of these as well as some other attempts to explain fermion masses and mixings within the framework of SO(10) GUTs has already been carried out by Chen and Mahanthappa<sup>192</sup>, however in the present case, our emphasis will be on the issue of the compatibility of the textures of the mass matrices within the constraints of the SO(10) formalism.

In particular, Fukuyama *et al.*<sup>194</sup> have carried out an analysis wherein they have investigated the compatibility of texture specific mass matrices, having similar forms for quarks and leptons, with the SO(10) inspired mass matrices. However, their analysis is not able to simultaneously fit the quark mixing and the lepton mixing data, in particular they are not able to reproduce the solar mixing angle with

the constraints on the neutrino masses coming from the oscillation data. Further, Joshipura and Patel<sup>193</sup> have also recently carried out an extensive analysis of mass matrices based on SO(10), however, they do not apply any ‘textures’ as well as the condition of ‘naturalness’ on these mass matrices. Similarly, the emphasis of analysis by Dev *et al.*<sup>195</sup> is to fit the lepton mixing data in the context of mass matrices based on SO(10), however again the condition of ‘naturalness’ on these mass matrices has not been imposed as well as the quark textures have not been taken into consideration. Very recently a detailed and comprehensive analysis of the texture 4 zero mass matrices in the context of SO(10), with the latest constraints of quark and lepton mixing parameters has been carried out by Verma *et al.*<sup>196</sup> wherein the condition of ‘naturalness’ on these mass matrices has been imposed as well. In the sequel, we present the essentials of SO(10) and SO(10) based mass matrices and broad conclusions of the analysis carried out by Ref. 196.

### 7.1. Introduction to SO(10)

It may be noted that the SO(10) group incorporates several interesting features that makes it a very promising and a leading GUT group<sup>197</sup>. For example, the SO(10) group achieves complete quark-lepton symmetry by unifying all the 15 known fermions, along with the right handed neutrino of each family, into one sixteen dimensional spinor representation denoted by 16. Similarly, it is not only compatible with supersymmetry, but also includes the seesaw mechanism<sup>175–179</sup> for explaining the small neutrino masses.

The SO(10) group is a rank 5 orthogonal group with 10 dimensional fundamental or vector representation. The fifteen fermions of each generation that belong to the  $\bar{5} + 10$  of SU(5) and CP conjugate of right handed neutrino can be accommodated into the 16 dimensional spinor representation of SO(10) as

$$\begin{pmatrix} u_1 & u_2 & u_3 & \nu_e \\ d_1 & d_2 & d_3 & e^- \end{pmatrix} + \begin{pmatrix} u_1^c & u_2^c & u_3^c & \nu_e^c \\ d_1^c & d_2^c & d_3^c & e^+ \end{pmatrix} \quad (197)$$

where the symbols have their usual meanings<sup>198</sup>.

Since SO(10) is a rank 5 gauge group and the SM has a rank 4, there are many possible chains of symmetry breaking through which SO(10) can descend to the gauge group for the Standard Model,  $G_{SM} = SU(3)_c \times SU(2)_L \times U(1)_Y$ <sup>199</sup>. The two usually considered symmetry breaking chains of SO(10) are

$$\text{Chain 1 : } SO(10) \longrightarrow SU(5) \times U(1) \longrightarrow SU(5) \longrightarrow G_{SM},$$

$$\begin{aligned} \text{Chain 2 : } SO(10) &\longrightarrow SU(4)_c \times SU(2)_L \times SU(2)_R \longrightarrow \\ &SU(3)_c \times SU(2)_L \times SU(2)_R \times U(1)_{B-L} \longrightarrow \\ &G_{SM} \longrightarrow G_{EW}. \end{aligned}$$

The first one is ruled out as the proton decays in this case much faster than re-

quired, therefore the second possibility of symmetry breaking in  $SO(10)$  is usually adopted.

### 7.2. Yukawa sector in $SO(10)$

In renormalizable  $SO(10)$ , only three types of Higgs fields can couple to fermions, e.g.,

$$16 \times 16 = 10_S + 120_A + \overline{126}_S, \quad (198)$$

where the symbols  $S$  and  $A$  refer to the symmetry property under interchange of two family indices in the Yukawa couplings  $Y_{AB}$ . The gauge invariant Yukawa couplings are given as<sup>192</sup>

$$S_{AB}^{10}(16)_a(16)_b\phi_{10}, \quad A_{AB}^{120}(16)_a(16)_b\phi_{120}, \quad S_{AB}^{\overline{126}}(16)_a(16)_b\phi_{\overline{126}}. \quad (199)$$

The relevant  $SO(10)$  representations have the following decomposition in terms of the Pati Salam Group,  $SU(4)_c \times SU(2)_L \times SU(2)_R$ ,

$$10 = (6, 1, 1) + (1, 2, 2), \quad (200)$$

$$16 = (4, 2, 1) + (\bar{4}, 1, 2), \quad (201)$$

$$45 = (1, 3, 1) + (1, 1, 3) + (15, 1, 1) + (6, 2, 2), \quad (202)$$

$$54 = (1, 1, 1) + (1, 3, 3) + (20', 1, 1) + (6, 2, 2), \quad (203)$$

$$120 = (1, 2, 2) + (10, 1, 1) + (\overline{10}, 1, 1) + (6, 1, 3) + (6, 3, 1) + (15, 2, 2), \quad (204)$$

$$126 = (15, 2, 2) + (10, 1, 3) + (\overline{10}, 3, 1) + (6, 1, 1). \quad (205)$$

We know that  $16 = (4, 2, 1) + (\bar{4}, 1, 2)$  and  $(4, 2, 1) \times (\bar{4}, 1, 2) = (15, 2, 2) + (1, 2, 2)$  so the Dirac masses for quarks and leptons are generated when neutral components in  $(1, 2, 2)$  multiplet in  $10$ ,  $(15, 2, 2)$  and  $(1, 2, 2)$  in  $120$  and  $(15, 2, 2)$  in  $126$  dimensional representations acquire non vanishing expectation values. On the other hand, the  $(\overline{10}, 3, 1)$  and  $(10, 1, 3)$  components of  $126$  dimensional Higgs break the  $SU(2)_L$  and  $SU(2)_R$  symmetries and hence are responsible for the left and right handed Majorana neutrino masses through the Higgs lepton-lepton interactions  $(\overline{10}, 3, 1)$   $(4, 2, 1)$   $(4, 2, 1)$  and  $(10, 1, 3)$   $(\bar{4}, 1, 2)$   $(\bar{4}, 1, 2)$  respectively. Being able to achieve a complete quark-lepton symmetry,  $SO(10)$  has the promise for explaining the pattern of fermion masses and mixing in a renormalizable form wherein only three Yukawa coupling matrices  $S^{10}$ ,  $S^{\overline{126}}$ ,  $A^{120}$  and relative strengths between them determine six physical mass matrices  $M_f$  with  $f = u, d, e, \nu_D, \nu_L, \nu_R$ . The fermion masses are generated when the Higgs fields of  $10$ ,  $120$  and dimensional  $SO(10)$  representation (denoted by  $\phi_{10}$ ,  $\phi_{120}$  and  $\phi_{\overline{126}}$  respectively) develop non vanishing expectation values and lead to the following mass matrices<sup>200,201</sup>

$$M_u = S^{10} \langle \phi_{10}^+ \rangle + A^{120} (\langle \phi_{120}^+ \rangle + \frac{1}{3} \langle \phi_{120}'^+ \rangle) + S^{\overline{126}} \frac{1}{3} \langle \phi_{\overline{126}}^+ \rangle, \quad (206)$$



$$M_d = S^{10} \langle \phi_{10}^- \rangle + A^{120} (-\langle \phi_{120}^- \rangle + \frac{1}{3} \langle \phi_{120}'^- \rangle) - S^{\overline{126}} \frac{1}{3} \langle \phi_{\overline{126}}^- \rangle, \quad (207)$$

$$M_e = S^{10} \langle \phi_{10}^- \rangle + A^{120} (-\langle \phi_{120}^- \rangle - \langle \phi_{120}'^- \rangle) + S^{\overline{126}} \langle \phi_{\overline{126}}^- \rangle, \quad (208)$$

$$M_{\nu_D} = S^{10} \langle \phi_{10}^+ \rangle + A^{120} (\langle \phi_{120}^+ \rangle - \langle \phi_{120}'^+ \rangle) - S^{\overline{126}} \frac{1}{3} \langle \phi_{\overline{126}}^+ \rangle. \quad (209)$$

Note that a Clebsch-Gordon coefficient (-3) is generated in the lepton sectors when the  $SU(4)_c \times SU(2)_L \times SU(2)_R$  components (15,2,2) are involved. The Majorana neutrino mass matrices are given by

$$M_{\nu_L} = S^{\overline{126}} \langle \phi_{\overline{126}}'^0 \rangle, \quad (210)$$

$$M_{\nu_R} = S^{\overline{126}} \langle \phi_{\overline{126}}'^+ \rangle, \quad (211)$$

where the superscripts +/0/- refer to the sign of the hypercharge Y. Furthermore  $\langle \phi_{10}^\pm \rangle$  are the vacuum expectation values of the Higgs fields of  $\phi_{10}$ ,  $\phi_{120}'^\pm$  are those of  $\phi_{120}$  and  $\langle \phi_{\overline{126}}^\pm \rangle$ ,  $\langle \phi_{\overline{126}}'^0 \rangle$ ,  $\langle \phi_{\overline{126}}'^+ \rangle$  are those of  $\phi_{\overline{126}}$ . As already mentioned, the matrices  $S^{10}$  and  $S^{\overline{126}}$  are complex symmetric while  $A^{120}$  is complex anti-symmetric in nature.

### 7.3. $SO(10)$ based mass matrices

It is possible to define the fermion mass matrices by considering the minimal and non minimal approaches, both in the context of non Supersymmetric (non-SUSY) and SUSY  $SO(10)$  frameworks. The minimal approaches involve fermion mass matrices with Yukawa contributions coming from only two Higgs i.e.  $\phi_{10}$  and  $\phi_{126}$  or  $\phi_{120}$  and  $\phi_{126}$ . Keeping in mind the limitations involved<sup>193,200,201</sup> in these minimal scenarios, we discuss here the non minimal case incorporating the  $S_{AB}^{10}$ ,  $A_{AB}^{120}$  and  $S_{AB}^{126}$ . Although some investigations have been carried out<sup>135,194,195</sup> to check their compatibility with texture specific mass matrices, a detailed and comprehensive analysis is yet to be carried out. Further, the compatibility of the mass matrices based on  $SO(10)$  has not been carried out in the case of texture specific mass matrices incorporating 'weak' hierarchy.

To begin with, we consider the mass matrices formulated by several authors<sup>193,194,202-204</sup>, within the context of  $SO(10)$ . The approach adopted by Fukuyama *et al.*<sup>194</sup> wherein the 6 physical mass matrices in Eqs. (206)-(209) can be reduced to a simpler form as

$$M_u = S + \sigma S' + \xi' A, \quad (212)$$

$$M_d = \eta S + S' + A, \quad (213)$$

74 *Manmohan Gupta, Gulsheen Ahuja*

$$M_e = \eta S - 3S' + \xi A, \quad (214)$$

$$M_D = S - 3\sigma S' + \xi'' A, \quad (215)$$

$$M_{\nu_L} = \beta S', M_{\nu_R} = \gamma S', \quad (216)$$

where

$$S = S^{10} \langle \phi_{10}^+ \rangle, S' = -S^{\overline{126}} \frac{1}{3} \langle \phi_{126}^- \rangle, A = A^{120} (-\langle \phi_{120}^- \rangle + \frac{1}{3} \langle \phi_{120}'^- \rangle), \quad (217)$$

$$\eta = (\langle \phi_{10}^- \rangle / \langle \phi_{10}^+ \rangle), \quad (218)$$

$$\sigma = -(\langle \phi_{126}^+ \rangle / \langle \phi_{126}^- \rangle), \quad (219)$$

$$\xi = (-\langle \phi_{120}^- \rangle - \langle \phi_{120}'^- \rangle) / (-\langle \phi_{120}^- \rangle + 1/3 \langle \phi_{120}'^- \rangle), \quad (220)$$

$$\xi' = (\langle \phi_{120}^+ \rangle + 1/3 \langle \phi_{120}'^+ \rangle) / (-\langle \phi_{120}^- \rangle + 1/3 \langle \phi_{120}'^- \rangle), \quad (221)$$

$$\xi'' = (\langle \phi_{120}^+ \rangle - \langle \phi_{120}'^+ \rangle) / (-\langle \phi_{120}^- \rangle + 1/3 \langle \phi_{120}'^- \rangle), \quad (222)$$

$$\beta = -(\langle \phi_{126}^0 \rangle) / (1/3 \langle \phi_{126}^- \rangle), \quad (223)$$

$$\gamma = -(\langle \phi_{126}^+ \rangle) / (1/3 \langle \phi_{126}^- \rangle). \quad (224)$$

The matrices  $S$  and  $S'$  are complex symmetric while  $A$  is complex anti-symmetric in nature, and the parameters  $\sigma, \eta, \xi, \xi', \xi'', \beta, \gamma$  are dimensionless complex parameters of which  $\beta$  and  $\gamma$  can be chosen to be real without loss of generality<sup>193</sup>.

Similarly, using the approaches given by Altarelli and Blankenburg<sup>202</sup> as well as by Dutta *et al.*<sup>203</sup>, the above expressions take the form

$$M_u = r(H + sF + t_u G), \quad (225)$$

$$M_d = H + F + G, \quad (226)$$

$$M_e = H - 3F + t_e G, \quad (227)$$

$$M_{\nu_D} = r(H - 3sF + t_D G), \quad (228)$$

$$M_{\nu_L} = r_L F, \quad (229)$$

$$M_{\nu_R} = r_R^{-1} F, \quad (230)$$

where  $H$  and  $F$  are symmetric coupling matrices while  $G$  is anti-symmetric. It may also be mentioned that a few other authors<sup>193,204</sup> have also derived these relations, however all these approaches can be shown to be essentially equivalent. The parameters of the above mentioned two approaches are related as

$$S = rH = h, \quad S' = F = r_1 f, \quad A = G = r_1 h', \quad \eta = 1/r = r_1, \quad (231)$$

$$\sigma = sr = r_2/r_1, \quad \xi = t_e = c_e, \quad \xi' = rt_u = r_3/r_1, \quad (232)$$

$$\xi'' = rt_{D\nu} = c/r_1, \quad \beta = r_L = v, \quad \nu_R = r_R^{-1} = v. \quad (233)$$

It may be mentioned that the above mass matrices can easily be related to hermitian mass matrices in  $SO(10)$  incorporating L-R symmetry<sup>200,201,205</sup>. In such a case, the parameters  $\sigma, \eta, \xi, \xi', \xi'', \beta$  and  $\gamma$  can be treated as real. It is important to mention that the above mentioned approaches are valid in both the non SUSY  $SO(10)$  as well as the SUSY  $SO(10)$  scenarios.

#### 7.4. Compatibility of texture 4 zero hermitian mass matrices with $SO(10)$

As a next step, it becomes an interesting exercise to check the compatibility of texture specific mass matrices with  $SO(10)$  based mass matrices. To this end, we present the essentials of Refs. 180, 196 wherein the authors have imposed textures and hermiticity on the mass matrices given in Eqs. (225)-(230) and examined the compatibility of these. It may be mentioned that in case the matrices  $M_u, M_d, M_e$  and  $M_{\nu D}$  are considered to be texture 4 zero hermitian mass matrices, then the parameters  $r, s, t_u, t_e, t_D, r_L, r_R$  have to be real and the matrices  $H$  and  $F$  have to be real symmetric while  $G$  has to be purely imaginary and anti-symmetric.

To understand the constraints imposed by  $SO(10)$  on texture 4 zero fermion mass matrices, the authors have considered texture 4 zero Fritzsch-like mass matrices as

$$M_f = \begin{pmatrix} 0 & a_f e^{i\alpha_f} & 0 \\ a_f e^{-i\alpha_f} & d_f & b_f e^{i\beta_f} \\ 0 & b_f e^{-i\beta_f} & c_f \end{pmatrix}, \quad (234)$$

where  $f = u, d, l, \nu_D$ . It may be noted that the notation used in the above equation is somewhat different than the one used earlier. This has been done keeping in mind the unified treatment of quarks and leptons to be presented in the context of  $SO(10)$ . The corresponding left and right handed Majorana neutrino mass matrices are real symmetric and defined as

$$M_k = \begin{pmatrix} 0 & a_k & 0 \\ a_k & d_k & b_k \\ 0 & b_k & c_k \end{pmatrix}, \quad (235)$$

where  $k = \nu_L, \nu_R$ . Keeping in mind the texture imposed on  $M_u, M_d$ , etc., the

76 *Manmohan Gupta, Gulsheen Ahuja*

matrices  $H$ ,  $F$  and  $G$  can be defined as

$$H = \begin{pmatrix} 0 & a_H & 0 \\ a_H & d_H & b_H \\ 0 & b_H & c_H \end{pmatrix}, F = \begin{pmatrix} 0 & a_F & 0 \\ a_F & d_F & b_F \\ 0 & b_F & c_F \end{pmatrix}, G = \begin{pmatrix} 0 & ia_G & 0 \\ -ia_G & 0 & ib_G \\ 0 & -ib_G & 0 \end{pmatrix}, \quad (236)$$

resulting into Eqs. (225)-(230) being re-expressed as

$$M_u = r(H + sF + t_u G) = S_u + A_u, \quad (237)$$

$$M_d = H + F + G = S_d + A_d, \quad (238)$$

$$M_e = H - 3F + t_e G = S_e + A_e, \quad (239)$$

$$M_{\nu_D} = r(H - 3sF + t_D G) = S_D + A_D, \quad (240)$$

$$M_{\nu_L} = r_L F = S_L, M_{\nu_R} = r_R^{-1} F = S_R, \quad (241)$$

where the matrices  $S_u$ ,  $A_u$ , etc. respectively represent the real symmetric and the imaginary anti-symmetric parts of  $M_u$ , etc.. These are defined as

$$S_u = r(H + sF), \quad S_d = H + F, \quad S_e = H - 3F, \quad S_D = r(H - 3sF), \quad (242)$$

$$A_d = G, \quad A_u = rt_u G, \quad A_e = t_e G, \quad A_D = rt_D G. \quad (243)$$

Using Eqs. (237)-(241), one obtains

$$S_u = \begin{pmatrix} 0 & a_u \cos \alpha_u & 0 \\ a_u \cos \alpha_u & d_u & b_u \cos \beta_u \\ 0 & b_u \cos \beta_u & c_u \end{pmatrix}, \quad (244)$$

$$S_d = \begin{pmatrix} 0 & a_d \cos \alpha_d & 0 \\ a_d \cos \alpha_d & d_d & b_d \cos \beta_d \\ 0 & b_d \cos \beta_d & c_d \end{pmatrix}, \quad (245)$$

$$S_e = \begin{pmatrix} 0 & a_e \cos \alpha_e & 0 \\ a_e \cos \alpha_e & d_e & b_e \cos \beta_e \\ 0 & b_e \cos \beta_e & c_e \end{pmatrix}, \quad (246)$$

$$S_D = \begin{pmatrix} 0 & a_D \cos \alpha_D & 0 \\ a_D \cos \alpha_D & d_D & b_D \cos \beta_D \\ 0 & b_D \cos \beta_D & c_D \end{pmatrix}, \quad (247)$$

$$A_u = \begin{pmatrix} 0 & ia_u \sin \alpha_u & 0 \\ -ia_u \sin \alpha_u & d_u & ib_u \sin \beta_u \\ 0 & -ib_u \sin \beta_u & c_u \end{pmatrix}, \quad (248)$$

$$A_d = \begin{pmatrix} 0 & ia_d \sin \alpha_d & 0 \\ -ia_d \sin \alpha_d & d_d & ib_d \sin \beta_d \\ 0 & -ib_d \sin \beta_d & c_d \end{pmatrix}, \quad (249)$$

$$A_e = \begin{pmatrix} 0 & ia_e \sin \alpha_e & 0 \\ -ia_e \sin \alpha_e & d_e & ib_e \sin \beta_e \\ 0 & -ib_e \sin \beta_e & c_e \end{pmatrix}, \quad (250)$$

$$A_D = \begin{pmatrix} 0 & ia_D \sin \alpha_D & 0 \\ -ia_D \sin \alpha_D & d_D & ib_D \sin \beta_D \\ 0 & -ib_D \sin \beta_D & c_D \end{pmatrix}, \quad (251)$$

$$S_L = r_L \begin{pmatrix} 0 & a_F & 0 \\ a_F & d_F & b_F \\ 0 & b_F & c_F \end{pmatrix} = \begin{pmatrix} 0 & a_L & 0 \\ a_L & d_L & b_L \\ 0 & b_L & c_L \end{pmatrix}, \quad (252)$$

$$S_R = r_R^{-1} \begin{pmatrix} 0 & a_F & 0 \\ a_F & d_F & b_F \\ 0 & b_F & c_F \end{pmatrix} = \begin{pmatrix} 0 & a_R & 0 \\ a_R & d_R & b_R \\ 0 & b_R & c_R \end{pmatrix}. \quad (253)$$

It may be noted that the 17 real free parameters of  $M_u, M_d, M_e, M_{\nu D}, M_{\nu L}$  and  $M_{\nu R}$  correspond to 7 real parameters  $r, s, t_u, t_e, t_D, r_L, r_R$ , 4 parameters  $a_H, b_H, c_H, d_H$  of H, 4 parameters  $a_F, b_F, c_F, d_F$  of F and 2 parameters  $a_G, b_G$  of G. Using Eqs. (237)-(241) one obtains

$$H = \frac{1}{4}(S_d - S_e), F = \frac{1}{4}(3S_d + S_e), G = A_d, \quad (254)$$

$$r(1-s)S_e = 4S_u - (3+s)rS_d, \quad (255)$$

$$S_D = S_u - rs(S_d - S_e), \quad (256)$$

$$A_u = rt_u A_d, A_e = t_e A_d, A_D = rt_D A_d. \quad (257)$$

Using the above equations, along with Eqs. (244)-(253), one obtains the following relations among the elements of the texture specific mass matrices and the SO(10) based mass matrices, e.g.,

$$r(1-s)a_e \cos \alpha_e = 4a_u \cos \alpha_u - (3+s)ra_d \cos \alpha_d, \quad (258)$$

$$r(1-s)b_e \cos \beta_e = 4b_u \cos \beta_u - (3+s)rb_d \cos \beta_d, \quad (259)$$

$$r(1-s)d_e = 4d_u - (3+s)rd_d, \quad (260)$$

$$r(1-s)c_e = 4c_u - (3+s)rc_d, \quad (261)$$

$$a_D \cos \alpha_D = a_u \cos \alpha_u - rs(a_d \cos \alpha_d - a_e \cos \alpha_e), \quad (262)$$

$$b_D \cos \beta_D = b_u \cos \beta_u - rs(b_d \cos \beta_d - b_e \cos \beta_e), \quad (263)$$

$$d_D = d_u - rs(d_d - d_e), \quad (264)$$

$$c_D = c_u - rs(c_d - d_e), \quad (265)$$

$$a_e \sin \alpha_e = t_e a_d \sin \alpha_d, \quad (266)$$

$$b_e \sin \beta_e = t_e b_d \sin \beta_d, \quad (267)$$

$$a_u \sin \alpha_u = r t_u a_d \sin \alpha_d, \quad (268)$$

$$b_u \sin \beta_u = r t_u b_d \sin \beta_d, \quad (269)$$

$$a_D \sin \alpha_D = r t_D a_d \sin \alpha_d, \quad (270)$$

$$b_D \sin \beta_D = r t_D b_d \sin \beta_d. \quad (271)$$

The above large number of coupled equations need to be solved for checking the compatibility of texture specific mass matrices with the constraints imposed by  $SO(10)$ . The procedure being followed by Refs. 180, 196 is to construct the texture 4 zero mass matrices and check their viability with the available data. To this end, the authors consider the fermion masses at the GUT scale  $M_X = 2 \times 10^{16}$  GeV as provided in the Refs. 130 and 193. It may be mentioned that Ref. 193 considers the mixing angles to be scale independent, however, it has been shown<sup>192</sup> that in the case of quarks, there is a slight scale dependence of the elements of the CKM matrix. Therefore, both the cases where the CKM matrix elements  $V_{ub}$ ,  $V_{cb}$ ,  $V_{td}$  and  $V_{ts}$  are scale independent as well as when these are scale dependent have been considered. In the latter case, it can be shown<sup>192</sup> that at the GUT scale these elements get re-scaled as

$$V_{ij} = V_{ij}^0 B_t^{-1}, \quad (272)$$

where  $ij = ub, cb, td, ts$  and  $B_t$  is the running coupling constant induced by the top quark Yukawa coupling and varies between 0.7 to 0.9. For the leptonic sector, since the neutrino mass squared differences and the lepton mixing parameters do not show much scale dependence, their  $M_Z$  values as quoted by Fogli *et al.*<sup>95</sup> have been used for the purpose of calculations.

As a first step, the parameters of the mass matrices  $M_u$  and  $M_d$ , e.g.,  $a_u, b_u, c_u, d_u, a_d, b_d, c_d, d_d, \phi_1$  and  $\phi_2$  have been found by imposing the constraints of the quark mixing data. It may be noted that the mixing data does not impose any constraint on the absolute values of the phases  $\alpha_u, \alpha_d, \beta_u$  and  $\beta_d$  appearing in the quark mass matrices. As a next step, the element  $d_e$  of the mass matrix  $M_e$  is

considered as the free parameter to obtain the parameters  $r$  and  $s$  in terms of the diagonal elements of the mass matrices  $M_{u,d,e}$ , e.g.,

$$r = \frac{(d_u c_e - c_u d_e) + (d_d c_u - d_u c_d)}{(c_e d_d - c_d d_e)}, \quad (273)$$

$$s = 1 - \frac{4(d_u c_d - d_d c_u)}{r(d_e c_d - d_d c_e)}. \quad (274)$$

It may further be noted that by varying  $\alpha_u$ , it is possible to find  $\alpha_d$  through the condition  $\alpha_d = \alpha_u - \phi_1$ . This allows the calculation of the parameter  $t_u$ , e.g.,

$$t_u = \frac{a_u \sin \alpha_u}{r a_d \sin \alpha_d}. \quad (275)$$

Further, one can obtain the value of the phase  $\beta_u$  as

$$\beta_u = \tan^{-1} \left[ \frac{r t_u b_d \sin \phi_2}{(r t_u b_d \cos \phi_2) - b_u} \right], \quad (276)$$

using which the phase  $\beta_d$  can be found through the relation

$$\beta_d = \beta_u - \phi_2. \quad (277)$$

The phases  $\alpha_e$  and  $\beta_e$ , can also be found, e.g.,

$$\alpha_e = \tan^{-1} \left[ \frac{t_e a_d \sin \alpha_d}{a_u \cos \alpha_u \left( \frac{c_e d_d - d_e c_d}{c_u d_d - d_u c_d} \right) - a_d \cos \alpha_d \left( \frac{c_e d_u - d_e c_u}{c_u d_d - d_u c_d} \right)} \right], \quad (278)$$

$$\beta_e = \tan^{-1} \left[ \frac{t_e b_d \sin \beta_d}{b_u \cos \beta_u \left( \frac{c_e d_d - d_e c_d}{c_u d_d - d_u c_d} \right) - b_d \cos \beta_d \left( \frac{c_e d_u - d_e c_u}{c_u d_d - d_u c_d} \right)} \right], \quad (279)$$

wherein the parameter  $t_e$  can be considered to be free. Subsequently, considering  $\alpha_D$  as a free parameter, one gets

$$a_D = (a_u \cos \alpha_u - r s (a_d \cos \alpha_d - a_e \cos \alpha_e)) / \cos \alpha_D. \quad (280)$$

This allows one to calculate the parameter  $t_D$  as

$$t_D = \frac{a_D \sin \alpha_D}{r a_d \sin \alpha_d}. \quad (281)$$

The remaining elements of the Dirac neutrino mass matrix, in terms of the parameters already found, can be obtained as

$$b_D = \sqrt{(r t_D b_d \sin \beta_d)^2 + (b_u \cos \beta_u - r s (b_d \cos \beta_d - b_e \cos \beta_e))^2}, \quad (282)$$

$$d_D = d_u - r s (d_d - d_e), \quad (283)$$

$$c_D = c_u - r s (c_d - c_e). \quad (284)$$

This allows one to evaluate the elements of the mass matrices H and F as

$$a_H = \frac{1}{4}(3a_d \cos \alpha_d + a_e \cos \alpha_e), \quad (285)$$

$$b_H = \frac{1}{4}(3b_d \cos \beta_d + b_e \cos \beta_e), \quad (286)$$

$$d_H = \frac{1}{4}(3d_d + d_e), \quad (287)$$

$$c_H = \frac{1}{4}(3c_d + c_e), \quad (288)$$

$$a_F = \frac{1}{4}(a_d \cos \alpha_d - a_e \cos \alpha_e), \quad (289)$$

$$b_F = \frac{1}{4}(b_d \cos \beta_d - b_e \cos \beta_e), \quad (290)$$

$$d_F = \frac{1}{4}(d_d - d_e), \quad (291)$$

$$c_F = \frac{1}{4}(c_d - c_e). \quad (292)$$

As a next step,  $r_R$  can be considered as a free parameter and the elements of the right handed Majorana neutrino matrix can be evaluated as

$$a_R = r_R^{-1} a_F, b_R = r_R^{-1} b_F, d_R = r_R^{-1} d_F, c_R = r_R^{-1} c_F. \quad (293)$$

The light Majorana neutrino mass matrix may be obtained using the type-I seesaw mechanism,

$$M_\nu = -M_{\nu D}^T M_{\nu R}^{-1} M_{\nu D} = -r_R^{-1} M_{\nu D}^T F^{-1} M_{\nu D} \quad (294)$$

or by using the type-II seesaw mechanism defined as

$$M_\nu = M_{\nu L} - M_{\nu D}^T M_{\nu R}^{-1} M_{\nu D}. \quad (295)$$

However, the results obtained in the two cases are not very different, therefore Refs. 180 and 196 have discussed the results corresponding to the type-I seesaw mechanism only. The eigenvalues ( $m_{\nu 1}, m_{\nu 2}, m_{\nu 3}$ ) and the complex diagonalizing matrix  $O_\nu$  of the matrix  $M_\nu$  are then numerically computed and are used along with the diagonalizing transformations for the charged lepton matrix to compute the PMNS mixing matrix.

It may be noted that there are only 16 free parameters in case one uses type-I seesaw mechanism which further increases to 17 in the case of type-II seesaw mechanism. For the purpose of calculations, along with type-I seesaw mechanism, the parameters  $a_u, b_u, c_u, d_u, a_d, b_d, c_d, d_d, a_e, b_e, c_e, d_e, \alpha_u, \alpha_d, \alpha_e$  and  $r_R^{-1}$  have been used. Interestingly, one finds that the present fermion mixing data is very well accommodated by the texture 4 zero SO(10) inspired mass matrices. The constraints from the CKM matrix elements have implications only on the hierarchy of the quark mass matrices and on the phase differences  $\phi_1 = \alpha_u - \alpha_d$  and  $\phi_2 = \beta_u - \beta_d$ , without bearing any impressions on the absolute values of the phases  $\alpha_u, \alpha_d, \beta_u$  and  $\beta_d$  involved in the quark mass matrices. However, the fermion mixing data as well as



the observed neutrino mass square differences have implications not only on the hierarchy of the charged lepton mass matrices and the light neutrino mass matrix but also on the phases involved in these matrices. In particular, one finds that the quark mass matrices follow the ‘natural’ hierarchy whereas the lepton mass matrices do not exhibit the same, as is expected. Specifically the neutrinos follow a ‘normal’ hierarchy, whereas the hierarchy for the charged lepton mass matrix is different.

The analysis also leads to several interesting points regarding the phase structure of the elements of the mass matrices. In particular, the lepton mixing angle  $(s_{12}^l)^2$  supports the large values of  $d_e$  only wherein  $d_e > c_e$ . However, these large values of  $d_e$  are compatible with small values of  $d_u$  and  $d_d$  suggesting that the quark mass matrices continue to possess a ‘weak’ hierarchy as one goes from  $M_Z$  to  $M_X$  scale. Furthermore, it is observed that the parameter  $t_e$  along with the phase  $\alpha_D$  of the Dirac neutrino mass matrix has to be non zero in order to reproduce the observed values of the ratio  $\Delta m_{13}^2/\Delta m_{12}^2$  indicating that real  $M_e$  and  $M_{\nu D}$  may not be able to accommodate the lepton mixing data under the constraints of SO(10). Likewise it is also observed that the mixing angle  $(s_{23}^l)^2$  can be reproduced only by non vanishing values of the phase  $\alpha_u$  of the mass matrix  $M_u$  suggesting that within the SO(10) framework, the real  $M_u$  may not be allowed.

For the sake of completion, the allowed ranges of the elements of the various mass matrices in the SO(10) framework have also been presented, e.g.,

$$M_u = \begin{pmatrix} 0 & (0.0114 - 0.0125)e^{i(162)} & 0 \\ (0.0114 - 0.0125)e^{-i(162)} & 9 - 20 & (24.5 - 33.06)e^{i(-0.06)} \\ 0 & (24.5 - 33.06)e^{-i(-0.06)} & 53.77 - 64.77 \end{pmatrix}, \quad (296)$$

$$M_d = \begin{pmatrix} 0 & (0.0053 - 0.0057)e^{i(74)} & 0 \\ (0.0053 - 0.0057)e^{-i(74)} & 0.1 - 0.22 & (0.33 - 0.43)e^{i(-7)} \\ 0 & (0.33 - 0.43)e^{-i(-7)} & 0.76 - 0.88 \end{pmatrix}, \quad (297)$$

$$M_e = \begin{pmatrix} 0 & (0.0117 - 0.0182)e^{i(-37)} & 0 \\ (0.0117 - 0.0182)e^{-i(-37)} & 1.01 - 1.35 & (0.697 - 0.865)e^{i(-39)} \\ 0 & (0.697 - 0.865)e^{-i(-39)} & 0.2369 - 0.5769 \end{pmatrix}, \quad (298)$$

$$M_{\nu d} = \begin{pmatrix} 0 & (3.19 - 6.65)e^{i(83)} & 0 \\ (3.19 - 6.65)e^{-i(83)} & 71.17 - 90.24 & (-84.78 - -47.21)e^{i(45)} \\ 0 & (-84.78 - -47.21)e^{-i(45)} & 22.74 - 44.16 \end{pmatrix}, \quad (299)$$

$$M_\nu = \begin{pmatrix} 0 & (0.53 - 1.02) \times 10^{-11} & 0 \\ (0.53 - 1.02) \times 10^{-11} & (0.40 - 1.69) \times 10^{-11} & (0.270 - 2.19) \times 10^{-11} \\ 0 & (0.270 - 2.19) \times 10^{-11} & (3.38 - 5.19) \times 10^{-11} \end{pmatrix}, \quad (300)$$

$$M_R = \begin{pmatrix} 0 & (-1.42 - 6.89) \times 10^{12} & 0 \\ (-1.42 - 6.89) \times 10^{12} & (-1.5 - 0.283) \times 10^{14} & (-16.11 - 4.03) \times 10^{12} \\ 0 & (-16.11 - 4.03) \times 10^{12} & (1.28 - 4.87) \times 10^{13} \end{pmatrix}. \quad (301)$$

The corresponding CKM and PMNS matrices as well as the associated parameters are as follows,

$$V_{\text{CKM}} = \begin{pmatrix} 0.9738 - 0.9747 & 0.2235 - 0.2274 & 0.00367 - 0.00577 \\ 0.2233 - 0.2272 & 0.9720 - 0.9736 & 0.0454 - 0.0618 \\ 0.0009 - 0.0139 & 0.0446 - 0.0608 & 0.9981 - 0.9990 \end{pmatrix}, \quad (302)$$

$$\sin 2\beta = 0.6561 - 0.7058, J_q = (3.266 - 6.935) \times 10^{-5}, \delta_{13} = 55.73^\circ \text{ to } 81.16^\circ. \quad (303)$$

$$V_{\text{PMNS}} = \begin{pmatrix} 0.7791 - 0.8540 & 0.5025 - 0.6009 & 0.0709 - 0.2236 \\ 0.3050 - 0.4286 & 0.4785 - 0.7552 & 0.5724 - 0.7958 \\ 0.3712 - 0.5124 & 0.4004 - 0.7042 & 0.5865 - 0.8022 \end{pmatrix}, \quad (304)$$

$$(s_{12}^l)^2 = 0.265 - 0.364, (s_{13}^l)^2 = 0.005 - 0.05, (s_{23}^l)^2 = 0.3403 - 0.6399, \quad (305)$$

$$\Delta m_{12}^2 = (6.99 - 8.18) \times 10^{-23} \text{GeV}^2, \Delta m_{13}^2 = (2.06 - 2.67) \times 10^{-21} \text{GeV}^2 \quad (306)$$

$$m_{\nu 1} = (2.92 - 7.07) \times 10^{-12} \text{GeV}, m_{\nu 2} = (0.89 - 1.14) \times 10^{-11} \text{GeV}, \quad (307)$$

$$m_{\nu 3} = (4.55 - 5.20) \times 10^{-11} \text{GeV} \quad (308)$$

$$J_l = -0.0428 - 0.0353, \delta_l = -87.16^\circ - 71.31^\circ. \quad (309)$$

It is easy to check that the CKM matrix and the related parameters have good overlap with the PDG 2010 values. Similarly, the PMNS matrix and the related parameters are also in good agreement with a recent analysis<sup>99</sup>.

## 8. Summary and conclusion

The fermion masses and mixings not only provide a fertile ground to hunt for physics beyond the SM but also pose a big challenge to understand these from more fundamental considerations. In the present work, attempts have been made to present a comprehensive review of some of the aspects of fermion mixing phenomenon and texture specific mass matrices. In the context of fermion mixings, keeping in mind the role played by unitarity of the CKM matrix and unitarity triangles in establishing the CKM paradigm, implications of these on parameters like  $\sin 2\beta$ ,  $V_{ub}$  and phase  $\delta$  have been discussed. Interestingly, one finds that unitarity along with precisely measured  $V_{us}$ ,  $V_{cb}$ ,  $\sin 2\beta$  and angle  $\alpha$  provides important constraints on the CKM matrix element  $V_{ub}$  and the CP violating phase  $\delta$ .

The recent precision measurements of CKM phenomenological parameters along with several developments in the lattice QCD calculations of hadronic factors in the

case of  $K - \bar{K}$  and the  $B_d - \bar{B}_d$  mixings and the contribution of the long distance effects in the  $K - \bar{K}$  system provide motivation to investigate the implications of these for the CKM phenomenology. In this context, some authors<sup>51,52</sup> point towards the possibility of New Physics (NP) in these systems to the tune of 20% or so. However, a recent analysis<sup>53</sup> has made an attempt to re-look this issue and interestingly, one finds that both the  $K - \bar{K}$  and  $B_d - \bar{B}_d$  systems do not seem to provide any significant clues regarding the possibility of existence of NP and therefore, the presence of NP effects, if any, would be less than a few percent only.

The issues of unitarity of the PMNS matrix and unitarity triangles in the leptonic sector have also been discussed in the present work. To this end, attempts<sup>64</sup> have been made to explore the possibility of the construction of the leptonic unitarity triangle in the modified tribimaximal scenario of Bjorken *et al.*<sup>63</sup>. In particular, using the PMNS matrix constructed in this scenario and considering values of  $U_{e3}$  suggested by different theoretical models, the Dirac-like CP violating phase  $\delta$  in the leptonic sector has been found. Further, in light of recent T2K, MINOS, DAYA BAY and RENO observations regarding the mixing angle  $s_{13}$ , the possibility of existence of CP violation in the leptonic sector has been explored<sup>65</sup>, suggesting a good possibility of having non zero CP violation.

Coming to the texture specific hermitian fermion mass matrices, in the present work, we have given an overview of possible cases of Fritzsch-like as well as non Fritzsch-like texture 6 and 5 zero fermion mass matrices. Further, for the case of texture 4 zero Fritzsch-like quark mass matrices, the issue of the hierarchy of the elements of the mass matrices and the role of their phases have been discussed. Furthermore, the case of texture 4 zero Fritzsch-like lepton mass matrices has also been discussed with an emphasis on the hierarchy of neutrino masses for both Majorana and Dirac neutrinos.

For the case of quarks<sup>126</sup>, all the texture 6 zero combinations are completely ruled out whereas in the case of texture 5 zero mass matrices the only viable possibility looks to be that of Fritzsch-like matrices which shows only limited viability, depending upon the light quark masses used as input. Further, for the case of texture 4 zero quark mass matrices<sup>124,125</sup>, including the case of ‘weak hierarchy’ along with the usually considered ‘strong hierarchy’ case, one finds that the weakly hierarchical mass matrices are able to reproduce the strongly hierarchical mixing angles. Also, both the phases having their origin in the mass matrices have to be non zero to achieve compatibility of these matrices with the quark mixing data, in particular with the parameter  $\sin 2\beta$ .

Similar investigations have been presented for the neutrino mixing data considering normal/ inverted hierarchy and degenerate scenario of neutrino masses for Majorana as well as Dirac neutrinos. For the texture 6 zero case<sup>174</sup>, all the possibilities pertaining to normal/ inverted hierarchy and degenerate scenario of neutrino masses for Dirac neutrinos and inverted hierarchy as well as degenerate scenarios in the case of Majorana neutrinos are ruled out. Normal hierarchy of neu-

trino masses for Majorana neutrinos results into some combinations which are in accordance with the neutrino oscillation data. Regarding texture 5 zero lepton mass matrices<sup>180</sup>, interestingly, one finds that these can accommodate all hierarchies of neutrino masses.

For the Fritzsch-like texture 4 zero neutrino mass matrices<sup>172</sup>, analysis pertaining to both Majorana and Dirac neutrinos for different hierarchies of neutrino masses reveals that for both types of neutrinos, all the cases pertaining to inverted hierarchy and degenerate scenarios of neutrino masses are ruled out at  $3\sigma$  C.L. by the existing data. For the normal hierarchy cases, one gets viable ranges of neutrino masses, mixing angle  $s_{13}$ , Jarlskog's rephasing invariant parameter  $J_I$  and the CP violating Dirac-like phase  $\delta_I$ . Interestingly, a measurement of  $m_{\nu_1}$  and further refinements regarding mixing angle  $\theta_{13}$  could have important implications for the nature of neutrinos.

The success of texture 4 zero weakly hierarchical mass matrices warrants a closer look at the origin of these from more fundamental considerations. To this end, general concepts like naturalness<sup>186</sup> and weak basis transformations<sup>21,181,187–190</sup> for reducing the general mass matrices to texture specific form have been discussed. Using the condition of naturalness as well as the facility of WB transformations, the most general mass matrices  $M_{u,d}$  or/and  $M_{\nu,e}$  can be reduced to texture 1 zero hermitian mass matrices, the implications of fermion mixing data on these texture structures have been discussed. One finds that the additional (1,1) elements in these matrices do not show any significant effect on the CKM parameters. Similar observations have been made in the case of lepton mass matrices with similar texture structures wherein the entire range of the various lepton mixing parameters can be reproduced for the case of Dirac as well as Majorana neutrinos. From these observations one can conclude that for the purpose of accommodating the quark mixing data as well as the lepton mixing data, without loss of generality, the texture 4 zero hermitian mass matrices can be considered to be equivalent to texture 2 zero hermitian mass matrices. This also motivates one to understand the significance of texture 4 zero mass matrices from the 'top-down' perspective.

As a next step, the issue of compatibility of the texture 4 zero Fritzsch-like hermitian mass matrices with the SO(10) inspired mass matrices has been discussed. One notes that the texture 4 zero hermitian mass matrices  $M_u$ ,  $M_d$ ,  $M_e$  and  $M_{\nu D}$  can be expressed in terms of SO(10) inspired symmetric and anti-symmetric texture 4 zero mass matrices. Interestingly, one finds that a simultaneous fit to the fermion masses and mixings within the constraints of SO(10) and naturalness can be arrived at. The analysis also shows that quarks and the neutrino mass matrices follow normal hierarchy. Further, in the case of quarks, there are constraints on the hierarchy of the elements of the quark mass matrices and on the phase differences. In the case of leptons, the fermion mixing data has implications not only on the hierarchy of the charged lepton mass matrices and the light neutrino mass matrix but also on the phases involved in these. The weakly hierarchical quark mass matrices continue to be supported within the SO(10) framework.

In conclusion, we would like to remark that on the one hand there is a need to take the analysis of texture specific mass matrices towards completion. For example, besides carrying out the analysis of texture 4 zero non Fritzsch-like fermion mass matrices, one has to consider texture 3 zero cases also, the latter corresponding to general mass matrices after carrying out weak basis rotations. On the other hand, one may also consider breaking the hermiticity condition perturbatively as has been done recently<sup>206</sup> and to go into its detailed implications. Similarly, the compatibility of the texture 4 zero Fritzsch-like hermitian mass matrices with the SO(10) inspired mass matrices motivates one to find deeper understanding of the texture 4 zero *ansätze*, may be within SO(10), incorporating Abelian or Horizontal symmetries.

### Acknowledgments

The authors would like to thank Prof. K. K. Phua and the organizers of the ‘1st IAS-CERN School on Particle Physics and Cosmology and Implications for Technology’ held in NTU, Singapore, 9-31 January 2012, for giving an opportunity to present several aspects of the present work. The authors would also like to thank Prof. N. P. Chang, Rohit Verma, Priyanka Fakay and Samandeep for stimulating discussions and help as well as the Chairman, Department of Physics for providing facilities to work in the department. G.A. would also like to acknowledge DST, Government of India (Grant No: SR/FTP/PS-017/2012) for financial support.

### Appendix A. Diagonalizing transformation of texture 2 zero lepton mass matrices

The Fritzsch-like texture 2 zero lepton mass matrices can be expressed as

$$M_l = \begin{pmatrix} 0 & A_l & 0 \\ A_l^* & D_l & B_l \\ 0 & B_l^* & C_l \end{pmatrix}, \quad M_{\nu D} = \begin{pmatrix} 0 & A_\nu & 0 \\ A_\nu^* & D_\nu & B_\nu \\ 0 & B_\nu^* & C_\nu \end{pmatrix}, \quad (\text{A.1})$$

$M_l$  and  $M_{\nu D}$  respectively corresponding to charged lepton and Dirac neutrino mass matrices. It may be noted that each of the above matrix is texture 2 zero type with  $A_{l(\nu)} = |A_{l(\nu)}|e^{i\alpha_{l(\nu)}}$  and  $B_{l(\nu)} = |B_{l(\nu)}|e^{i\beta_{l(\nu)}}$ , in case these are symmetric then  $A_{l(\nu)}^*$  and  $B_{l(\nu)}^*$  should be replaced by  $A_{l(\nu)}$  and  $B_{l(\nu)}$ , as well as  $C_{l(\nu)}$  and  $D_{l(\nu)}$  should respectively be defined as  $C_{l(\nu)} = |C_{l(\nu)}|e^{i\gamma_{l(\nu)}}$  and  $D_{l(\nu)} = |D_{l(\nu)}|e^{i\omega_{l(\nu)}}$ .

Texture 6 zero mass matrices can be obtained from the above mentioned matrices by taking both  $D_l$  and  $D_\nu$  to be zero, which reduces the matrices  $M_l$  and  $M_{\nu D}$  each to texture 3 zero type. Texture 5 zero matrices can be obtained by taking either  $D_l = 0$  and  $D_\nu \neq 0$  or  $D_\nu = 0$  and  $D_l \neq 0$ , thereby, giving rise to two possible cases of texture 5 zero matrices, referred to as texture 5 zero  $D_l = 0$  case pertaining to  $M_l$  texture 3 zero type and  $M_{\nu D}$  texture 2 zero type and texture 5 zero  $D_\nu = 0$  case pertaining to  $M_l$  texture 2 zero type and  $M_{\nu D}$  texture 3 zero type.

To fix the notations and conventions, we detail the formalism connecting the mass matrix to the neutrino mixing matrix. The mass matrices  $M_l$  and  $M_{\nu D}$  given in Eq. (A.1), for hermitian as well as symmetric case, can be exactly diagonalized. To facilitate diagonalization, the mass matrix  $M_k$ , where  $k = l, \nu D$ , can be expressed as

$$M_k = Q_k M_k^r P_k \quad (\text{A.2})$$

or

$$M_k^r = Q_k^\dagger M_k P_k^\dagger, \quad (\text{A.3})$$

where  $M_k^r$  is a real symmetric matrix with real eigenvalues and  $Q_k$  and  $P_k$  are diagonal phase matrices. For the hermitian case  $Q_k = P_k^\dagger$ , whereas for the symmetric case under certain conditions  $Q_k = P_k$ . In general, the real matrix  $M_k^r$  is diagonalized by the orthogonal transformation  $O_k$ , e.g.,

$$M_k^{diag} = O_k^T M_k^r O_k, \quad (\text{A.4})$$

which on using Eq. (A.3) can be rewritten as

$$M_k^{diag} = O_k^T Q_k^\dagger M_k P_k^\dagger O_k. \quad (\text{A.5})$$

To facilitate the construction of diagonalization transformations for different hierarchies, we introduce a diagonal phase matrix  $\xi_k$  defined as  $\text{diag}(1, e^{i\pi}, 1)$  for the case of normal hierarchy and as  $\text{diag}(1, e^{i\pi}, e^{i\pi})$  for the case of inverted hierarchy. Eq. (A.5) can now be written as

$$\xi_k M_k^{diag} = O_k^T Q_k^\dagger M_k P_k^\dagger O_k, \quad (\text{A.6})$$

which can also be expressed as

$$M_k^{diag} = \xi_k^\dagger O_k^T Q_k^\dagger M_k P_k^\dagger O_k. \quad (\text{A.7})$$

Making use of the fact that  $O_k^* = O_k$  it can be further expressed as

$$M_k^{diag} = (Q_k O_k \xi_k)^\dagger M_k (P_k^\dagger O_k), \quad (\text{A.8})$$

from which one gets

$$M_k = Q_k O_k \xi_k M_k^{diag} O_k^T P_k. \quad (\text{A.9})$$

The case of leptons is fairly straight forward, for the neutrinos the diagonalizing transformation is hierarchy specific as well as requires some fine tuning of the phases of the right handed neutrino mass matrix  $M_R$ . To clarify this point further, in analogy with Eq. (A.9), we can express  $M_{\nu D}$  as

$$M_{\nu D} = Q_{\nu D} O_{\nu D} \xi_{\nu D} M_{\nu D}^{diag} O_{\nu D}^T P_{\nu D}. \quad (\text{A.10})$$

Substituting the above value of  $M_{\nu D}$  in Eq. (143) one obtains

$$M_\nu = -(Q_{\nu D} O_{\nu D} \xi_{\nu D} M_{\nu D}^{diag} O_{\nu D}^T P_{\nu D})^T (M_R)^{-1} (Q_{\nu D} O_{\nu D} \xi_{\nu D} M_{\nu D}^{diag} O_{\nu D}^T P_{\nu D}). \quad (\text{A.11})$$

On using  $P_{\nu D}^T = P_{\nu D}$ , the above equation can further be written as

$$M_\nu = -P_{\nu D} O_{\nu D} M_{\nu D}^{diag} \xi_{\nu D} O_{\nu D}^T Q_{\nu D}^T (M_R)^{-1} Q_{\nu D} O_{\nu D} \xi_{\nu D} M_{\nu D}^{diag} O_{\nu D}^T P_{\nu D}. \quad (\text{A.12})$$

Assuming fine tuning, the phase matrices  $Q_{\nu D}^T$  and  $Q_{\nu D}$  along with  $-M_R$  can be taken as  $m_R \text{diag}(1, 1, 1)$  as well as using the unitarity of  $\xi_{\nu D}$  and orthogonality of  $O_{\nu D}$ , the above equation can be expressed as

$$M_\nu = P_{\nu D} O_{\nu D} \frac{(M_{\nu D}^{diag})^2}{(m_R)^{-1}} O_{\nu D}^T P_{\nu D}. \quad (\text{A.13})$$

The lepton mixing matrix, obtained from the matrices used for diagonalizing the mass matrices  $M_l$  and  $M_\nu$ , is expressed as

$$U = (Q_l O_l \xi_l)^\dagger (P_{\nu D} O_{\nu D}). \quad (\text{A.14})$$

Eliminating the phase matrix  $\xi_l$  by redefinition of the charged lepton phases, the above equation becomes

$$U = O_l^\dagger Q_l P_{\nu D} O_{\nu D}, \quad (\text{A.15})$$

where  $Q_l P_{\nu D}$ , without loss of generality, can be taken as  $(e^{i\phi_1}, 1, e^{i\phi_2})$ ,  $\phi_1$  and  $\phi_2$  being related to the phases of mass matrices and can be treated as free parameters.

To understand the relationship between diagonalizing transformations for different hierarchies of neutrino masses as well as their relationship with the charged lepton case, we reproduce the general diagonalizing transformation  $O_k$ , e.g.,

$$O_k = \begin{pmatrix} \pm O_k(11) \pm O_k(12) \pm O_k(13) \\ \pm O_k(21) \mp O_k(22) \pm O_k(23) \\ \mp O_k(31) \pm O_k(32) \pm O_k(33) \end{pmatrix}, \quad (\text{A.16})$$

88 *Manmohan Gupta, Gulsheen Ahuja*

where

$$\begin{aligned}
O_k(11) &= \sqrt{\frac{m_2 m_3 (m_3 - m_2 - D_k)}{(m_1 - m_2 + m_3 - D_k)(m_3 - m_1)(m_1 + m_2)}} \\
O_k(12) &= \sqrt{\frac{m_1 m_3 (m_1 + m_3 - D_k)}{(m_1 - m_2 + m_3 - D_k)(m_2 + m_3)(m_2 + m_1)}} \\
O_k(13) &= \sqrt{\frac{m_1 m_2 (m_2 - m_1 + D_k)}{(m_1 - m_2 + m_3 - D_k)(m_3 + m_2)(m_3 - m_1)}} \\
O_k(21) &= \sqrt{\frac{m_1 (m_3 - m_2 - D_k)}{(m_3 - m_1)(m_1 + m_2)}} \\
O_k(22) &= \sqrt{\frac{m_2 (m_3 + m_1 - D_k)}{(m_2 + m_3)(m_2 + m_1)}} \\
O_k(23) &= \sqrt{\frac{m_3 (m_2 - m_1 + D_k)}{(m_2 + m_3)(m_3 - m_1)}} \\
O_k(31) &= \sqrt{\frac{m_1 (m_2 - m_1 + D_k)(m_1 + m_3 - D_k)}{(m_1 - m_2 + m_3 - D_k)(m_1 + m_2)(m_3 - m_1)}} \\
O_k(32) &= \sqrt{\frac{m_2 (D_k - m_1 + m_2)(m_3 - m_2 - D_k)}{(m_1 - m_2 + m_3 - D_k)(m_2 + m_3)(m_2 + m_1)}} \\
O_k(33) &= \sqrt{\frac{m_3 (m_3 - m_2 - D_k)(m_1 + m_3 - D_k)}{(m_1 - m_2 + m_3 - D_k)(m_3 - m_1)(m_3 + m_2)}}, \quad (A.17)
\end{aligned}$$

$m_1, -m_2, m_3$  being the eigenvalues of  $M_k$ . In the case of charged leptons, because of the hierarchy  $m_e \ll m_\mu \ll m_\tau$ , the mass eigenstates can be approximated respectively to the flavor eigenstates. Using the approximation,  $m_{l1} \simeq m_e, m_{l2} \simeq m_\mu$  and  $m_{l3} \simeq m_\tau$ , the first element of the matrix  $O_l$  can be obtained from the corresponding element of Eq. (A.17) by replacing  $m_1, -m_2, m_3$  by  $m_e, -m_\mu, m_\tau$ , e.g.,

$$O_l(11) = \sqrt{\frac{m_\mu m_\tau (m_\tau - m_\mu - D_l)}{(m_e - m_\mu + m_\tau - D_l)(m_\tau - m_e)(m_e + m_\mu)}}. \quad (A.18)$$

For normal hierarchy defined as  $m_{\nu_1} < m_{\nu_2} \ll m_{\nu_3}$ , as well as for the corresponding degenerate case given by  $m_{\nu_1} \lesssim m_{\nu_2} \sim m_{\nu_3}$ , Eq. (A.17) can also be used to obtain the first element of diagonalizing transformation for Dirac neutrinos as well as Majorana neutrinos. The first element of the diagonalizing transformation for Dirac neutrinos can be obtained from the corresponding element of Eq. (A.17) by replacing  $m_1, -m_2, m_3$  by  $m_{\nu_1}, -m_{\nu_2}, m_{\nu_3}$  and is given by

$$O_{\nu D}(11) = \sqrt{\frac{m_{\nu_2} m_{\nu_3} (m_{\nu_3} - m_{\nu_2} - D_\nu)}{(m_{\nu_1} - m_{\nu_2} + m_{\nu_3} - D_\nu)(m_{\nu_3} - m_{\nu_1})(m_{\nu_1} + m_{\nu_2})}}, \quad (A.19)$$



where  $m_{\nu_1}$ ,  $m_{\nu_2}$  and  $m_{\nu_3}$  are neutrino masses. Similarly, for Majorana neutrinos, replacing  $m_1$ ,  $-m_2$ ,  $m_3$  by  $\sqrt{m_{\nu_1}m_R}$ ,  $-\sqrt{m_{\nu_2}m_R}$ ,  $\sqrt{m_{\nu_3}m_R}$  in the equation, we get

$$O_\nu(11) = \sqrt{\frac{\sqrt{m_{\nu_2}}\sqrt{m_{\nu_3}}(\sqrt{m_{\nu_3}} - \sqrt{m_{\nu_2}} - D_\nu)}{(\sqrt{m_{\nu_1}} - \sqrt{m_{\nu_2}} + \sqrt{m_{\nu_3}} - D_\nu)(\sqrt{m_{\nu_3}} - \sqrt{m_{\nu_1}})(\sqrt{m_{\nu_1}} + \sqrt{m_{\nu_2}})}}. \quad (\text{A.20})$$

The parameter  $D_\nu$  is to be divided by  $\sqrt{m_R}$ , however as  $D_\nu$  is arbitrary therefore we retain it as it is.

In the same manner, for Dirac and Majorana neutrinos one can obtain the elements of diagonalizing transformation for the inverted hierarchy case defined as  $m_{\nu_3} \ll m_{\nu_1} < m_{\nu_2}$  as well as for the corresponding degenerate case given by  $m_{\nu_3} \sim m_{\nu_1} \lesssim m_{\nu_2}$ . For the case of Dirac neutrinos, the first element, obtained by replacing  $m_1$ ,  $-m_2$ ,  $m_3$  with  $m_{\nu_1}$ ,  $-m_{\nu_2}$ ,  $-m_{\nu_3}$  in Eq. (A.17), is given by

$$O_{\nu D}(11) = \sqrt{\frac{m_{\nu_2}m_{\nu_3}(m_{\nu_3} + m_{\nu_2} + D_\nu)}{(-m_{\nu_1} + m_{\nu_2} + m_{\nu_3} + D_\nu)(m_{\nu_3} + m_{\nu_1})(m_{\nu_1} + m_{\nu_2})}}. \quad (\text{A.21})$$

For Majorana neutrinos, by replacing  $m_1$ ,  $-m_2$ ,  $m_3$  in Eq. (A.17) with  $\sqrt{m_{\nu_1}m_R}$ ,  $-\sqrt{m_{\nu_2}m_R}$ ,  $-\sqrt{m_{\nu_3}m_R}$ , we obtain

$$O_\nu(11) = \sqrt{\frac{\sqrt{m_{\nu_2}}\sqrt{m_{\nu_3}}(D_\nu + \sqrt{m_{\nu_2}} + \sqrt{m_{\nu_3}})}{(-\sqrt{m_{\nu_1}} + \sqrt{m_{\nu_2}} + \sqrt{m_{\nu_3}} + D_\nu)(\sqrt{m_{\nu_1}} + \sqrt{m_{\nu_3}})(\sqrt{m_{\nu_1}} + \sqrt{m_{\nu_2}})}}. \quad (\text{A.22})$$

The other elements of diagonalizing transformations in the case of neutrinos as well as charged leptons can similarly be found.

## Appendix B. Elements of the PMNS mixing matrix

In this Appendix, we present the elements of the PMNS mixing matrix in the case of Dirac neutrinos corresponding to texture 4 zero mass matrices. For Majorana neutrinos, the elements of the PMNS mixing matrix can be derived from those presented below by replacing  $m_1$ ,  $-m_2$ ,  $m_3$  by  $\sqrt{m_{\nu_1}m_R}$ ,  $-\sqrt{m_{\nu_2}m_R}$ ,  $\sqrt{m_{\nu_3}m_R}$ .

Further, the corresponding relations for the texture 5 and 6 zero mass matrices can be easily derived from these. For example, considering both  $D_l$  and  $D_\nu$  to be zero the relations for texture 6 zero mass matrices are obtained, whereas for the texture 5 zero mass matrices either  $D_l$  or  $D_\nu$  is considered to be zero. The expressions for

the elements of the PMNS mixing matrix are given by

$$\begin{aligned}
 U_{e1} = & \sqrt{\frac{m_1(-D_\nu + m_2 + m_3)}{(m_1 - m_2)(-m_1 + m_3)}} \sqrt{\frac{m_e(-D_l + m_\mu + m_\tau)}{(m_e - m_\mu)(-m_e + m_\tau)}} + \\
 & \sqrt{\frac{-m_2 m_3(-D_\nu + m_2 + m_3)}{C_\nu(m_1 - m_2)(-m_1 + m_3)}} \sqrt{\frac{-m_\mu m_\tau(-D_l + m_\mu + m_\tau)}{C_l(m_e - m_\mu)(-m_e + m_\tau)}} \phi_1 + \\
 & \sqrt{\frac{m_1(D_\nu - m_1 - m_2)(-D_\nu + m_1 + m_3)}{C_\nu(m_1 - m_2)(-m_1 + m_3)}} \times \\
 & \sqrt{\frac{m_e(D_l - m_e - m_\mu)(-D_l + m_e + m_\tau)}{C_l(m_e - m_\mu)(-m_e + m_\tau)}} \phi_2
 \end{aligned} \tag{B.1}$$

$$\begin{aligned}
 U_{e2} = & \sqrt{\frac{-m_2(-D_\nu + m_1 + m_3)}{(m_1 - m_2)(-m_2 + m_3)}} \sqrt{\frac{m_e(-D_l + m_\mu + m_\tau)}{(m_e - m_\mu)(-m_e + m_\tau)}} - \\
 & \sqrt{\frac{m_1 m_3(-D_\nu + m_1 + m_3)}{C_\nu(m_1 - m_2)(-m_2 + m_3)}} \sqrt{\frac{-m_\mu m_\tau(-D_l + m_\mu + m_\tau)}{C_l(m_e - m_\mu)(-m_e + m_\tau)}} \phi_1 + \\
 & \sqrt{\frac{-m_2(D_\nu - m_1 - m_2)(-D_\nu + m_2 + m_3)}{C_\nu(m_1 - m_2)(-m_2 + m_3)}} \times \\
 & \sqrt{\frac{m_e(D_l - m_e - m_\mu)(-D_l + m_e + m_\tau)}{C_l(m_e - m_\mu)(-m_e + m_\tau)}} \phi_2
 \end{aligned} \tag{B.2}$$

$$\begin{aligned}
 U_{e3} = & \sqrt{\frac{m_3(D_\nu - m_1 - m_2)}{(-m_1 + m_3)(-m_2 + m_3)}} \sqrt{\frac{m_e(-D_l + m_\mu + m_\tau)}{(m_e - m_\mu)(-m_e + m_\tau)}} + \\
 & \sqrt{\frac{-m_1 m_2(D_\nu - m_1 - m_2)}{C_\nu(-m_1 + m_3)(-m_2 + m_3)}} \sqrt{\frac{-m_\mu m_\tau(-D_l + m_\mu + m_\tau)}{C_l(m_e - m_\mu)(-m_e + m_\tau)}} \phi_1 - \\
 & \sqrt{\frac{m_3(-D_\nu + m_1 + m_3)(-D_\nu + m_2 + m_3)}{C_\nu(-m_1 + m_3)(-m_2 + m_3)}} \times \\
 & \sqrt{\frac{m_e(D_l - m_e - m_\mu)(-D_l + m_e + m_\tau)}{C_l(m_e - m_\mu)(-m_e + m_\tau)}} \phi_2
 \end{aligned} \tag{B.3}$$

$$\begin{aligned}
U_{\mu 1} = & \sqrt{\frac{m_1(-D_\nu + m_2 + m_3)}{(m_1 - m_2)(-m_1 + m_3)}} \sqrt{\frac{-m_\mu(-D_l + m_e + m_\tau)}{(m_e - m_\mu)(-m_\mu + m_\tau)}} - \\
& \sqrt{\frac{-m_2 m_3(-D_\nu + m_2 + m_3)}{C_\nu(m_1 - m_2)(-m_1 + m_3)}} \sqrt{\frac{m_e m_\tau(-D_l + m_e + m_\tau)}{C_l(m_e - m_\mu)(-m_\mu + m_\tau)}} \phi_1 + \\
& \sqrt{\frac{m_1(D_\nu - m_1 - m_2)(-D_\nu + m_1 + m_3)}{C_\nu(m_1 - m_2)(-m_1 + m_3)}} \times \\
& \sqrt{\frac{-m_\mu(D_l - m_e - m_\mu)(-D_l + m_\mu + m_\tau)}{C_l(m_e - m_\mu)(-m_\mu + m_\tau)}} \phi_2
\end{aligned} \tag{B.4}$$

$$\begin{aligned}
U_{\mu 2} = & \sqrt{\frac{-m_2(-D_\nu + m_1 + m_3)}{(m_1 - m_2)(-m_2 + m_3)}} \sqrt{\frac{-m_\mu(-D_l + m_e + m_\tau)}{(m_e - m_\mu)(-m_\mu + m_\tau)}} + \\
& \sqrt{\frac{m_1 m_3(-D_\nu + m_1 + m_3)}{C_\nu(m_1 - m_2)(-m_2 + m_3)}} \sqrt{\frac{m_e m_\tau(-D_l + m_e + m_\tau)}{C_l(m_e - m_\mu)(-m_\mu + m_\tau)}} \phi_1 + \\
& \sqrt{\frac{-m_2(D_\nu - m_1 - m_2)(-D_\nu + m_2 + m_3)}{C_\nu(m_1 - m_2)(-m_2 + m_3)}} \times \\
& \sqrt{\frac{-m_\mu(D_l - m_e - m_\mu)(-D_l + m_\mu + m_\tau)}{C_l(m_e - m_\mu)(-m_\mu + m_\tau)}} \phi_2
\end{aligned} \tag{B.5}$$

$$\begin{aligned}
U_{\mu 3} = & \sqrt{\frac{m_3(D_\nu - m_1 - m_2)}{(-m_1 + m_3)(-m_2 + m_3)}} \sqrt{\frac{-m_\mu(-D_l + m_e + m_\tau)}{(m_e - m_\mu)(-m_\mu + m_\tau)}} - \\
& \sqrt{\frac{-m_1 m_2(D_\nu - m_1 - m_2)}{C_\nu(-m_1 + m_3)(-m_2 + m_3)}} \sqrt{\frac{m_e m_\tau(-D_l + m_e + m_\tau)}{C_l(m_e - m_\mu)(-m_\mu + m_\tau)}} \phi_1 - \\
& \sqrt{\frac{m_3(-D_\nu + m_1 + m_3)(-D_\nu + m_2 + m_3)}{C_\nu(-m_1 + m_3)(-m_2 + m_3)}} \times \\
& \sqrt{\frac{-m_\mu(D_l - m_e - m_\mu)(-D_l + m_\mu + m_\tau)}{C_l(m_e - m_\mu)(-m_\mu + m_\tau)}} \phi_2
\end{aligned} \tag{B.6}$$

$$\begin{aligned}
U_{\tau 1} = & \sqrt{\frac{m_1(-D_\nu + m_2 + m_3)}{(m_1 - m_2)(-m_1 + m_3)}} \sqrt{\frac{m_\tau(D_l - m_e - m_\mu)}{(-m_e + m_\tau)(-m_\mu + m_\tau)}} + \\
& \sqrt{\frac{-m_2 m_3(-D_\nu + m_2 + m_3)}{C_\nu(m_1 - m_2)(-m_1 + m_3)}} \sqrt{\frac{-m_e m_\mu(D_l - m_e - m_\mu)}{C_l(-m_e + m_\tau)(-m_\mu + m_\tau)}} \phi_1 - \\
& \sqrt{\frac{m_1(D_\nu - m_1 - m_2)(-D_\nu + m_1 + m_3)}{C_\nu(m_1 - m_2)(-m_1 + m_3)}} \times \\
& \sqrt{\frac{m_\tau(-D_l + m_e + m_\tau)(-D_l + m_\mu + m_\tau)}{C_l(-m_e + m_\tau)(-m_\mu + m_\tau)}} \phi_2
\end{aligned} \tag{B.7}$$

$$\begin{aligned}
U_{\tau 2} = & \sqrt{\frac{-m_2(-D_\nu + m_1 + m_3)}{(m_1 - m_2)(-m_2 + m_3)}} \sqrt{\frac{m_\tau(D_l - m_e - m_\mu)}{(-m_e + m_\tau)(-m_\mu + m_\tau)}} - \\
& \sqrt{\frac{m_1 m_3(-D_\nu + m_1 + m_3)}{C_\nu(m_1 - m_2)(-m_2 + m_3)}} \sqrt{\frac{-m_e m_\mu(D_l - m_e - m_\mu)}{C_l(-m_e + m_\tau)(-m_\mu + m_\tau)}} \phi_1 - \\
& \sqrt{\frac{-m_2(D_\nu - m_1 - m_2)(-D_\nu + m_2 + m_3)}{C_\nu(m_1 - m_2)(-m_2 + m_3)}} \times \\
& \sqrt{\frac{m_\tau(-D_l + m_e + m_\tau)(-D_l + m_\mu + m_\tau)}{C_l(-m_e + m_\tau)(-m_\mu + m_\tau)}} \phi_2
\end{aligned} \tag{B.8}$$

$$\begin{aligned}
U_{\tau 3} = & \sqrt{\frac{m_3(D_\nu - m_1 - m_2)}{(-m_1 + m_3)(-m_2 + m_3)}} \sqrt{\frac{m_\tau(D_l - m_e - m_\mu)}{(-m_e + m_\tau)(-m_\mu + m_\tau)}} + \\
& \sqrt{\frac{-m_1 m_2(D_\nu - m_1 - m_2)}{C_\nu(-m_1 + m_3)(-m_2 + m_3)}} \sqrt{\frac{-m_e m_\mu(D_l - m_e - m_\mu)}{C_l(-m_e + m_\tau)(-m_\mu + m_\tau)}} \phi_1 - \\
& \sqrt{\frac{m_3(-D_\nu + m_1 + m_3)(-D_\nu + m_2 + m_3)}{C_\nu(-m_1 + m_3)(-m_2 + m_3)}} \times \\
& \sqrt{\frac{m_\tau(-D_l + m_e + m_\tau)(-D_l + m_\mu + m_\tau)}{C_l(-m_e + m_\tau)(-m_\mu + m_\tau)}} \phi_2
\end{aligned} \tag{B.9}$$

### Appendix C. Diagonalizing transformation of texture 1 zero hermitian mass matrix

To facilitate diagonalization, the mass matrices  $M_q$  may be expressed as  $M_q = P_q^\dagger M_q^r P_q$  or  $M_q^r = P_q M_q P_q^\dagger$  where  $M_q^r$  are real symmetric matrices with real eigenvalues and  $P_q$  are the diagonal phase matrices, e.g.,

$$M_q^r = \begin{pmatrix} e_q & |a_q| & 0 \\ |a_q| & d_q & |b_q| \\ 0 & |b_q| & c_q \end{pmatrix}, \quad P_q = \begin{pmatrix} e^{i\alpha_q} & 0 & 0 \\ 0 & 1 & 0 \\ 0 & 0 & e^{i\beta_q} \end{pmatrix}. \tag{C.1}$$

The matrix  $M_q^r$  can be diagonalized using the following transformations

$$M_q^{diag} = O_q^T M_q^r O_q = O_q^T P_q M_q P_q^\dagger O_q = \text{Diag}(m_1, -m_2, m_3), \quad (\text{C.2})$$

where the subscripts 1, 2 and 3 refer respectively to  $u, c, t$  for the up sector,  $d, s, b$  for the down sector,  $e, \mu, \tau$  for the charged lepton sector and  $\nu_1, \nu_2, \nu_3$  for the neutrino sector. The exact diagonalization of the mass matrix  $M_q^r$  can be carried out using the three invariants, Trace  $M_q^r$ , Trace  $(M_q^r)^2$  and Determinant  $M_q^r$ . Using these, the elements of the mass matrix  $|a_q|$ ,  $|b_q|$  and  $c_q$  can be expressed in terms of the free parameters  $e_q, d_q$  and the respective fermion mass eigenvalues as

$$\begin{aligned} c_q &= (m_1 - m_2 + m_3 - d_k - e_q), \\ |a_k| &= \sqrt{\frac{(m_1 - e_q)(m_2 + e_q)(m_3 - e_q)}{c_k - e_q}} \\ |b_k| &= \sqrt{\frac{(c_q - m_1)(m_3 - c_q)(c_q + m_2)}{c_q + e_q}}. \end{aligned} \quad (\text{C.3})$$

In order that the diagonalizing transformations remain real, the free parameters  $e_q$  and  $d_q$  get constrained within the limits

$$(m_3 - m_2 - e_q) > d_q > (m_1 - m_2 - e_q), \quad (\text{C.4})$$

and

$$m_1 > e_q > -m_2. \quad (\text{C.5})$$

The exact diagonalizing transformation  $O_q$  for the matrix  $M_q^r$  is given by

$$O_q = \begin{pmatrix} \sqrt{\frac{(e_q+m_2)(m_3-e_q)(c_q-m_1)}{(c_q-e_q)(m_3-m_1)(m_2+m_1)}} & \sqrt{\frac{(m_1-e_q)(m_3-e_q)(c_q+m_2)}{(c_q-e_q)(m_3+m_2)(m_2+m_1)}} & \sqrt{\frac{(m_1-e_q)(e_q+m-2)(m_3-c_q)}{(c_q-e_q)(m_3+m_2)(m_3-m_1)}} \\ \sqrt{\frac{(c_q-m_1)(m_1-e_q)}{(m_3-m_1)(m_2+m_1)}} & -\sqrt{\frac{(e_q+m_2)(c_q+m_2)}{(m_3+m_2)(m_2+m_1)}} & \sqrt{\frac{(m_3-e_q)(m_3-c_q)}{(m_3+m_2)(m_3-m_1)}} \\ -\sqrt{\frac{(m_1-e_q)(m_3-c_q)(c_q+m_2)}{(c_q-e_q)((m_3-m_1)(m_2+m_1))}} & \sqrt{\frac{(e_q+m_2)(c_q-m_1)(m_3-c_q)}{(c_q-e_q)((m_3+m_2)(m_2+m_1))}} & \sqrt{\frac{(m_3-e_q)(c_q-m_1)(c_q+m_2)}{(c_q-e_q)(m_3+m_2)(m_3-m_1)}} \end{pmatrix}. \quad (\text{C.6})$$

## References

1. N. Cabibbo, *Phys. Rev. Lett.* **10**, 531 (1963).
2. S. L. Glashow, J. Illiopoulos and L. Maiani, *Phys. Rev. D* **2**, 1285 (1970).
3. M. Kobayashi and T. Maskawa, *Prog. Theor. Phys.* **49**, 652 (1973).
4. S. L. Glashow, *Nucl. Phys.* **22**, 597 (1961).
5. S. Weinberg, *Phys. Rev. Lett.* **19**, 1264 (1967).
6. A. Salam, Proc. of the 8<sup>th</sup> Nobel Symposium on *Elementary Particle Theory, Relativistic Groups and Analyticity*, edited by N. Svartholm (1969).
7. H. Fritzsch, M. Gell-Mann and H. Leutwyler, *Phys. Lett. B* **47**, 365 (1973).
8. For excellent reviews on the Standard Model see J. F. Donoghue, E. Golowich and B. R. Holstein, *Dynamics of the Standard Model*, (Cambridge University Press, 1992).
9. T2K Collab. (K. Abe *et al.*), *Phys. Rev. Lett.* **107**, 041801 (2011).

10. MINOS Collab. (P. Adamson *et al.*), *Phys. Rev. Lett.* **107**, 181802 (2011).
11. DAYA BAY Collab. (F. P. An *et al.*), arXiv:1203.1669.
12. RENO Collab. Soo-Bong Kim, arXiv:1204.0626.
13. A. Yu. Smirnov, hep-ph/0604213.
14. C. D. Froggatt and H. B. Nielsen, *Nucl. Phys. B* **147**, 277 (1979).
15. Y. Nir and N. Seiberg, *Phys. Lett. B* **309**, 337 (1993).
16. M. Leurer, Y. Nir and N. Seiberg, *Nucl. Phys. B* **420**, 468 (1994).
17. L. E. Ibanez and G. G. Ross, *Phys. Lett. B* **332**, 100 (1994).
18. G. Altarelli and F. Feruglio, arXiv:1002.0211.
19. A. J. Buras, C. Grojean, S. Pokorski and R. Ziegler, arXiv:1105.3725 and references therein.
20. Z. Guo and B. Ma, *JHEP* **0909**, 091 (2009) and references therein.
21. H. Fritzsch and Z. Z. Xing, *Prog. Part. Nucl. Phys.* **45**, 1 (2000) and references therein.
22. Z. Z. Xing, *Int. J. Mod. Phys. A* **19**, 1 (2004) and references therein.
23. Belle Collab. (K. Abe *et al.*), *Phys. Rev. Lett.* **89**, 142001 (2002).
24. BABAR Collab. (B. Aubert *et al.*), *Phys. Rev. D* **73**, 031101 (2006).
25. K. Nakamura *et al.*, *JPG* **37**, 075021 (2010), updated results available at <http://pdg.lbl.gov/>.
26. UTfit Collab. (M. Bona *et al.*), *PMC Phys. A* **3**, 6 (2009), updated results available at <http://www.utfit.org/>.
27. CKMfitter Group (J. Charles *et al.*), arXiv: 0905.1572, updated results available at <http://ckmfitter.in2p3.fr/>.
28. Heavy Flavor Averaging Group (HFAG) (E. Barberio *et al.*), arXiv: 0808.1297, updated results available at <http://www.slac.stanford.edu/xorg/hfag/>.
29. C. Jarlskog, *CP Violation*, *World Scientific Publishing Co. Pte. Ltd.* (1989).
30. L. Wolfenstein, *Phys. Rev. Lett.* **51**, 1945 (1983).
31. A. J. Buras, M. E. Lautenbacher and G. Ostermaier, *Phys. Rev. D* **50**, 3433 (1994).
32. G. Buchalla, A. J. Buras and M. E. Lautenbacher, *Rev. Mod. Phys.* **68**, 1125 (1996).
33. L. L. Chau and W. Y. Keung, *Phys. Rev. Lett.* **53**, 1802 (1984).
34. H. Fritzsch, *Phys. Lett. B* **70**, 436 (1977).
35. H. Fritzsch, *Phys. Lett. B* **73**, 317 (1978).
36. M. Antonelli, *Phys. Rept.* **494**, 197 (2010).
37. M. Ciuchini *et al.*, *JHEP* **0107**, 013 (2001).
38. J. Charles *et al.*, *Eur. Phys. J. C* **41**, 1 (2005).
39. G. Ahuja, M. Gupta, S. Kumar and M. Randhawa, *Phys. Lett. B* **647**, 394 (2007).
40. M. Randhawa, V. Bhatnagar, P. S. Gill and M. Gupta, *Mod. Phys. Lett. A* **15**, 2363 (2000).
41. M. Randhawa and M. Gupta, *Phys. Lett. B* **516**, 446 (2001).
42. F. J. Botella, G. C. Branco, M. Nebot and M. N. Rebelo, *Nucl. Phys. B* **725**, 155 (2005).
43. W.-M. Yao *et al.*, *J. Phys. G* **33**, 1 (2006).
44. M. Gronau, hep-ph/0607282.
45. A. Hocker *et al.*, *Eur. Phys. J. C* **21**, 225 (2001), updated results available at <http://ckmfitter.in2p3.fr/>.
46. A. J. Buras, R. Fleischer, S. Recksiegel and F. Schwab, *Eur. Phys. J. C* **45**, 701 (2006).
47. K. Kleinknecht and B. Renk, *Phys. Lett. B* **639**, 612 (2006).
48. J. L. Rosner and M. Gronau, arXiv:1105.1923.
49. C. Aubin, J. Laiho and R. S. Van de Water, *Phys. Rev. D* **81**, 014507 (2010).
50. R. S. Van de Water, *PoS LAT 2009*, 014 (2009).
51. A. J. Buras and D. Guadagnoli, *Phys. Rev. D* **78**, 033005 (2008).

52. E. Lunghi and A. Soni, *Phys. Lett. B* **666**, 162 (2008).
53. G. Ahuja, R. Verma, P. Fakay, P. S. Gill and M. Gupta, *Mod. Phys. Lett. A* **27**, 1250125 (2012).
54. Y. Grossman, A. Hocker, Z. Ligeti and D. Pirjol, *Phys. Rev. D* **72**, 094033 (2005).
55. M. Gronau, *Int. J. Mod. Phys. A* **22**, 1953 (2007).
56. M. Artuso, E. Barberio and S. Stone, *PMC Physics A* **3**, 3 (2009).
57. Private communication with Y. Nir.
58. B. Pontecorvo, *Zh. Eksp. Teor. Fiz. (JETP)* **33**, 549 (1957).
59. B. Pontecorvo, *Zh. Eksp. Teor. Fiz. (JETP)* **34**, 247 (1958).
60. B. Pontecorvo, *Zh. Eksp. Teor. Fiz. (JETP)* **53**, 1717 (1967).
61. Z. Maki, M. Nakagawa and S. Sakata, *Prog. Theor. Phys.* **28**, 870 (1962).
62. Y. Farzan and A. Yu. Smirnov, *Phys. Rev. D* **65**, 113001 (2002).
63. J. D. Bjorken, P. F. Harrison and W. G. Scott, *Phys. Rev. D* **74**, 073012 (2006).
64. G. Ahuja and M. Gupta, *Phys. Rev. D* **77**, 057301 (2008).
65. G. Ahuja, *Mod. Phys. Lett. A* **26**, 2597 (2011).
66. G. C. Branco, R. Gonzalez Felipe and F. R. Joaquim, arXiv:1111.5332.
67. P. F. Harrison, D. H. Perkins and W. G. Scott, *Phys. Lett. B* **530**, 167 (2002).
68. Z. Z. Xing, *Phys. Lett. B* **533**, 85 (2002).
69. P. F. Harrison and W. G. Scott, *Phys. Lett. B* **535**, 163 (2002).
70. P. F. Harrison and W. G. Scott *Phys. Lett. B* **547**, 219 (2002).
71. P. F. Harrison and W. G. Scott *Phys. Lett. B* **557**, 76 (2003).
72. P. F. Harrison and W. G. Scott, hep-ph/0402006.
73. P. F. Harrison and W. G. Scott, *Phys. Lett. B* **594**, 324 (2004).
74. SUPER-KAMIOKANDE Collab. (R. Wendell *et al.*), *Phys. Rev. D* **81**, 092004 (2010).
75. K2K Collab. (M. H. Ahn *et al.*), *Phys. Rev. D* **74**, 072003 (2006).
76. CHOOZ Collab. (M. Appolonio *et al.*), *Eur. Phys. J. C* **27**, 331 (2003).
77. C. H. Albright and M. C. Chen, *Phys. Rev. D* **74**, 113006 (2006).
78. W. Marciano and Z. Parsa, hep-ph/0610258.
79. H. Minakata, hep-ph/0604088.
80. C. Giunti and M. Tanimoto, *Phys. Rev. D* **66**, 113006 (2002).
81. K. R. S. Balaji, G. Couture and C. Hamzaoui, *Phys. Rev. D* **74**, 033013 (2006).
82. H. Sugiyama, hep-ph/0411209.
83. R. N. Mohapatra *et al.*, hep-ph/0510213.
84. R. Davis, *Prog. Part. Nucl. Phys.* **32**, 13 (1994).
85. HOMESTAKE Collab. (B. T. Cleveland *et al.*), *Astrophys. J.* **496**, 505 (1998).
86. GALLEX Collab. (W. Hampel *et al.*), *Phys. Lett. B* **447**, 127 (1999).
87. GNO Collab. (M. Altmann *et al.*), *Phys. Lett. B* **616**, 174 (2005).
88. SUPER-KAMIOKANDE Collab. (J. P. Cravens *et al.*), *Phys. Rev. D* **78**, 032002 (2008).
89. SAGE Collab. (J. N. Abdurashitov *et al.*), *Phys. Rev. C* **80**, 015807 (2009).
90. SNO Collab. (B. Aharmim *et al.*), *Phys. Rev. C* **81**, 055504 (2010).
91. KamLAND Collab. (A. Gando *et al.*), *Phys. Rev. D* **83**, 052002 (2011).
92. MINOS Collab. (L. Whitehead), Recent results from MINOS, Joint Experimental-Theoretical Seminar (24 June 2011, Fermilab, USA). Websites: theory.fnal.gov/jetp, [http://www.numi.fnal.gov/pr\\_plots/](http://www.numi.fnal.gov/pr_plots/)
93. T. Schwetz, M. Tortola and J. W. F. Valle, *New J. Phys.* **10**, 113011 (2008).
94. G. L. Fogli, E. Lisi, A. Marrone, A. Palazzo and A. M. Rotunno, *Phys. Rev. Lett.* **101**, 141801 (2008).
95. G. L. Fogli, E. Lisi, A. Marrone, A. Palazzo and A. M. Rotunno, *Phys. Rev. D* **84**, 053007 (2011).

96. OPERA Collab. (N. Agafonova *et al.*), *Phys. Lett. B* **691**, 138 (2010).
97. A. Strumia and F. Vissani, hep-ph/0606054.
98. C. Giunti, *Nucl. Phys. Proc. Suppl.* **169**, 309 (2007).
99. M. C. Gonzalez-Garcia and M. Maltoni, *Phys. Rept.* **460**, 1 (2008).
100. G. C. Branco and J. I. Silva-Marcos, *Phys. Rev. D* **80**, 073016 (2009).
101. B. Stech, *Phys. Lett. B* **130**, 189 (1983).
102. M. Gronau, R. Johnson and J. Schechter, *Phys. Rev. Lett.* **54**, 2176 (1985).
103. G. C. Branco, L. Lavoura and F. Mota, *Phys. Rev. D* **39**, 3443 (1989).
104. G. C. Branco, D. Emmanuel-Costa and C. Simoes, arXiv:1001.5065.
105. S. Weinberg, *Transaction of the New York Academy of Sciences*, Series II, 38, 185 (1977).
106. P. Ramond, R. G. Roberts and G. G. Ross, *Nucl. Phys. B* **406**, 19 (1993).
107. P. S. Gill and M. Gupta, *J. Phys. G: Nuc. Part. Phys.* **21**, 1 (1995).
108. A. Rasin, *Phys. Rev. D* **58**, 096012 (1998).
109. H. D. Kim and G. H. Wu, hep-ph/0004036.
110. B. R. Desai and A. R. Vaucher, *Phys. Rev. D* **63**, 113001 (2001).
111. N. G. Deshpande, M. Gupta and P. B. Pal, *Phys. Rev. D* **45**, 953 (1992).
112. P. S. Gill and M. Gupta, *Pramana* **45**, 333 (1995).
113. P. S. Gill and M. Gupta, *J. Phys. G* **23**, 335 (1997).
114. P. S. Gill and M. Gupta, *Phys. Rev. D* **56**, 3143 (1997).
115. M. Randhawa and M. Gupta, *Phys. Rev. D* **63**, 097301 (2001).
116. L. J. Hall and A. Rasin, *Phys. Lett. B* **315**, 164 (1993).
117. R. Barbieri, L. J. Hall and A. Romanino, *Phys. Lett. B* **401**, 47 (1997).
118. R. G. Roberts, A. Romanino, G. G. Ross and L. Velasco-Sevilla, *Nucl. Phys. B* **615**, 358 (2001).
119. H. Fritzsch and Z. Z. Xing, *Phys. Lett. B* **555**, 63 (2003).
120. H. D. Kim, S. Raby and L. Schradin, *Phys. Rev. D* **69**, 092002 (2004).
121. G. C. Branco, M. N. Rebelo and J. I. Silva-Marcos, *Phys. Rev. D* **76**, 033008 (2007).
122. M. Bando, S. Kaneko, M. Obara and M. Tanimoto, *Prog. Theor. Phys.* **116**, 1105 (2007).
123. Z. Z. Xing and H. Zhang, *J. Phys. G* **30**, 129 (2004).
124. R. Verma, G. Ahuja and M. Gupta, *Phys. Lett. B* **681**, 330 (2009).
125. R. Verma, G. Ahuja, N. Mahajan, M. Randhawa and M. Gupta, *J. Phys. G: Nucl. Part. Phys.* **37**, 075020 (2010) and references therein.
126. N. Mahajan, R. Verma and M. Gupta, *Int. J. Mod. Phys. A* **25**, 2037 (2010).
127. P. S. Gill and M. Gupta, *Phys. Rev. D* **57**, 3917 (1998).
128. M. Randhawa, V. Bhatnagar, P. S. Gill and M. Gupta, *Phys. Rev. D* **60**, 051301 (1999).
129. H. Leutwyler, hep-ph/9602255.
130. Z. Z. Xing, H. Zhang and S. Zhou, *Phys. Rev. D* **77**, 113016 (2008).
131. W. Grimus, hep-ph/0511078.
132. K. Kang and S. K. Kang, *Phys. Rev. D* **56**, 1511 (1997).
133. P. S. Gill and M. Gupta, *Phys. Rev. D* **57**, 3971 (1998).
134. H. Nishiura, K. Matsuda and T. Fukuyama, *Phys. Rev. D* **60**, 013006 (1999).
135. K. Matsuda, T. Fukuyama and H. Nishiura, *Phys. Rev. D* **61**, 053001 (2000).
136. K. Kang, S. K. Kang, C. S. Kim and S. M. Kim, *Mod. Phys. Lett. A* **16**, 2169 (2001).
137. P. H. Frampton, S. L. Glashow and D. Marfatia, *Phys. Lett. B* **536**, 79 (2002).
138. M. Frigerio and A. Yu. Smirnov, *Nucl. Phys. B* **640**, 233 (2002).
139. E. Ma, *Mod. Phys. Lett. A* **17**, 2361 (2002).
140. E. Ma, *Phys. Rev. D* **66**, 117301 (2002).



141. Z. Z. Xing, *Phys. Lett. B* **530**, 159 (2002).
142. E. Ma, *Phys. Lett. B* **539**, 85 (2002).
143. A. Kageyama, S. Kaneko, N. Simoyama and M. Tanimoto, *Phys. Lett. B* **538**, 96 (2002).
144. W. L. Guo and Z. Z. Xing, hep-ph/0211315.
145. M. Randhawa, G. Ahuja and M. Gupta, *Phys. Rev. D* **65**, 093016 (2002).
146. M. Fukugita, M. Tanimoto and T. Yanagida, *Phys. Lett. B* **562**, 273 (2003).
147. M. Frigerio and A. Yu. Smirnov, *Phys. Rev. D* **67**, 013007 (2003).
148. K. S. Babu, E. Ma and J. W. F. Valle, *Phys. Lett. B* **552**, 207 (2003).
149. W. L. Guo and Z. Z. Xing, *Phys. Rev. D* **67**, 053002 (2003).
150. S. Kaneko and M. Tanimoto, *Phys. Lett. B* **551**, 127 (2003).
151. B. R. Desai, D. P. Roy and A. R. Vaucher, *Mod. Phys. Lett. A* **18**, 1355 (2003).
152. K. Hasegawa, C. S. Lim and K. Ogure, *Phys. Rev. D* **68**, 053006 (2003).
153. M. Honda, S. Kaneko and M. Tanimoto, *JHEP* **0309**, 028 (2003).
154. G. Bhattacharyya, A. Raychaudhuri and A. Sil, *Phys. Rev. D* **67**, 073004 (2003).
155. Z. Z. Xing, invited talk given at NOON (2004), hep-ph/0406049.
156. M. Bando, S. Kaneko, M. Obara and M. Tanimoto, *Phys. Lett. B* **580**, 229 (2004).
157. O. L. G. Peres and A. Yu. Smirnov, *Nucl. Phys. B* **680**, 479 (2004).
158. C. H. Albright, *Phys. Lett. B* **599**, 285 (2004).
159. J. Ferrandis and S. Pakvasa, *Phys. Lett. B* **603**, 184 (2004).
160. Z. Z. Xing and S. Zhou, *Phys. Lett. B* **593**, 156 (2004).
161. S. Zhou and Z. Z. Xing, *Eur. Phys. J. C* **38**, 495 (2005).
162. Z. Z. Xing and S. Zhou, *Phys. Lett. B* **606**, 145 (2005).
163. S. T. Petcov and W. Rodejohann, *Phys. Rev. D* **71**, 073002 (2005).
164. S. S. Masood, S. Nasri and J. Schechter, *Phys. Rev. D* **71**, 093005 (2005).
165. R. Dermisek and S. Raby, *Phys. Lett. B* **622**, 327 (2005).
166. F. Plentinger and W. Rodejohann, *Phys. Lett. B* **625**, 264 (2005).
167. M. Randhawa, G. Ahuja and M. Gupta, *Phys. Lett. B* **643**, 175 (2006).
168. K. Matsuda and H. Nishiura, *Phys. Rev. D* **74**, 033014 (2006) and references therein.
169. S. Dev and S. Kumar, *Mod. Phys. Lett. A* **22**, 1401 (2007).
170. S. Dev, S. Kumar, S. Verma and S. Gupta, *Nucl. Phys. B* **784**, 103 (2007).
171. S. Dev, S. Kumar, S. Verma and S. Gupta, *Phys. Rev. D* **76**, 013002 (2007).
172. G. Ahuja, S. Kumar, M. Randhawa, M. Gupta and S. Dev, *Phys. Rev. D* **76**, 013006 (2007).
173. G. Ahuja, M. Gupta, M. Randhawa and R. Verma, *Phys. Rev. D* **79**, 093006 (2009).
174. N. Mahajan, M. Randhawa, M. Gupta and P. S. Gill, arXiv:1010.5640.
175. P. Minkowski, *Phys. Lett. B* **67**, 421 (1977).
176. T. Yanagida, in *Proceedings of the Workshop on Unified Theory and the Baryon Number of the Universe*, eds. O. Sawada and A. Sugamoto (KEK, Tsukuba, 1979), p. 95.
177. M. Gell-Mann, P. Ramond and R. Slansky, in *Supergravity*, eds. F. van Nieuwenhuizen and D. Freedman (North Holland, Amsterdam, 1979), p. 315.
178. S. L. Glashow, in *Quarks and Leptons*, eds. M. Lévy *et al.* (Plenum, New York, 1980), p. 707.
179. R. N. Mohapatra and G. Senjanovic, *Phys. Rev. Lett.* **44**, 912 (1980).
180. M. Gupta, Invited talk entitled *Texture specific fermion mass matrices and their compatibility with SO(10) inspired mass matrices* delivered at *1st IAS-CERN winter school on High Energy Physics and Cosmology* on 27 January 2012 at IAS, NTU, Singapore.
181. G. C. Branco *et al.*, *Phys. Lett. B* **670**, 340 (2009).

182. Heidelberg-Moscow Collab., (H. V. Klapdor-Kleingrothaus *et al.*), *Eur. Phys. J. A* **12**, 147 (2001).
183. H. V. Klapdor-Kleingrothaus *et al.*, *Phys. Lett. B* **586**, 198 (2004) and references therein.
184. H. Ejiri, R. Hazama, P. Krastev, N. Kudomi and R. G. H. Robertson, *Phys. Rev. Lett.* **85**, 2917 (2000).
185. CUORE Collab., R. Ardito *et al.*, hep-ex/0501010.
186. R. D. Peccei and K. Wang, *Phys. Rev. D* **53**, 2712 (1996).
187. G. C. Branco *et al.*, *Phys. Rev. Lett.* **82**, 683 (1999).
188. G. C. Branco *et al.*, *Phys. Lett. B* **477**, 147 (2000).
189. H. Fritzsch and Z. Z. Xing, *Phys. Lett. B* **413**, 396 (1997) and references therein.
190. H. Fritzsch and Z. Z. Xing, *Nucl. Phys. B* **556**, 49 (1999) and references therein.
191. J. C. Pati, *Phys. Rev. D* **68**, 072002 (2003).
192. M. C. Chen and K. T. Mahanthappa, *Int. J. Mod. Phys. A* **18**, 5819 (2003).
193. A. Joshipura and K. Patel, *Phys. Rev. D* **83**, 095002 (2011).
194. T. Fukuyama, K. Matsuda and H. Nishiura, *Int. J. Mod. Phys. A* **22**, 5235 (2007).
195. S. Dev, S. Kumar, S. Verma, S. Gupta and R. R. Gautam, *Eur. Phys. J. C* **72**, 1940 (2012).
196. R. Verma, S. Sharma, P. Fakay, G. Ahuja and M. Gupta, *Compatibility of textures and  $SO(10)$  inspired mass matrices*, presented at *V International Pontecorvo Neutrino Physics School*, 6-16 September 2012, Ukraine.
197. J. C. Pati and A. Salam, *Phys. Rev. D* **10**, 275 (1974).
198. U. Sarkar, in *Particle and Astroparticle Physics*, Taylor and Francis, (2007), ISBN: 978-1-58488-931-1.
199. R. N. Mohapatra, in *Unification and Supersymmetry: The frontiers of quark-lepton physics*, Springer (2003), ISBN: 0387955348.
200. A. Bottino, C. W. Kim and H. Nishiura, *Phys. Rev. D* **30**, 1046 (1984).
201. G. Senjanovic, hep-ph/0612312.
202. G. Altarelli and G. Blankenburg, *JHEP* **1103**, 133 (2011).
203. B. Dutta, Y. Mimura and R. N. Mohapatra, *JHEP* **34**, 1005 (2010).
204. W. Grimus and H. Kuhbock, *EPJ C* **51**, 721 (2007).
205. R. G. Moorehouse, *Phys. Rev. D* **77**, 053006 (2008).
206. H. Fritzsch, Z. Z. Xing and Y. L. Zhou, *Phys. Lett. B* **697**, 357 (2011).